Understanding the Mutual Antagonism Between HIV and Autophagy

by

Sergio Castro Gonzalez, M.Sc.

A Dissertation

In

Biology

Submitted to the Graduate Faculty
of Texas Tech University in
Partial Fulfillment of
the Requirements for
the Degree of

DOCTOR OF PHILOSOPHY

Approved

Ruth Serra-Moreno
Chair of Committee

Catherine Wakeman

Lauren Gollahon

Peter Keyel

Sharilyn Almodovar

Mark Sheridan
Dean of the Graduate School

December, 2020

ACKNOWLEDGMENTS

First and foremost, I would like to thank my advisor Dr. Ruth Serra-Moreno not only for offering me the great opportunity to become a graduate student in her lab, but also for her relentless guidance and support. I will always be indebted to Dr. Serra-Moreno for the most inspiring and complete mentorship I could have wished for when I first joined Texas Tech University four years ago. Thank you.

I would like to extend my gratitude to my PhD committee members: Dr. Catherine Wakeman, Dr. Lauren Gollahon, Dr. Peter Keyel, Dr. Sharilyn Almodovar and Dr. Brian Reilly. I am extremely grateful for the valuable input and advice they have provided throughout the different steps of my graduate experience. They all have contributed, along with Dr. Serra-Moreno, to my growth as a researcher. As Isaac Newton said, "if I have seen further, it is by standing on the shoulders of giants."

I would also like to thank all the members of Dr. Serra-Moreno's lab, who have not only been lab mates, but also have become very good friends. I had great pleasure of working and getting to know each of them. To the former postdoc Marta, thank you for making my first months in the lab so easy, and thank you for your continuous support and helpful advice. To Yuhang and Yuexuan, I cannot express how lucky I feel for working side by side with you two. You have been crucial for the progress of my project, through your constant feedback and assistance, but what I think is more important, you have made this process a fun and enjoyable experience.

Also, my sincere gratitude to my friends in Lubbock for providing the sometimes underestimated moral and emotional support that living in a foreign country requires. Thank you all: Belinda, Bipush, Caroline, Karishma, Michael, Mike, Moamen, Neha, Neil, Nick, Nikhil and Varun. Thank you for making Lubbock feel like home.

I cannot finish this section without acknowledging my friends from Spain, especially my dear friends Paola and Pablo, who made this PhD adventure possible in the first place. Thank you for always being my career compass.

Finally, I would like to express my deepest appreciation to my parents, Sagrario and Gonzalo, my sister, Malva, and my partner, Claudia, for all their sacrifices and unconditional support during this journey. To them, I dedicate my dissertation.

TABLE OF CONTENTS

ABSTRACT

Autophagy is a conserved cell survival pathway that is activated in response to stress to target cargo for lysosomal degradation. This pathway has recently gained attention as a potent mechanism of defense against viruses, since it can target virions and/or viral components to autophagosomes and halt virus replication. Furthermore, the autophagy-mediated breakdown of these viral structures facilitates (a) their engagement with endosomal pattern recognition receptors, and (b) their presentation through MHC-I/II molecules. Hence, besides its role in the direct elimination of viruses, autophagy also assists in shaping adaptive immune responses against these pathogens. Consistent with this, autophagy effectively protects from important infectious agents such as herpesviruses or flaviviruses. However, the role of autophagy in HIV infection remains controversial. Whereas some studies indicate that its degradative nature is detrimental for this virus, others have claimed that HIV triggers autophagy to increase its infectivity. Moreover, these contrasting findings seem to differ in a cell type-specific manner.

Here, we show that autophagy restricts HIV replication through the clearance of the viral protein Gag, the main driver of virion assembly and release. Upon autophagy activation, Gag is targeted to autophagosomes for its subsequent degradation in autolysosomes. However, HIV has evolved its virulence factor Nef to protect from autophagy through a previously unappreciated mechanism. A thorough analysis of the interactions between HIV Nef and the autophagy machinery revealed that Nef enhances the association between the initiator of autophagy BECN1 and its natural inhibitor BCL2, impeding the early steps of autophagy and consequently autophagosome biogenesis. As a consequence of this, Gag levels and virion production are restored. Nef achieves this by promoting changes in the post-translational modification patterns of BCL2. In particular, HIV Nef recruits the E3 ubiquitin ligase PRKN to promote the mono-ubiquitination of BCL2. This post-translational modification renders BCL2 more stable and, thus, enhances its inhibitory effect over BECN1. Our structural analysis revealed that the N-terminal portion of Nef is responsible for this newly discovered anti-autophagic function. Remarkably, this

ability of Nef to counteract autophagy is conserved in the most prevalent HIV-1 M subtypes as well as their direct ancestor SIV_{cpz}, but largely missing in the HIV-2/SIV_{sm} linage, which suggests that this activity has been a critical evolutionary trait for the pathogenesis and spread of HIV-1.

In conclusion, autophagy poses an important hurdle for HIV, but the virus uses the *nef* gene – a notorious virulence factor that facilitates immune evasion – to counteract this block. Therefore, the identification of the cellular molecules targeted by Nef (i.e. BECN1-BCL2) represents an instrumental step to design approaches to make HIV susceptible to autophagy elimination.

LIST OF TABLES

LIST OF FIGURES

CHAPTER 1

INTRODUCTION

The figures presented in this chapter are derived from the following publications[1,2] in which I am first or co-first author and I have permission from the journal editorial to reproduce the figures in this thesis.

Sergio Castro-Gonzalez, Yuhang Shi, Yuexuan Chen, Marta Colomer-Lluch, Jayc Waller, Ying Song, Anju Bansal, Frank Kirchhoff, Konstantin Sparrer, Chengyu Liang and Ruth Serra-Moreno. HIV-1 Nef counteracts autophagy restriction by enhancing the association between BECN1 and its inhibitor BCL2 in a PRKN-dependent manner. *Autophagy*, 1-25, doi:10.1080/15548627.2020.1725401 (2020).

Marta Colomer-Lluch, Sergio Castro-Gonzalez and Ruth Serra-Moreno. Ubiquitination and SUMOylation in HIV Infection: Friends and Foes. *Curr Issues Mol Biol* **35**, 159-194, doi:10.21775/cimb.035.159 (2020).

Human Immunodeficiency Virus (HIV) and Acquired Immunodeficiency Syndrome (AIDS)

Origin and distribution

Acquired Immunodeficiency Syndrome (AIDS) in humans is caused by the Human Immunodeficiency Virus (HIV). Since the first AIDS cases were ever reported in the early 80s, AIDS has grown to become one of the most devastating pandemics that humanity has ever encountered, with a shocking death toll of 36 million people. Based on the latest report from UNAIDS in 2020, 38 million individuals are currently infected with HIV and this virus is causing the death of around 700,000 people every year[3].

AIDS first arose as a new infectious disease in the United States in 1981, when many young and previously healthy individuals started to exhibit symptoms of severe immunodeficiency. The immunodeficiency usually preceded a variety of rare cancers and opportunistic infections such as Kaposi's Sarcoma or *Pneumocystis carinii* pneumonia[4,5]. These unusual cases were initially observed among white homosexual males, which led the press to unofficially name this disease GRID (Gay-related disease) or Gay cancer[6]. As a consequence of this, an already very stigmatized community became further defamed. The term AIDS and its definition was finally designated by the Centers for Disease Control and Prevention (CDC) at the end of 1982. One year later, the collaborative efforts devoted by the international scientific

community allowed the identification of a novel human retrovirus as the causative agent of this infection. The retrovirus was initially called LAV for lymphadenopathy associated virus, and finally renamed as human immunodeficiency virus or HIV[7-9]. By that time, nearly 1,450 cases of AIDS had been reported, which had already caused the death of at least a third of those individuals[10,11]. In 1985, AIDS was declared a pandemic with the presence of at least one reported case of HIV in each region of the world[10].

Remarkably, in 1986, another human retrovirus also capable of causing AIDS was found in West Africa, although this virus seemed less pathogenic than the virus isolated in the US and Europe[12]. Phylogenetic analyses determined that both retroviruses were related but different enough to be considered different species. In consequence, the original HIV was renamed as HIV-1 and the African retrovirus as HIV-2. Importantly, HIV-1 is the most predominant species of HIV worldwide, being responsible for at least 95% of all infections, which consequently makes this species the main focus of the international research efforts[13,14]. Early studies revealed important facts about these viruses, including the methods of transmission as well as their evolutionary origins. Both viruses could be transmitted through direct contact between bodily fluids containing the virus, such as (1) blood, (2) sexual fluids, from both men and women (in contrast to what it was originally speculated), and also (3) vertically, from mother to child during birth as well as through the breast milk[15].

With regard to their evolutionary origins, HIV-1 and HIV-2 arose from different Simian Immunodeficiency Viruses (SIVs), as a result of zoonotic infections from their natural hosts to humans. Researchers believe that the first infections in humans occurred when hunters were exposed to blood from apes and monkeys infected with SIV. These events would have normally ended up in a non-productive infection, but occasionally these viruses adapted within the new host, leading to the generation of the new primate lentiviral species HIV-1 and HIV-2[16,17]. Phylogenetic analyses indicate that, whilst HIV-1 is the result of cross-species transmissions of SIVs infecting chimpanzees and gorillas (SIV_{cpz} and SIV_{gor}), HIV-2 originated from an

interspecific transmission of SIVs infecting Sooty Mangabeys (SIV_{smm})[17-21]. In addition, SIV_{smm} was also able to infect rhesus macaques, originating the simian pathogenic species SIV_{mac}[16,22]. Interestingly, as a result of a co-adaptation process, the predecessor SIVs (SIV_{cpz}, SIV_{gor} or SIV_{smm}) are usually nonpathogenic in their natural hosts, whereas the newly originated species HIV-1, HIV-2 and SIV_{mac} cause AIDS to humans and macaques, respectively[16,21]. For this reason, and given the immune similarities between macaques and humans, the SIV_{mac}/rhesus macaque has become an important animal model for the study of AIDS[23,24].

Due to its global distribution and multiple origins (from SIVs infecting chimpanzees as well as gorillas) HIV-1 has diversified more than HIV-2, which has led to the emergence of the distinct worldwide distributed phylogenetic groups of HIV-1: M, N, O and P. From these four groups, the vast majority of the global infections with HIV are caused by a few clades or subtypes belonging to the major group M. Specifically, the HIV-1 subtypes A, B and C account for more than 80% of all HIV/AIDS cases worldwide[25-28]. These subtypes have heterogeneously spread throughout the human population for the past 30 years, resulting in the current distribution of these viruses around the globe. Whereas the subtype C of HIV-1 is

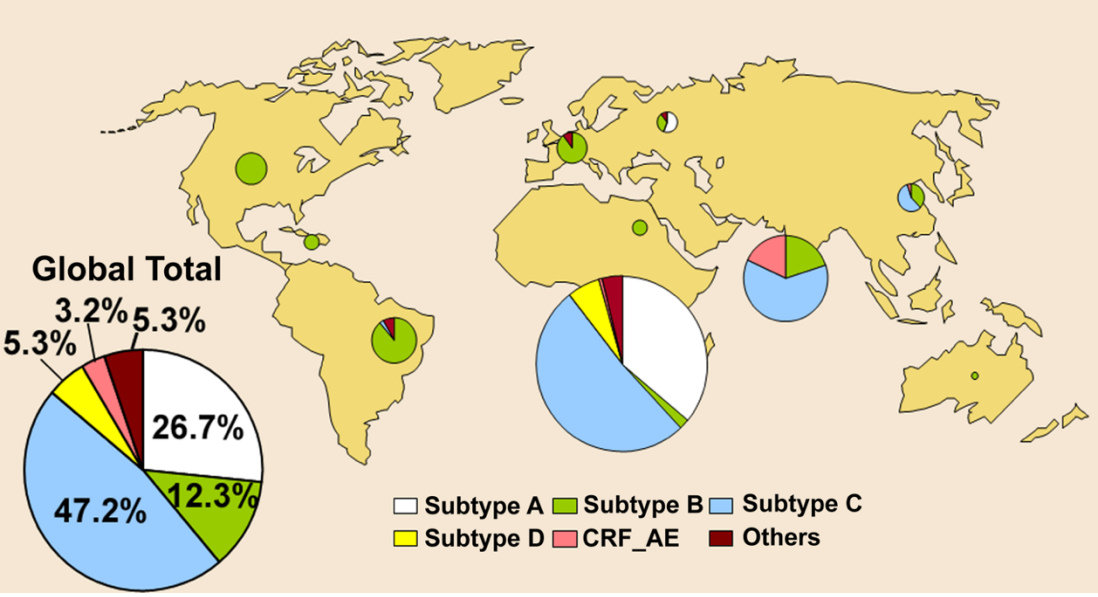

Figure 1.1. Map showing HIV-1 subtype prevalence. Figure adapted from Osmanov *et al*., 2000.

responsible for most infections, the subtype B is the most geographically distributed pandemic clade of HIV-1, being present in almost every continent (**Fig. 1.1**). The successful dispersion of some of these clades is frequently the result of an underlying increase in the evolutionary fitness acquired by those particular virus isolates during the adaptation process to the new host[16,29,30].

Virus particle

HIVs and SIVs belong to the *Retroviridae* family, which is the only representative member of the category VI in the Baltimore classification. Retroviruses are considered diploid because they enclose two identical copies of a positive sense single-stranded RNA (ssRNA) genome. Of note, positive sense RNA refers to the potential of this molecule to be used as messenger RNA (mRNA) by the cellular machinery. As for other retroviruses, the genome needs to be reverse transcribed (*Retro*- transcription) into a double-stranded DNA (dsDNA) molecule to allow the replication of these viruses. Both HIV-1 and HIV-2 are complex retroviruses that cluster within the *Lentivirus* genus, characterized by their long incubation periods (*Lente*-, Latin for "slow")[31].

The intermediate DNA molecule, known as provirus, is over 9 Kb long and it is flanked by two long terminal repeat (LTR) sequences generated during the reverse transcription reaction. The LTR found at the 5' end is used as a promoter for the transcription of the viral genes[31,32]. The HIV-1 genome encodes the three essential structural genes that are present in all retroviruses (*gag*, *pol* and *env*). Additionally, HIV encodes for two regulatory proteins (Tat and Rev) and four accessory proteins (Vif, Vpr, Nef and Vpu), which are not essential for viral replication *in vitro*, but they significantly improve viral fitness *in vivo* and are associated with pathogenesis[31-33]. Unlike HIV-1, the lentiviral species SIV_{sm}, HIV-2 and SIV_{mac}, do not encode *vpu,* but they encode *vpx*, which is a gene specific for the HIV-2/SIV_{sm} lineage[34,35] (**Fig. 1.2**).

During the maturation process of the viral particles, the structural proteins Gag, Gag-Pol and Env undergo a protease-mediated cleavage that results in the generation

of a variety of mature structural proteins that will constitute the fully infectious virions[31,32,36] (**Fig. 1.3**):

- Gag (p55)-derived proteins provide the internal structural proteins: Matrix (MA; p17), capsid (CA; p24) and nucleocapsid (NC; p7).
- Pol-derived proteins comprise the virus enzymes: Integrase (IN), reverse transcriptase (RT) and protease (PR).
- Env-derived proteins will form the external structural proteins, which form the envelope spikes: Glycoprotein 120 (gp120) and glycoprotein 41 (gp41).

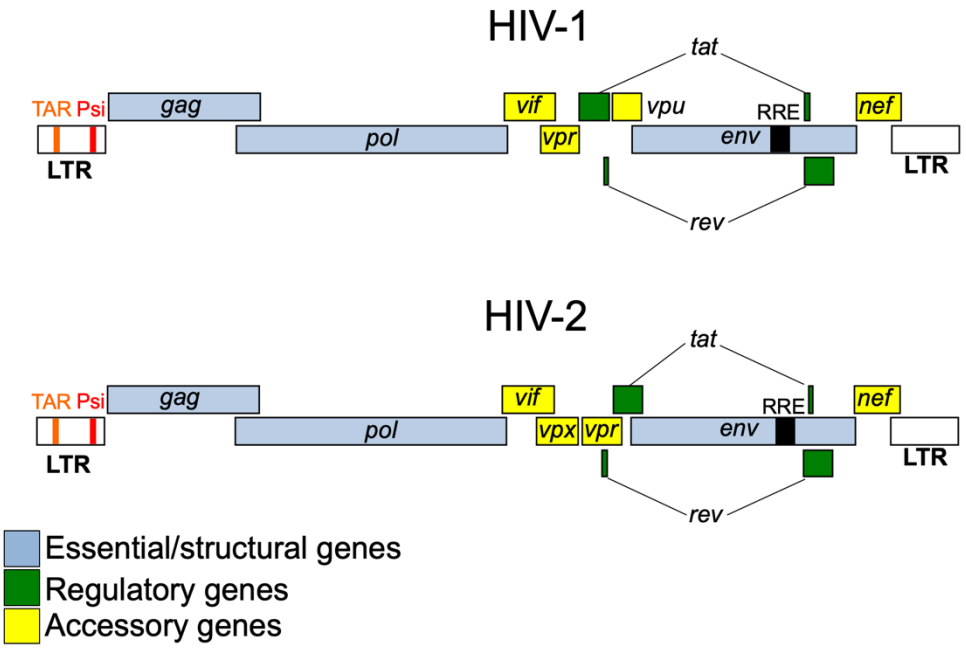

Figure 1.2. The HIV genome. Representation of the HIV-1 and HIV-2 genomes as dsDNA. Figure adapted from Colomer-Lluch *et al.*, 2020.

In the HIV virus particle, the RNA genome is wrapped by the positively charged NC protein and further enclosed in the virus capsid or core, which is built from CA monomers. This capsid has a conical shape and icosahedral symmetry. In addition to the virus genome and nucleocapsid, the capsid also encloses the enzymes RT and IN. The capsid is found underneath a matrix layer, made from multiple copies of the MA protein (**Fig. 1.3**). In between the MA and the core, additional structural proteins can

be found, including the enzymatic protein PR and the accessory proteins Nef, Vpx (in the case of HIV-2) and Vpr[2,32] (**Fig. 1.3**). All these elements are surrounded by a round-shaped lipid bilayer envelope that displays around 14 spikes or knobs. The spikes are formed by trimers of gp120, which are attached to the virion envelope by association with trimers of the transmembrane protein gp41 (**Fig. 1.3**). The envelope protein gp120 is the only viral protein exposed in HIV virions and, therefore, it is susceptible to become neutralized by antibodies[37,38]. HIV circumvents this vulnerability by heavily glycosylating gp120, a post-translational modification that shields antibody-binding sites and also increases the variability of virus epitopes,

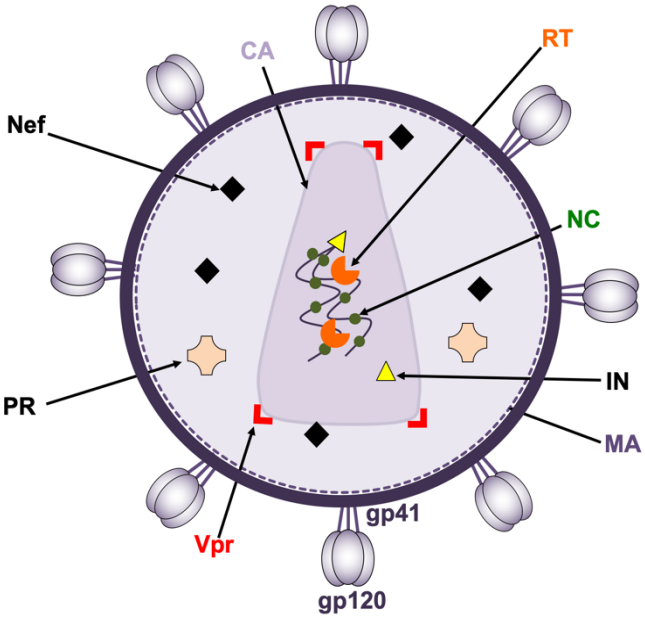

Figure 1.3. The HIV-1 virus particle. CA, capsid; IN, integrase; MA, matrix; NC, nucleocapsid; PR, protease; RT, reverse transcriptase. Figure adapted from Colomer-Lluch *et al.*, 2020.

hindering the efficacy of potential antibody-mediated immune responses mounted by the host[38,39].

Replicative cycle

As for any other virus, the replication cycle of HIV consists of five steps: attachment, entry, replication, assembly and release (**Fig. 1.4**).

Attachment and entry. Attachment takes place when a HIV virion associates to its target cells ($CD4^+$ cells) through a specific interaction with the surface receptor CD4. The envelope protein gp120 selectively binds to CD4, which promotes conformational changes in gp120 that facilitate its interaction with a secondary receptor, often referred to as co-receptor. HIV can use two different cellular surface molecules as co-receptors, namely CXCR4 or CCR5, and its ability to interact with one or another (or both) dictates the virus-specific tropism[40] (**Fig. 1.4**). The interactions between gp120 and the cell receptor/co-receptor leads to further conformational modifications that enable gp41 to pierce through the plasma membrane of the target cell. This process ends up with the fusion of both the virus envelope and the cellular membrane, allowing in turn the entry of the virus capsid/core inside the target cell[32]. Immediately after entry, uncoating of the core begins (**Fig. 1.4**). Uncoating is a multi-step process that is synchronized with reverse transcription. Of note, acceleration as well as deceleration of uncoating can significantly impair reverse transcription. CA monomers strip from the viral core to allow the entry of cytoplasmic nucleotides to the remaining of the virus core, so RT can initiate reverse transcription[41,42]. In consequence, RT synthesizes a dsDNA molecule (often referred to as copy DNA, cDNA, or proviral DNA) using the virus ssRNA genome as a template[43]. During or shortly after reverse transcription, the cDNA along with other virus proteins (Vpr, IN, and portions of CA) conform the pre-integration complex (PIC), which is transported via microtubules to the nuclear pores (**Fig. 1.4**). The PIC, assisted mostly by Vpr, is then translocated to the nucleus, where IN mediates the integration of the provirus into the cellular genome[44]. The next events in the HIV replication cycle, generally referred to as post-integration steps, rely on the transcriptional activity of infected cells. If the virus infects resting cells, characterized by a low transcriptional profile, HIV establishes a latent infection. However, infections of transcriptionally active $CD4^+$ cells lead to proviral transcription and synthesis of viral proteins, causing a productive infection[31,45].

Replication. For this step, HIV takes advantage of the machinery of the cell in order to replicate its genome and to synthesize the different virus proteins. The proviral

transcription starts when cellular transcription factors, including NF-κB, NFAT, AP-1 and SP1, bind to their responsive elements in the 5' LTR of the provirus**.** However, during the first rounds of gene expression, transcription elongation occurs with a relatively low efficiency[45,46]. Additionally, these transcripts are susceptible to undergo differential splicing processes, giving rise to multiple spliced variants: non-spliced, singly-spliced and multiply-spliced. Of note, the splicing process for the singly- and multiply-spliced transcripts can have different "flavors" by using distinct splicing donor and accepting sites, resulting in different species of singly-spliced and multiply-spliced HIV RNAs. As a consequence of such intricate splicing processes, HIV generates sufficient mRNA species to allow the translation of all its virus proteins. Despite the fact that all these RNA variants are generated almost simultaneously, HIV is characterized by having early and late phases for gene expression[31,46,47].

In the 'early' gene expression phase, only HIV transcripts that are multiply-spliced can be transported to the cytoplasm. Therefore, only genes encoded in these RNAs will be translated. In particular, *tat*, *rev* and *nef*. The protein Nef (Negative regulatory factor) is myristoylated and localizes at different membranous structures in the cell (**Fig. 1.4**). Its presence in the plasma membrane is critical for its role in circumventing host immune responses. This is achieved through the antagonism of cellular restrictions factors as well as downregulation of immune-related membrane receptors[48]. As for the proteins Tat (Transactivator of transcription) and Rev (Regulator of expression of virion proteins), the presence of nuclear localization signals in their amino acid sequences allows their nuclear translocation. Once in the nucleus, both Tat and Rev will enhance the expression of the rest of virus proteins through their ability to bind to specific sequences found within the virus transcripts[31,47]. Tat enhances transcription by associating to a secondary structure in the nascent HIV RNA called TAR (Trans-Activation Response element), which increases the efficiency of the RNA Pol II activity, and thus, accelerates transcription elongation, which, as stated earlier, was severely impaired[46,49]. Rev binds to a region within the non-spliced and singly-spliced HIV RNAs termed RRE (Rev-response element)[47,50]. Rev association with these RNA species assists in their transport to the

cytoplasm, where they can be translated into the remaining 'late' virus proteins (Vif, Vpr, Vpu, Env, Gag and Gag-Pol) (**Fig. 1.4**). Importantly, the non-spliced transcripts also represent the HIV genome. Hence, besides being translated, they can also be assembled into the new HIV virions[31,36].

The 'late' phase of gene expression is characterized by the translation of singly-spliced and non-spliced HIV RNAs. In the case of the singly-spliced HIV RNA encoding the *env* gene, not only does this transcript allow the synthesis of the Env precursor protein (gp160), but also Vpu[31,47] (**Fig. 1.4**). Vpu is translated in the ER, transported to Golgi and from there to the virion assembly regions found at the plasma membrane, where it promotes the internalization of the receptor CD4 to prevent superinfection, in addition to antagonize the activity of the antiviral factor BST-2 (bone marrow stromal antigen 2). BST-2, also known as Tetherin, prevents viral release by tethering nascent virions to the plasma membrane[51,52].

Through a process of leaky scanning and ribosomal frameshifting, the same transcript that encodes for *vpu* can be translated into gp160. Gp160 is co-translationally glycosylated in the ER and later in Golgi, where gp160 is ultimately cleaved by furin proteases into the mature envelope glycoproteins gp120 and gp41. These two glycoproteins are next transported to the plasma membrane, where they remain as integral membrane proteins and associated with each other as trimers. Similar to Vpu, gp120/gp41 trimers can also associate with the CD4 receptor during their transport to the plasma membrane and promote its down-regulation, as an additional mechanism to prevent superinfection and immune activation[53,54]. The rest of the singly-spliced RNAs are used to synthesize the accessory proteins Vif and Vpr (**Fig. 1.4**). Vif works as an inhibitor of the host restriction factor apolipoprotein B mRNA editing enzyme, catalytic polypeptide-like 3G (APOBEC3G), preventing the incorporation of this enzyme into virions, which otherwise would interfere and impair the reverse transcription process in future rounds of replication. The role of Vpr in HIV replication is not very well understood yet. However, besides being able to induce cell cycle arrest, Vpr can be incorporated into virions to facilitate the transport

of the PIC to the nucleus in the new round of infection[31,55]. In some lentiviral lineages, Vpr has also been involved in the degradation of the HIV restriction factor Sterile alpha motif and histidine aspartate domain-containing protein 1 (SAMHD-1)[56]. As mentioned above, the non-spliced HIV RNA can also work as genomic RNA. Therefore, this molecule can either be used as new genomes in the assembly of new viral particles or be translated into the immature structural proteins Gag (p55) and Gag-Pol (p160). These three elements (non-spliced RNA, Gag and Gag-Pol) will lead the last steps of the replication cycle of HIV[31,36].

Assembly and release. Both Gag and Gag-Pol polyproteins are post-translationally modified by the addition of a myristoyl group in their Gly_2, which serves as a membrane targeting signal. In addition, Gag and Gag-Pol harbor amino acid sequences within the NC portion of Gag that specifically recognize and interact with the

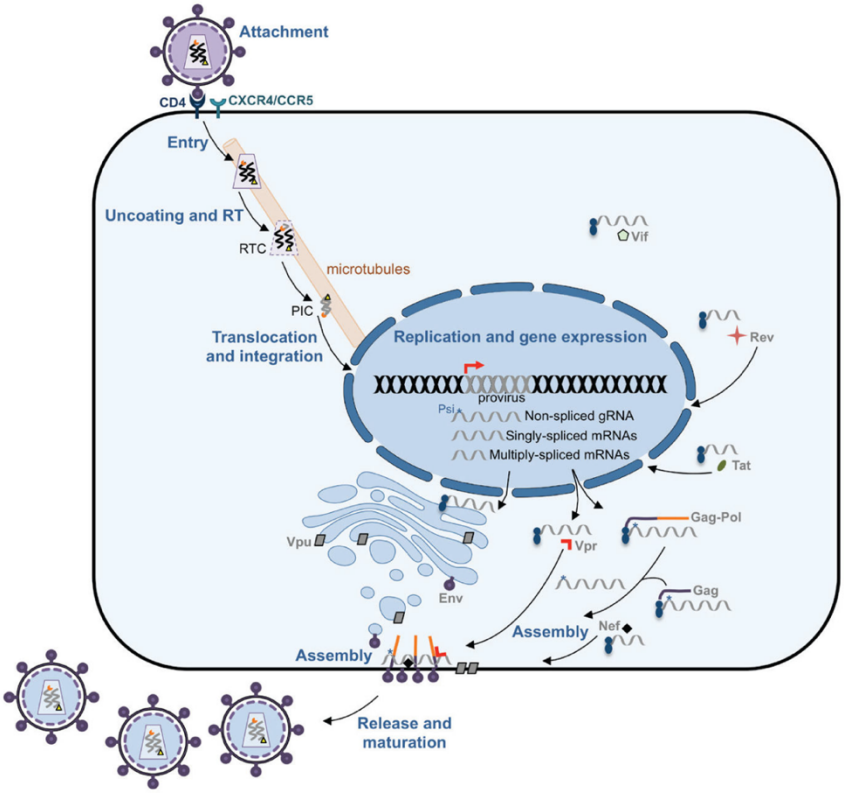

Figure 1.4. The HIV replication cycle. Representation of the different steps (bolded blue) and virus proteins (grey) involved in the life cycle of HIV. PIC, pre-integration complex; RT, reverse transcription; RTC, reverse transcription complex. Figure adapted from Colomer-Lluch *et al.*, 2020.

packaging signal (Psi) found only in the non-spliced HIV RNA molecules (**Fig. 1.2**). Both, the myristoyl group and the ability to recognize the virus genome, dictates the assembly process of nascent virions: by targeting genome-bound Gag and Gag-Pol proteins to cholesterol enriched locations at the plasma membrane, where gp120/gp41 are already present[57] (**Fig. 1.4**). Here, once again HIV uses the cellular resources to promote the release of the nascent virions. This is achieved by recruiting the endosomal sorting complexes required for transport (ESCRT) through ubiquitinated residues in Gag. The ESCRT machinery promotes the curvature and scission of the membrane and in consequence, virion budding and release[58] (**Fig. 1.4**). Upon release, the Pol portion within Gag-Pol is self-cleaved and facilitates its own processing as well as the processing of Gag into the mature MA, CA, NC, RT, IN and PR[31,57]. This process is known as virus maturation and is essential for the infectivity of the HIV progeny virions.

Pathogenesis and treatment

HIV attacks cells expressing the CD4 receptor on their surface, which are a set of very important cells for the immune system. The infection of these cells can lead to immune disorders (AIDS) and ultimately, if untreated, to the death of the host due to other opportunistic pathogens and cancers, such as the commonly AIDS-associated Kaposi's Sarcoma or *Pneumocystis carinii* pneumonia[5,59]. The main target of HIV amongst the $CD4^+$ cell population are the $CD4^+$ T lymphocytes, and in lower frequency, macrophages and dendritic cells[45,60]. Importantly, $CD4^+$ T lymphocytes, also known as T helper cells, are completely essential for an adequate regulation of all adaptive responses against invading pathogens. Not only does HIV cause the depletion of the productively infected cells, but also can induce the death of non-infected $CD4^+$ T cells (bystander T cells), although the underlying mechanism is not well understood yet[31,60,61]. Furthermore, the detrimental effect that HIV exerts on bystander $CD4^+$ T cells seems to be the main cause of the progressive immunological impairment observed in infected individuals[62,63]. The natural transition from being HIV^+ to developing AIDS is characterized by three distinct stages (**Fig. 1.5**):

1- Acute phase: This first period starts around 4 weeks after transmission, and it is associated with flu-like symptoms that usually last for up to two weeks. This stage is characterized by an increase of the viral load in blood (viremia) and a drastic decrease of the levels of $CD4^+$ T cells . This is a critical stage of HIV-1 infection. Noteworthy, early antiviral treatments after HIV exposure significantly improve long-term patient outcomes[64-66].

2- Clinical latency: This asymptomatic, although contagious period, can last up to 10 years and is characterized by a relatively low, but stable, level of $CD4^+$ T cells and a slight decrease of viremia. Even though at this point the immune system is relatively able to control HIV-1 replication, the infection cannot be completely cleared and will lead to a slow increase in the viral load and a concomitant reduction of $CD4^+$ T cells. The host's inability to clear this infection is partially due to the high variability of HIV-1 antigens, which poses a hurdle for the efficacy of antibody-mediated immune responses elicited by the host[64-66].

3- AIDS: The host immune system can handle the infection for a while, by replacing depleted cells to a certain extent. Nonetheless, there is a moment at which the level of $CD4^+$ T cells counts drops below 200 cells per μL of blood (**Fig. 1.5**). These levels are commonly associated with AIDS, since in this scenario the individual is fully immunosuppressed and may die due to a wide range of AIDS-associated disorders[64-66].

Despite the absence of a cure or an effective vaccine against HIV, currently available antiretroviral therapy (ART) is very effective at preventing the progression to the late stages of the disease and subsequent symptoms. Importantly, when individuals are diagnosed in the early acute phase and remain under ART treatment, the viremia can be suppressed to undetectable levels and the $CD4^+$ T cell counts can be stabilized within healthy limits for a prolonged period of time, which has immensely increased the lifespan of HIV^+ individuals as well as their life quality[67,68]

(**Fig. 1.5**). Moreover, the probability of HIV transmission from individuals controlling HIV under ART treatments is also drastically reduced by around 96%[69].

The drugs that are currently applied in ART are able to target various steps of the replication cycle of HIV. For instance, some drugs block the entry and attachment through the inhibition of gp120 or antagonism of CCR5, while other available compounds specifically inhibit the activity of the viral enzymes IN, RT or PR, impairing the processes of integration, reverse transcription or maturation, respectively[60,70-74]. However, even whilst these drugs effectively block active HIV replication, some infected cells such as memory $CD4^+$ T cells, characterized by their resting phenotype, may carry transcriptionally inactive integrated proviruses and therefore, will remain both unrecognized by the immune system as well as refractory to the action of ART. This pool of cells has been denominated as *latent reservoir* and conserves the full potential to become reactivated by a number of factors, promoting

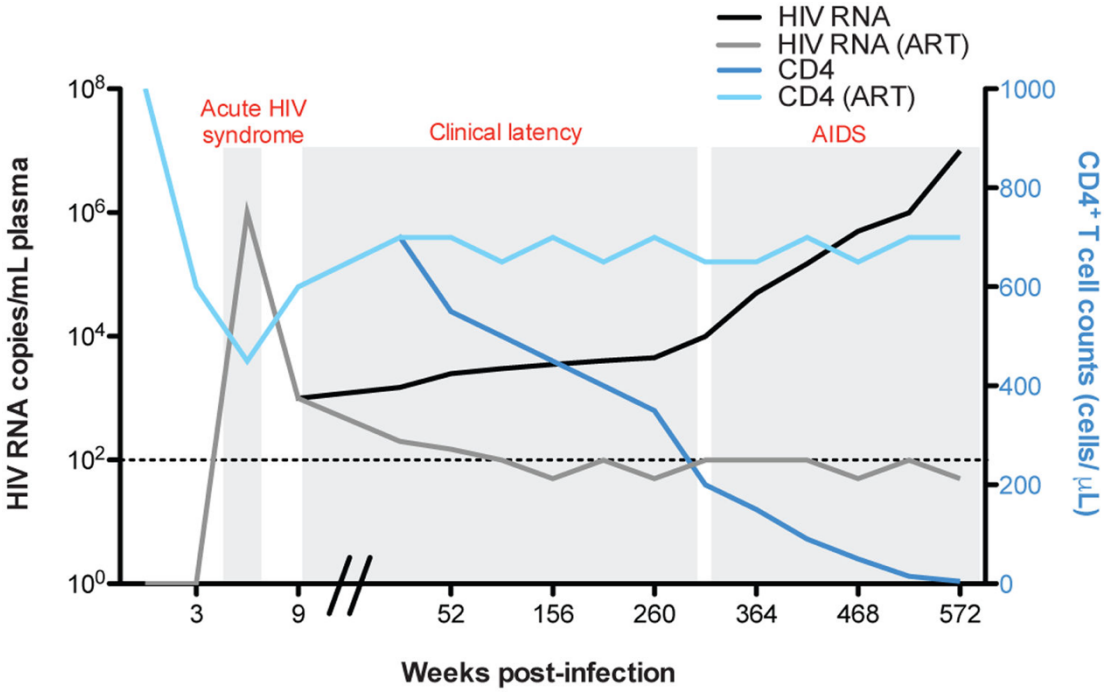

Figure 1.5. Progression of HIV infection to AIDS. Schematic representation of the different phases of HIV infection to AIDS, in the presence and absence of ART. The graph depicts the levels of viremia (HIV RNA copies/mL plasma) and $CD4^+$ T cell counts (cells/μL) over time (weeks) from infected individuals under ART regimens (grey and light blue lines) or untreated (black and dark blue lines). Figure adapted from Colomer-Lluch *et al.*, 2020.

the subsequent reactivation of the integrated provirus and, in the absence of ART, the normal progression of the infection. Hence, the discontinuation of ART is always associated with a viral rebound, which forces HIV^+ individuals to remain under these treatments uninterruptedly[45,75-77].

Importantly, life-long ART regimens not only represent a very costly burden for infected individuals, but they are also associated with several problems such as the emergence of drug-resistant strains in addition to adverse side effects or drug interactions[64,78-81]. The fact that the enzyme reverse transcriptase lacks proofreading activity increases genetic diversity and evolution, which contributes to viral escape from ART-mediated selective pressure and thus, increases the risk of drug resistance compared to other viruses[71,82]. In order to prevent this, patients are usually treated with a combination of ART (cART), further elevating the risk of potential side effects and adverse drug interactions. Fortunately, most detrimental alterations associated with HIV^+ individuals under cART are manageable, but in few occasions, they can have a significant impact on the quality of life of people living with HIV, such as premature aging or HIV-associated neurocognitive disorders (HAND), amongst others[83-85].

In spite of the fact that the benefits of current ART far exceed its drawbacks, the scientific community continuously works to improve the current treatments and search for new therapeutic approaches to lower their impact on people living with HIV, in addition to their associated costs. In this regard, some studies have recently explored the possibility of manipulating the host innate immune responses with the ultimate goal of eliminating the virus from infected individuals and/or preventing the establishment of a chronic infection[86-90]. In order to succeed in the development of these approaches, an extensive understanding of the interaction between host innate immunity, and more precisely restriction factors, and HIV countermeasure strategies against these innate barriers is needed.

Restriction factors and immune evasion

The innate immunity of the host is naturally equipped with a full set of cellular molecules capable of suppressing the replication of many pathogens, which are termed restriction factors or intrinsic resistance factors. Far from surrendering, HIV has developed a number of strategies in order to circumvent the effect of each of those restriction factors. Specific examples of the restriction factors that play a role in the defense against HIV are the cellular molecules TRIM5α, Mx2, APOBEC3, SAMHD-1, SERINC5, and BST-2[91-97].

TRIM5α. Tripartite motif-containing protein 5 is a cytoplasmic E3 ubiquitin ligase that interacts with incoming retroviral capsids to promote their proteasomal degradation. As a consequence of this, the uncoating process is accelerated and, thus, the reverse transcription is significantly impaired[92,98]. As a countermeasure to mitigate this innate restriction, the capsid protein CA of HIV has accumulated enough mutations to avoid being recognized by the human TRIM5α (hTRIM5α). Nevertheless, TRIM5α from non-human primates are still able to bind to the capsid core of HIV and to promote its degradation[99,100]. This finding has encouraged the use of genetic editing approaches to deliver non-human primate versions of TRIM5α to HIV-infected individuals, although these studies are still in the early stages of investigation.

Mx2: Myxovirus resistance 2 protein is a nuclear GTPase that regulates nucleocytoplasmic transport. This recently discovered HIV restriction factor is primarily enriched at the nuclear pores and inhibits the viral replication of primate lentiviruses by diminishing the PIC nuclear import in a CA-dependent manner. Therefore, in the same way that mutations in the CA allow HIV to prevent hTRIM5α recognition, HIV CA has also evolved to partially circumvent the effect of the restriction mediated by Mx2[96,101].

APOBEC3. Apolipoprotein B mRNA editing enzyme catalytic polypeptide-like 3 proteins belong to the family of cytidine deaminase enzymes. The APOBEC3 family

comprises eight different types of proteins (APOBEC3 A–H), being APOBEC3G (A3G) the one exerting the strongest restrictive effect on HIV replication. A3G can become incorporated into nascent HIV virions and catalyze the deamination of cytosine to uracil on the virus DNA strands that are synthesized during reverse transcription. Therefore, the incorporation of A3G in virions will only have a fitness impact in the next replication cycle. A3G causes virus hypermutation and, consequently, the reduction of the viability of the virus progeny[94,102]. However, HIV counteracts the restriction imposed by A3G through the accessory protein Vif. HIV Vif, despite lacking any catalytic activity, binds to both, A3G and the enzymatic ubiquitin ligase complex Elonging C/B-Cullin 5 to promote the poly-ubiquitination and subsequent degradation of A3G through the proteasomal pathway, thus preventing A3G incorporation into nascent virions[103].

SAMHD-1. Sterile alpha motif and histidine aspartate domain-containing protein 1 is another enzymatic restriction factor that, along with A3G, affects HIV reverse transcription. SAMHD-1 hydrolyzes the pool of cytoplasmic dNTPs into deoxynucleosides and inorganic phosphates, halting the reverse transcriptase-mediated synthesis of the provirus DNA[93,104]. In order to antagonize SAMHD-1, HIV-2 and some SIVs use the auxiliary protein Vpx, while other lentiviral lineages employ Vpr for the same purpose. Both Vpx and Vpr can interact with the CRL4 ubiquitin ligase complex and with SAMHD-1 to promote the poly-ubiquitination and proteasomal degradation of this cytoplasmic restriction factor[93,105,106].

SERINC5. Serine incorporator 5 is a transmembrane protein located at the plasma membrane. Specifically, SERINC5 and its paralog SERINC3 are enriched at locations of HIV virion assembly and release. Consequently, they can be incorporated into the envelope of nascent HIV virions. Unlike the BST-2 restriction factor (addressed in detail below), SERINC3/5 incorporation into particles does not affect virion budding, but significantly affects the entry into new target cells. Particularly, SERINC3/5 impedes the fusion between the virus envelope and the plasma membrane. Not only this activity blocks virus replication, but also increases the exposure of the non-fused

virions to the immune surveillance. Therefore, the actions of SERINC3/5 may contribute to the immune clearance of these trapped virions as well as the cells surrounded by them[97,107,108]. As a result of this selective pressure, HIV has evolved two distinct mechanisms to overcome SERINC5 and SERINC3-mediated barriers. On the one hand, HIV uses Nef to decrease the surface levels of these restriction factors and, consequently, it reduces the incorporation of these molecules into nascent HIV virions[97,109]. Not only Nef enhances virion infectivity by preventing virion incorporation of SERINC3/5, but it has also been reported that the relative strength of Nef to counteract SERINC3/5 is proportionally related with the prevalence of the different primate lentiviral species in their natural habitats[107]. On the other hand, some strains of HIV-1 have evolved Env to evade SERINC5, which may work in combination with Nef. Although these Env proteins do not promote the downregulation of SERINC5, and thus, SERINC5 is still present in virions, they exhibit a higher fusogenicity, which compensates for SERINC5 actions[110].

BST-2. Bone marrow stromal antigen 2, also called Tetherin, is a transmembrane protein with the ability to trap or tether HIV viral particles during their budding process. By virtue of keeping one domain anchored to the plasma membrane and the other one attached to the envelope of budding virions, this protein prevents the release of viral particles and halts the propagation of the infection[95,111]. In this regard, primate lentiviruses have evolved three different strategies in order to antagonize BST-2. Firstly, HIV-1 uses its accessory transmembrane protein Vpu to downregulate the levels of BST-2 from the plasma membrane. The transmembrane portion of Vpu interacts with BST-2 transmembrane domain, promoting BST-2 downregulation from the cell surface and subsequent degradation through both the lysosomal as well as proteasomal pathways[95,111,112]. HIV-2 and some SIVs do not encode a *vpu* gene and have evolved different strategies to counteract BST-2. Whereas HIV-2 uses Env, the majority of the SIVs use the accessory protein Nef to downregulate the surface levels of this restriction factor[51,113-115]. Of note, certain HIV-1 isolates seem to also use Nef instead of Vpu to counteract BST-2[116]. Therefore, due to the multiple roles of Nef in counteracting restriction factors such as BST-2, SERINC5, SERINC3, as well as other

immune related components, which will be discussed further below, this accessory protein is considered a central player in the HIV-mediated evasion of the immune system.

Nef

The HIV protein Nef is an accessory protein that deserves special attention when studying the ability of this virus to counteract host antiviral responses. Although this auxiliary protein is not essential for viral replication *in vitro*, it is crucial for viral success *in vivo*[48,117]. Nef possesses the ability to mediate the internalization and degradation multiple cell surface molecules with antiviral activity, playing a crucial role in host immune evasion. In the first place, Nef is able downregulate the surface levels of BST-2, SERINC3 and SERINC5, which is linked with HIV infectivity and pathogenesis [48,97,113,118]. In addition, HIV Nef is able to prevent immune surveillance by depleting various cell surface receptors associated with immune activation such as CD4, CD3, CD28, MHC-I and MHC-II[119-124]. Structurally, Nef is a small (25-34 KDa) and promiscuous protein able to interact with a fairly large number of molecules through different motifs that are distributed along its four domains: N-terminus, Globular core, Flexible loop and C-terminus[125] (**Fig. 1.6**). Although the primary sequence of Nef differs amongst primate lentiviral species, its functional domains are preserved[125-127]. The N-terminal domain is post-translationally modified by the addition of a myristoyl group at Gly_2, allowing Nef to bind to cellular membranes. Its membrane association allows Nef to interact with the different immune related surface molecules[125]. Furthermore, Nef harbors motifs that interact with multiple components of the intracellular trafficking network, driving the endocytosis, re-localization and even degradation of the molecules that Nef interacts with. Nef achieves this by hijacking the vesicular trafficking system through the direct association with AP-1, AP-2, AP-3, COP-I and PACS-1[122,125,128,129]. These interactions allow Nef to modulate the intracellular traffic at the plasma membrane, endosomes, lysosomes, Golgi apparatus and endoplasmic reticulum (ER), with the ultimate goal of counteracting different host-imposed restrictions.

One of the most recent properties attributed to Nef is its ability to interfere with the machinery of the immune-related pathway of autophagy[130-132]. In addition to this effect of Nef, other studies have reported that HIV has developed different strategies to intersect with this pathway through other viral proteins such as Tat, Vif or Env, suggesting that autophagy might be playing an important role in the replication cycle of HIV[133-135]. However, whereas the general antiviral activity of autophagy is well established, its capacity as a restriction factor for HIV has not yet been fully explored. Therefore, a deeper understanding of the untapped potential of autophagy in the fight against HIV is imperative.

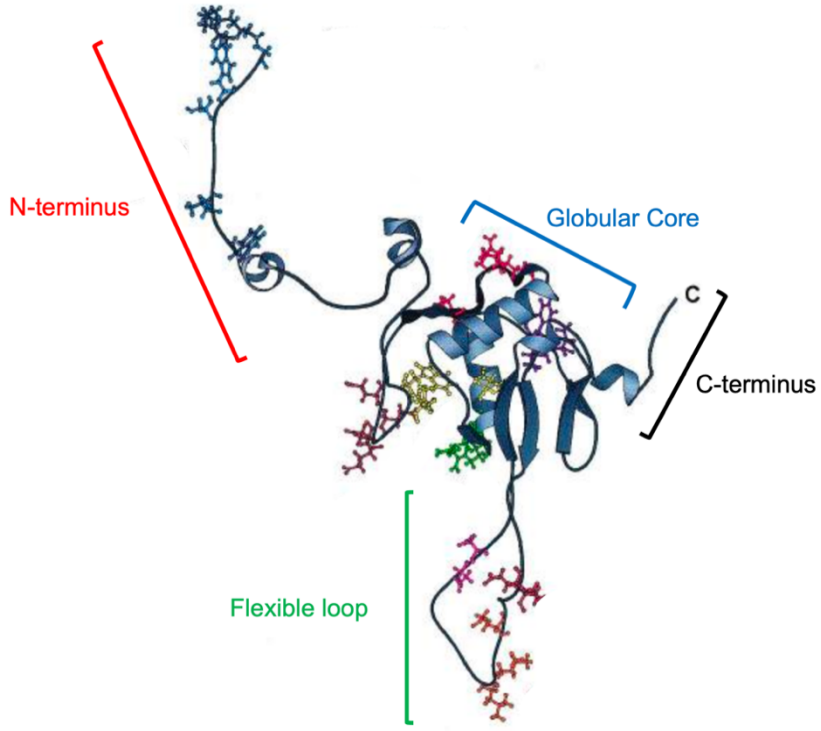

Figure 1.6. HIV-1 Nef structure and domains. Figure adapted from Geyer *et al.*, 2001.

Autophagy

Machinery

Etymologically the word autophagy comes from the two Greek words “auto” and “phagos”, which mean “self-eating”. Autophagy is a degradative process essential

for cell quality control and is characterized by the recruitment and delivery of intracellular targets to lysosomes for their degradation. Autophagy is activated under conditions of stress such as cell starvation or infections. The autophagic cargo is engulfed in specialized vesicles called autophagosomes, which eventually fuse with lysosomes to promote the degradation of their content. Importantly, the autophagy machinery is highly conserved among all eukaryotic organisms, which already denotes the relevance of this pathway[136-140]. Interestingly, in 2016, Dr. Yoshinori Ohsumi received the Nobel Prize in Physiology and Medicine for his work on elucidating the components and underlying mechanisms for the regulation of the autophagy machinery.

The multi-step process of autophagy, also known as macroautophagy (hereafter autophagy), orchestrates more than 30 autophagy-related proteins (ATG) to mediate (1) the activation and formation of double membrane vesicles (autophagosomes), (2) the recruitment of selective cargo, and (3) its final delivery to lysosomes, where the degradation of the targeted substrates and the inner membrane of the autophagosomes will take place[136,138] (**Fig. 1.7**). Autophagy consists of three stages: initiation, elongation and maturation.

Initiation. Several factors can trigger autophagy such as the absence of amino acids (starvation), intracellular pathogens, or the pharmacological action of drugs like rapamycin[138,141-143]. These stimuli have something in common, they all lead to the inhibition of the pleiotropic molecule mTOR (Mammalian Target of Rapamycin)[140,144]. The kinase mTOR inhibits by default the initiation of the pathway through the phosphorylation and inactivation of ULK1, one of the initiators of autophagy[145]. ULK1 is responsible for the phosphorylation and activation of BECN1/Beclin-1, which is a master regulator of autophagy with a crucial role in the isolation of membranes to form autophagosomes. BECN1 binds to the enzymatic complex class III phosphatidylinositol 3 kinase complex 1 (Class III PtdIns3K C1) at the initiation sites, which in the vast majority of the cases is the surface of the ER[132,146-148]. The class III PtdIns3K C1 generates phosphatidylinositol 3-phosphate

(PtdIns3P) at these locations, which in turn, recruits PtdIns3P-interacting proteins required for the for nucleation of a double membranous structure called phagophore, used as a primer for the formation of autophagosomes (**Fig. 1.7**). One of the PtdIns3P binding partners is the ZFYVE1/DFCP-1 protein, which is involved in the nucleation and curvature of the phagophore. Additionally, PtdIns3P also recruits an E3-like enzymatic complex formed by the E1 activating enzyme ATG7, the E2 conjugating enzyme ATG3 and the E3 ligase ATG-12-ATG5-ATG16L1[146,149-151]. This complex mediates a key reaction in the autophagy pathway: the conjugation of phosphatidylinositol ethanolamine (PE) to the microtubule associated protein 1 light chain 3 (MAPILC3 or LC3), converting the inactive isoform of LC3 (LC3-I) into the autophagy-competent LC3-II isoform. LC3-II is found on both, the inner as well as the outer membrane of the autophagosomes. LC3 is encoded by the gene *MAPILC3B* and is synthesized first as proLC3, which is instantly cleaved to generate the cytosolic isoform LC3-I. Upon autophagy activation, LC3-I is lipidated and converted into LC3-II. Membrane-associated LC3-II plays a very important role in the elongation of autophagosomes, cargo recruitment and final fusion with the lysosome[136,138] (**Fig. 1.7**). Furthermore, intracellular levels and relative abundance of LC3-I and LC3-II are one

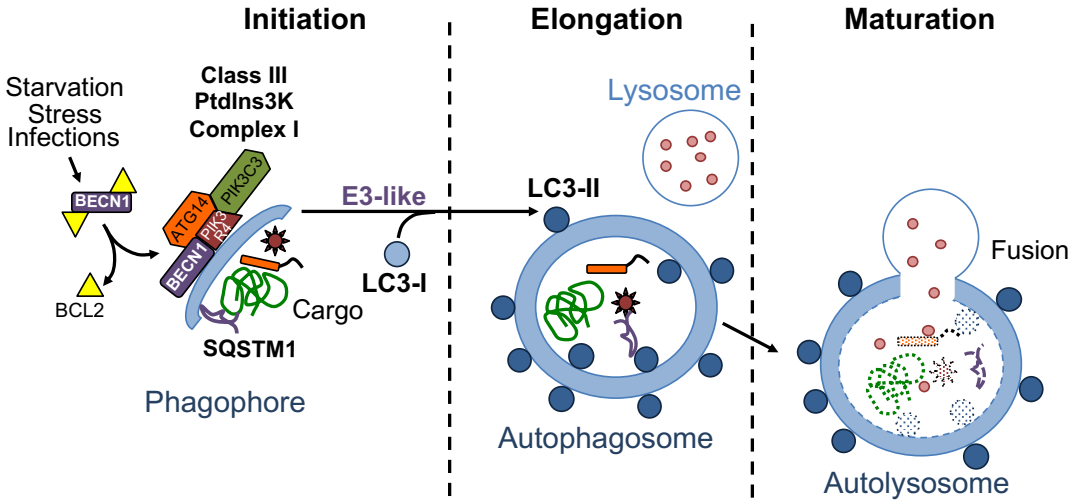

Figure 1.7. Schematic diagram of the autophagy pathway. Representation of the main steps of autophagy as well as molecules that play an important role in the progression of this pathway, and are relevant to this study. Figure adapted from Castro-Gonzalez *et al.*, 2020.

of the main indicators used to study and measure autophagy flux, being LC3-II the only protein reliably present on the autophagosome[152-154].

Besides BENC1 and LC3, BCL2 is another regulatory molecule that, although not included in the list of ATG proteins, plays a crucial role in the initiation of autophagy. BCL2 is able to inhibit this pathway by directly binding to the BCL2 Homology domain 3 (BH-3 domain) in BECN1, preventing thereby the association of BECN1 with the class III PtdIns3K C1 necessary for the formation of autophagosomes[155-157] (**Fig. 1.7**). The association between BCL2 and BECN1 is mainly regulated by two post-translational modifications on BCL2. On the one hand, autophagy stimuli can lead to the phosphorylation of this protein, which promotes its dissociation from BECN1 and thus, the activation of the first stages of autophagy. Conversely, the ubiquitination of BCL2 is associated with the inhibition of autophagy. Specifically, the E3 ubiquitin ligase PRKN/Parkin mediates the mono-ubiquitination of BCL2, which enhances BCL2 association with BECN1 and, therefore, further prevents BECN1 from associating with the class III PtdIns3K C1[158-160].

Elongation. The expansion and curvature of the autophagic double membrane is a complex process that involves more than 20 ATGs, yet ultimately achieved by the ATG12–ATG5 ubiquitin-like complex. For this, ATG12–ATG5 recruit intracellular membranes to the elongation site. The expansion of the autophagosome double membranes is coupled and assisted by the lipidation and incorporation of LC3-II to the forming vesicles. The recruitment of cargo also takes place during the elongation phase[138,139]. Targets for autophagy are usually poly-ubiquitinated proteins and large structures, such as viral capsids or damage mitochondria (mitophagy), which are recognized by different autophagy receptors[161-164]. These receptors or adaptor proteins work as a bridge between poly-ubiquitin tagged substrates and the LC3-II molecules found on the inner membrane of the growing autophagosomes. In this regard, sequestosome-1 (SQSTM1), also known as p62, is one of the main adaptor proteins, which works together with other autophagy receptors such as Optineurin or NBR1. This set of proteins is responsible for substrate recognition and sequestration, but

provides additional structural support for the formation and final enclosure of autophagosomes[164-167] (**Fig. 1.7**).

Maturation. This last stage involves the fusion between the autophagosome and a lysosome creating the so-called autophagolysosome or autolysosome. This fusion is regulated by many different proteins involved in vesicle biogenesis and vesicle trafficking, including GTPases, the ESCRT family and the enzymatic complex class III phosphatidylinositol 3 kinase complex 2 (Class III PtdIns3K C2)[168-170]. This Class III PtdIns3K complex 2 is very similar to the complex 1 described earlier, which is required for autophagy initiation. However, whilst both complexes have the proteins BECN1, Vps34 and Vps15 in common, complex 1 and complex 2 differ by one molecular subunit. Complex 1 harbors ATG14L while complex 2 carries UVRAG, which are responsible for the differential membrane targeting of both complexes (ER vs. autophagosome)[171,172]. Once the fusion between autophagosomes and lysosomes is accomplished, the autophagosome cargo is degraded due to the action of the lysosomal acid hydrolases (**Fig. 1.7**). Moreover, the inner membrane of the autophagosome and the associated proteins LC3-II and SQSTM1 are degraded along with the cargo. Hence, the relative levels of SQSTM1 are also informative when studying autophagy progression and execution[152,153,173].

Autophagy and immunity

The potential of autophagy to target specific intracellular components to the lysosomes equips cells with the ability to: first, maintain homeostasis and quality control through the degradation of different molecules, structures and damaged organelles in stress situations, working as a 'Recycling Factory' within the cell, and second, target intracellular pathogens, such as viruses, for lysosomal degradation[136-138,163,174]. Therefore, autophagy is considered an essential pathway for the immune system, and thus, its deficiency is associated with a multitude of pathologies, including cancers, cardiovascular diseases, neurodegenerative disorders, aging and infectious diseases[175-178].

Autophagy is associated with different components of the innate sensing system. Eukaryotic cells are equipped with a set of pattern recognition receptors (PRR) capable of detecting various damage-associated molecular patterns (DAPMS) and pathogen-associated molecular patterns (PAMPs), which ultimately trigger the activation of different innate immune pathways, including autophagy, to employ their protective capacity in stress situations. For instance, in the context of an intracellular infection, autophagy restriction does not merely cause the direct degradation of microbial structures, but also assists in mounting a more effective immune response against invading pathogens in a 'multi-hit' process[143,179,180]. The autophagosome-associated degradation of pathogens results in the generation of residual molecules (antigens) that activate additional immune responses through the association of these antigens with both, cytoplasmic PRRs as well as the antigen-presenting complexes MHC-I and MHC-II, which present these molecules as non-self structures for their recognition by immune cells[180,181]. Therefore, autophagy activation helps elicit both innate and also adaptive immune responses against intracellular parasites.

The involvement of autophagy in the activation of innate responses through the engagement of PRRs leads to pro-inflammatory responses that are linked to the selective production of the immune regulatory molecules known as cytokines. For instance, autophagy has been shown to boost the activation of the toll-like receptor 3 (endosome-associated PRR) by its engagement with the genomic RNA of Influenza A virus (IAV), leading to the secretion of the cytokine TNFα and thus, the amplification of the pro-inflammatory response necessary for the elimination of this virus. Conversely, autophagy can also mediate the degradation of signaling substrates from different pathways in order to downregulate the production of a particular pro-inflammatory cytokine once the response is over, preventing the potential damage associated with the overstimulation of inflammatory responses[180,182-184].

The autophagy-mediated breakdown of virus structures additionally provides a source of antigens to be loaded onto MHC-I and MHC-II molecules. MHC-I molecules are present on the surface of all human cells, where they are continuously

presenting cellular peptides to allow their recognition as "self" structures to the Natural Killer (NK) cells. This represents a strategy to show that the presenting cells are healthy. However, if the MHC-I molecule is presenting a non-self peptide, maybe derived from autophagy-mediated degradation of a virus pathogen, the engagement of the MHC-I with the NK cell results in the killing of the presenting cell, since it is considered infected. MHC-I molecules loaded with non-self peptides can also be recognized by specialized $CD8^+$ T cells (cytotoxic lymphocytes), which can promote the direct elimination of the infected cells. MHC-II molecules are only present in a subset of immune cells denominated antigen-presenting cells (APC) that includes B cells, macrophages and dendritic cells. $CD4^+$ T cells are responsible for recognizing MHC-II loaded with non-self peptides presented by APCs. This association in turn, promotes the stimulation and regulation of the activity of other immune cells, such as the antibody-secreting B cells, in order to mount and modulate a more tailored antibody-based response (adaptive immunity) that facilitates the clearance of the pathogen and, in most cases, provide immunity for future encounters with the same pathogen[179-182,185]. In this regard, different studies have described how the autophagy-mediated degradation of viral proteins from Influenza or Epstein Barr viruses has a proportional effect on antigen recognition by $CD4^+$ T cell and further humoral responses against these viruses[186,187]. Therefore, autophagy plays a pivotal role in the successful activation and modulation of the immune system when fighting viral infections.

Autophagy and HIV

The well-established protective effect of autophagy in the context of viral infections has led the scientific community to consider the pharmacological manipulation of this pathway as a strategy to enhance current therapeutic options[188-190]. Numerous studies have described the restrictive role of autophagy in the replication cycle of many viruses, including Chikungunya virus (CHIKV), Herpes Simplex virus type 1 (HSV-1) or West Nile virus (WNV), among others[189,191-193]. In response to the selective pressure posed by autophagy, some of these viruses have developed a variety of strategies to circumvent the autophagy-mediated restriction. For

example, HSV-1 synthesizes the protein ICP34.5 that binds to BECN1 and thereby inhibits the initiation of autophagy[194]. In line with this observation in HSV-1, the Kaposi's sarcoma-associated herpesvirus (KSHV) encodes for a viral homolog of BCL2 (vBCL2) that reinforces the anti-autophagic efforts of the endogenous BCL2 at preventing BECN1-dependent activation and initiation of autophagy[195]. Surprisingly, some other viruses have acquired the ability to hijack the autophagy machinery for their own replicative benefits. One example is the zika virus (ZIKV), which deliberately activates autophagy through the inhibition of the Akt-mTOR signaling to promote viral propagation. Although the mechanism is not yet understood, autophagy seems to facilitate ZIKV particle release by enhancing certain vesicle secretory pathways[196,197]. Similarly, some positive sense ssRNA viruses like MERS-CoV, SARS-CoV and possibly SARS-CoV-2 exploit autophagy by usurping autophagosomes for the creation of double membranous structures that work as viral replication factories or viroplasms[198-201]. Yet, in order for this strategy to be successful, the full potential of the autophagic machinery needs to be avoided. In the case of MERS-CoV, the virus protein SKP2 is able to impede the final formation of autophagolysosomes and associated degradation[202]. In contrast, SARS-CoV achieves the modulation of autophagy through the action of the virus protein NSP6 that, whilst increasing the number of autophagosomes, bypasses the detrimental effect of autophagy by drastically limiting the size of such autophagosomes[201,203]. Therefore, the pharmacological inhibition of these virus proteins would render them susceptible to autophagic degradation and thus, significantly attenuate their infection[202,204].

As proposed for other viruses, exploiting the autophagy machinery with antiviral purposes in the battle against HIV is an attractive strategy. However, the role of this pathway in the context of an HIV infection still remains uncertain. Whereas extensive research has been conducted on this subject, the conclusions drawn seem very scattered and, in some cases, conflicting. On the one hand, some studies defend that HIV induces autophagy to enhance viral replication[130,205,206]. On the other hand, numerous investigations uphold the restrictive role of autophagy in HIV replication. Supporting this position, we find different reports describing the role of TRIM5α in

restricting HIV by promoting the autophagic degradation of incoming viral capsids[207-209]. Furthermore, the viral proteins Vif and Tat have been reported as targets for autophagy elimination, which consequently impairs virus infectivity and propagation[210,211]. Other studies have reported that, as a consequence of this, HIV has evolved Nef, Vif and Env to inhibit autophagy and support virus replication[130,131,133,134]. The controversial reports on the role of autophagy in HIV infection are exacerbated even further when investigating cell specific molecular interactions between HIV and autophagy. For example, whereas Env is able to stimulate autophagy in bystander $CD4^+$T cells, it can inhibit this pathway in dendritic cells[134,183]. Similarly, Tat has been shown to down-regulate autophagy in neurons but is also reported to activate it in glial cells[135,206]. Therefore, a deeper understanding of the interplay between HIV and autophagy is utterly required in order to settle the current controversial situation and, consequently, evaluate the potential manipulation of autophagy in future antiretroviral therapeutic designs.

CHAPTER 2

OBJECTIVE

The main objective of this thesis is to analyze the association between HIV and autophagy using a comprehensive approach across different cell types in order to assess the overall effect of autophagy on HIV replication and to characterize the potential HIV-mediated manipulation of this molecular pathway.

CHAPTER 3

PRELIMINARY DATA AND HYPOTHESES

The figures presented in this chapter are derived from the following publication[1] in which I am first author and I have permission from the journal editorial to reproduce the figures in this thesis.

Sergio Castro-Gonzalez, Yuhang Shi, Yuexuan Chen, Marta Colomer-Lluch, Jayc Waller, Ying Song, Anju Bansal, Frank Kirchhoff, Konstantin Sparrer, Chengyu Liang and Ruth Serra-Moreno. HIV-1 Nef counteracts autophagy restriction by enhancing the association between BECN1 and its inhibitor BCL2 in a PRKN-dependent manner. *Autophagy*, 1-25, doi:10.1080/15548627.2020.1725401 (2020).

Despite the high degree of conservation of the autophagy machinery among eukaryotic organisms, the study of this system becomes specially challenging when working on different cell types, mainly due to the high dynamism of this pathway and the large number of underlying factors that can modulate its activation and progression[138,152]. Therefore, the first approach in this thesis was aimed at evaluating (i) autophagy's sensitivity to pharmacological stimulation and (ii) the basal autophagy levels in different cells frequently used in HIV research, such as HEK293T, Jurkat $CD4^+$ T cells, THP-1 monocytes, THP-1 derived macrophages and primary $CD4^+$ T cells. Unlike the rest of the selected cell types, HEK293T are not natural target cells for HIV. However, HEK293T cells are one of the most universally used human cell lines in cellular and molecular biology research due to their reliable growth and high transfection efficiency. Secondly, the lab-generated cell lines Jurkat $CD4^+$ T cells and THP-1 monocytes represent a very useful tool for the study of HIV, since they are human immortalized cell lines as well as natural HIV target cells. Lastly, the primary $CD4^+$ T cells were obtained from human peripheral blood mononuclear cells (PBMC) from healthy donors and therefore, they constitute the most physiological cell model in these experimental approaches. However, primary cells present a couple of limitations. First, the source from different individuals increases variability in results. Second, they have a limited number of divisions that often complicates experimental design. Each of these cell types were treated with the autophagy-activating drug rapamycin, at different concentrations and time exposures. Next, we assessed the activation of autophagy by measuring the relative conversion of LC3-I into LC3-II (LC3 lipidation)

and concomitant reduction of the relative abundance of SQSTM1, using western blot analysis. (**Fig. 3.1**). From these analyses we learned that these cell types exhibit a different degree of responsiveness to rapamycin stimulation as well as different basal levels and kinetics of autophagy. For instance, the increase in LC3 lipidation and associated SQSTM1 decline in HEK293T cells is clearly evident with relatively low doses and short exposure times to rapamycin (**Fig. 3.1A**). This denotes their higher capacity to respond to the drug compared to other cell types such as the $CD4^+$ T cells, which required higher doses and longer incubations with rapamycin in order to

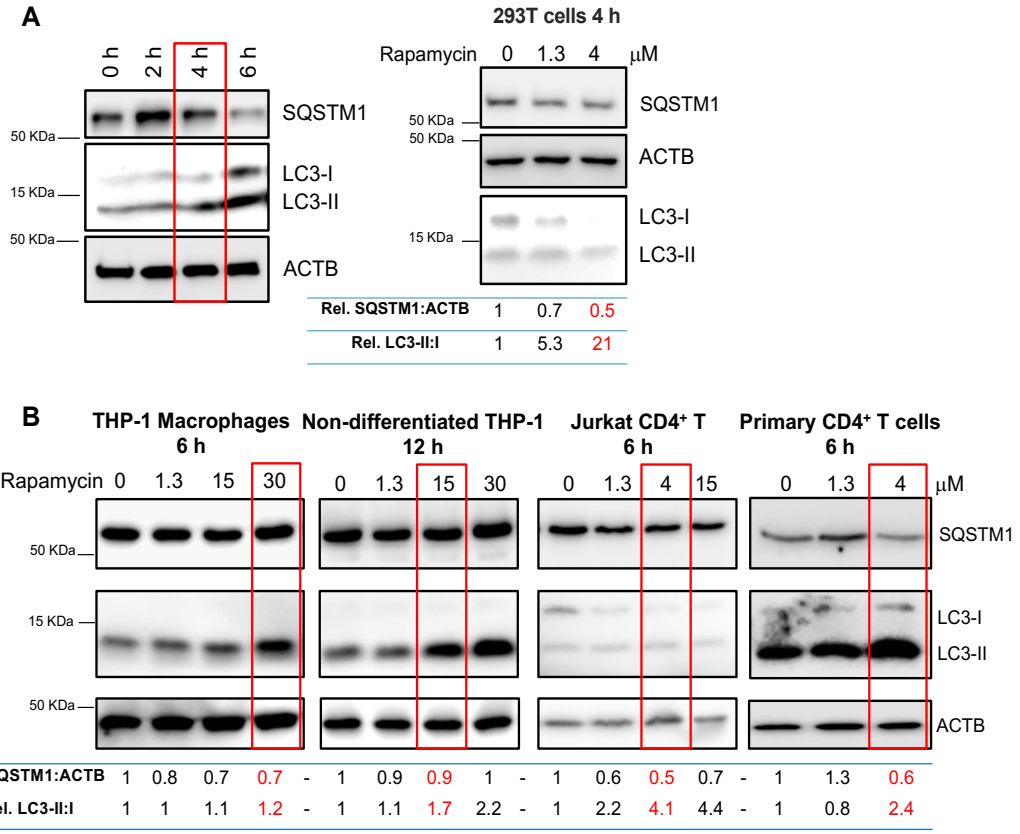

Figure 3.1. Cell-specific differences in the activation of autophagy in response to rapamycin. (**A, B**) Representative data of HEK293T cells, THP-1-derived macrophages, non-differentiated THP-1 monocytes, Jurkat $CD4^+$ T cells, and primary $CD4^+$ T cells showing their threshold and sensitivity to autophagy activation. Cells were treated with rapamycin (0-30 µM) at different time exposures (0-12 h). Cell lysates were analyzed by western blot for the autophagy markers SQSTM1, LC3, and the housekeeping protein ACTB/β-actin. Densitometric analyses were performed to determine the ratios of LC3-II over LC3-I as well as the SQSTM1:ACTB levels relative to the no-rapamycin treatment. Red boxes indicate optimal conditions for autophagy activation. Images are representative of 3 independent experiments.

achieve a rather moderate activation of autophagy (**Fig. 3.1B**). Interestingly, when comparing immortalized (Jurkat) and primary $CD4^+$ T cells, we found that primary $CD4^+$ T cells displayed higher endogenous levels of LC3-II than Jurkat cells, and additionally, Jurkat cells seemed to be more responsive to rapamycin stimulation, since they exhibited a more robust increase in the LC3-II:LC3-I ratio under the same treatment conditions (**Fig. 3.1B**).

Since primary $CD4^+$ T cells were activated and expanded (using anti-CD3/anti-CD28 antibodies and IL2, respectively) prior to their treatment with rapamycin, the relative high levels of LC3-II detected in these cells might be due to the major regulatory functions autophagy plays during T cell activation and proliferation[212,213]. Similarly, non-differentiated as well as macrophage-differentiated THP-1 cells exhibited very elevated basal levels of autophagy, indicated by the inherently high amounts of LC3-II and almost undetectable LC3-I (**Fig 3.1B**). Their high innate autophagy activation is in line with their high lysosomal function and their phagocytic nature[187]. In consequence, non-differentiated and THP-1-derived macrophages required higher doses (10 and 20 times more than the HEK293T cells, respectively) and longer exposure (6 and 12 h) with rapamycin in order to further increase their autophagic profile, which is evidenced by a moderate increment in LC3-II (**Fig. 3.1B**). Altogether these observations contribute to our better understanding of the differential autophagy dynamics in each of these cell types, which becomes of particular importance when using these cells to understand the interactions between HIV and autophagy.

Due to their high responsiveness to autophagy stimulation and their high transfection efficiency, our initial experiments were carried out in HEK293T cells. In order to have an unbiased evaluation of the interplay between HIV and autophagy, we transfected HEK293T cells with the full-length provirus DNA of the HIV-1 molecular clone NL4-3 as well as different mutants of this clone – of note, proviral transfections allow all post-integration events of the replicative cycle of HIV. As controls, we included cells transfected with an empty retroviral vector and untransfected cells that were either DMSO-treated (mock) or treated with rapamycin. 48 h post-transfection, we analyzed the effects of NL4-3 on autophagy by monitoring the autophagosome

markers LC3 and SQSTM1 using western blot; the levels of ACTB/β-actin and HIV Gag (p55 and p24) were used as loading control and proviral transfection control, respectively. (**Fig. 3.2**). As expected, mock treated cells exhibited very low levels of autophagy activation, with most LC3 detected as LC3-I and very high levels of SQSTM1. By contrast, cells treated with rapamycin displayed a significant transition to LC3-II and some decrease in SQSTM1 (**Fig. 3.2**). Consistent with the role of cytosolic DNA in triggering autophagy through the engagement of PRRs[214,215], autophagy was potently induced in all the transfected cells, particularly with the empty retroviral vector. In this case, we observed a prominent conversion of LC3-I into LC3-II (almost no detectable LC3-I) and a significant decay of SQSTM1 (**Fig. 3.2**). Contrary to the empty vector control, cells transfected with HIV NL4-3 were

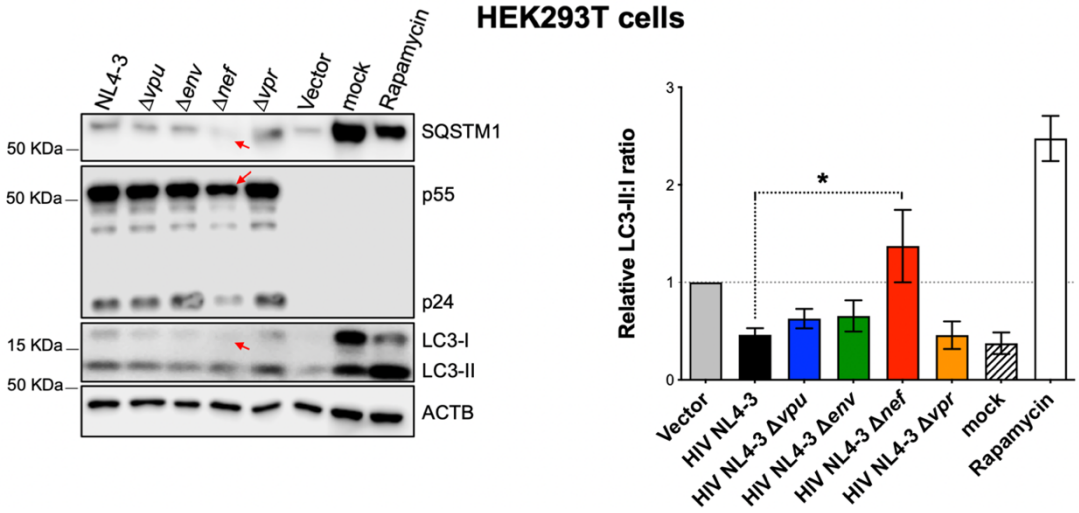

Figure 3.2. HIV Nef effect on autophagy progression in HEK293T cells. Left panel: HEK293T cells were transfected with the full-length proviral DNA of HIV-1 NL4-3, different mutants of this molecular clone (Δ*vpu*, Δ*env*, Δ*nef* and Δ*vpr*), or an empty retroviral vector. As controls for autophagy, cells were treated with 4 μM of rapamycin or mock (DMSO) for 4 h. 48 h post-transfection, cells were lysed and analyzed by western blot for SQSTM1, Gag (p55 and p24), LC3 and ACTB/β-actin. Right Panel: Densitometric analyses were performed to determine the ratio of LC3-II over LC3-I relative to the empty vector control. Data represent the mean and standard error of the mean (SEM) from 4 independent biological replicates. *: $p \leq 0.05$. Red arrow indicates decreased Gag and SQSTM1 levels as well as rapid LC3-I-to-LC3-II transition.

characterized by an impairment in the progression of autophagy, since the conversion rate of LC3-I into LC3-II (LC3-I was still detected) and the concomitant degradation of SQSTM1 was reduced (**Fig. 3.2**). These observations indicate that HIV impacts autophagy flux. Similar results were observed with the HIV NL4-3 mutants, except for HIV Δ*nef*. In the absence of a functional *nef* gene, the ability to restrain autophagy was lost, and thus, the relative levels of LC3 lipidation and SQSTM1 were similar to those seen in the empty vector transfected cells, indicating a normal activation and transition of autophagy. Interestingly, this normal progression of autophagy in the absence of *nef* is associated with a decrease in the expression of the HIV protein Gag (**Fig. 3.2; red arrows**). We consistently obtained similar findings in all four biological replicates, in which we measured the progression of autophagy by calculating the LC3-II:I ratios relative to the empty retroviral vector (**Fig. 3.2; right panel**). Samples where the relative LC3-II:I ratios were <1 represent conditions in which autophagy had not been activated (i.e., mock) or where autophagy had been impaired (in the presence of Nef). By contrast, samples where the relative LC3-II:I ratios were equal or >1 represent conditions of autophagy activation (i.e. treated with rapamycin or in the absence of

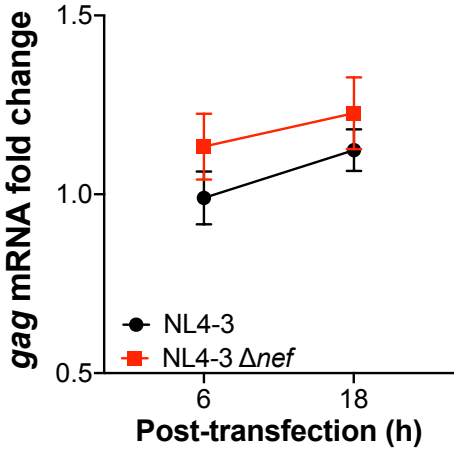

Figure 3.3. The reduction of Gag in HIV Δ*nef* is not due to transfection deficiencies. HEK293T cells were co-transfected with the proviral constructs of HIV-1 NL4-3 and HIV-1 NL4-3 Δ*nef*. 6 and 18 h post-transfection, cells were lysed, total RNA was extracted, converted to cDNA by reverse transcription, and analyzed for the mRNA levels of *gag* relative to the first time point of HIV-1 NL4-3, after normalization to *GAPDH*. Data represent the mean and standard error of the mean (SEM) from 3 independent biological replicates.

Nef) (**Fig. 3.2; right panel**). After ruling out by qPCR that this reduction in Gag in the absence of *nef* is not a consequence of differences in transfection efficiencies (**Fig. 3.3**), we concluded that autophagy might be posing a reciprocal inhibitory effect on HIV by targeting the virus protein Gag for autophagy-mediated clearance.

To investigate the reproducibility of this phenotype in HIV target cells, we infected Jurkat $CD4^+$ T cells, THP-1-derived macrophages, and primary $CD4^+$ T cells with wild type HIV-1 NL4-3 or NL4-3 Δ*nef*. In the case of the macrophage infection, we VSV-G pseudotyped NL4-3 Δ*env* and NL4-3 Δ*env*Δ*nef* to allow the infection of these cells, since the gp120 protein in the NL4-3 clone does not exhibit tropism for macrophages. We collected cell lysates at different time intervals to assess Gag, Nef, LC3, SQSTM1, and ACTB levels, and we calculated the ratios of LC3-II:I relative to the first time point. This normalization allowed us to compare the effect of HIV on autophagy among the different cell types (**Fig. 3.4**). Although macrophages and T cells differ in their sensitivity to autophagy triggers, and they exhibit differences in their basal levels of LC3-II (**Fig. 3.1B**), the impact of Nef on autophagy activation/progression remained evident in these cells. In the case of the Jurkat cells, the accumulation of LC3-I, and thus the defect in the emergence of LC3-II, was obvious at 48 h post-infection, which coincided with the time when Nef expression became apparent. However, cells infected with *nef*-deficient viruses showed normal transition of LC3-I to LC3-II, faster decline of SQSTM1 over time, and lower Gag expression levels compared to cells infected with the wild type virus (**Fig. 3.4A; western blots**). We obtained similar results in all 3 biological replicates, in which we found a significant reduction in the relative LC3-II:I ratios for cells infected with *nef*-competent viruses, particularly at the later time points (**Fig. 3.4A; graphs**).

We had similar observations in macrophages. Although these cells have inherently high basal levels of LC3-II, and the VSV-G pseudotyped viruses are restricted to one cycle of infection, macrophages infected with viruses harboring a functional *nef* gene showed detectable levels of LC3-I compared to cells infected with *nef*-defective viruses (**Fig. 3.4B; red arrows**). This result caused, in turn, a reduction in the LC3-II:I

ratios. The Nef-mediated impairment in the emergence of LC3-II was also accompanied by higher levels of SQSTM1, indicating that the presence of Nef hindered autophagy. Accordingly, the levels of Gag (p55) normalized to ACTB were lower in cells infected with NL4-3 Δ*env*Δ*nef* than NL4-3 Δ*env*-infected cells (**Fig. 3.4B; western blot**). Consistent with the data obtained in HEK293T and Jurkat cells, the differences in the relative LC3-II:I ratios were statistically significant between *nef*-competent and *nef*-defective viruses (**Fig. 3.4B; graph**).

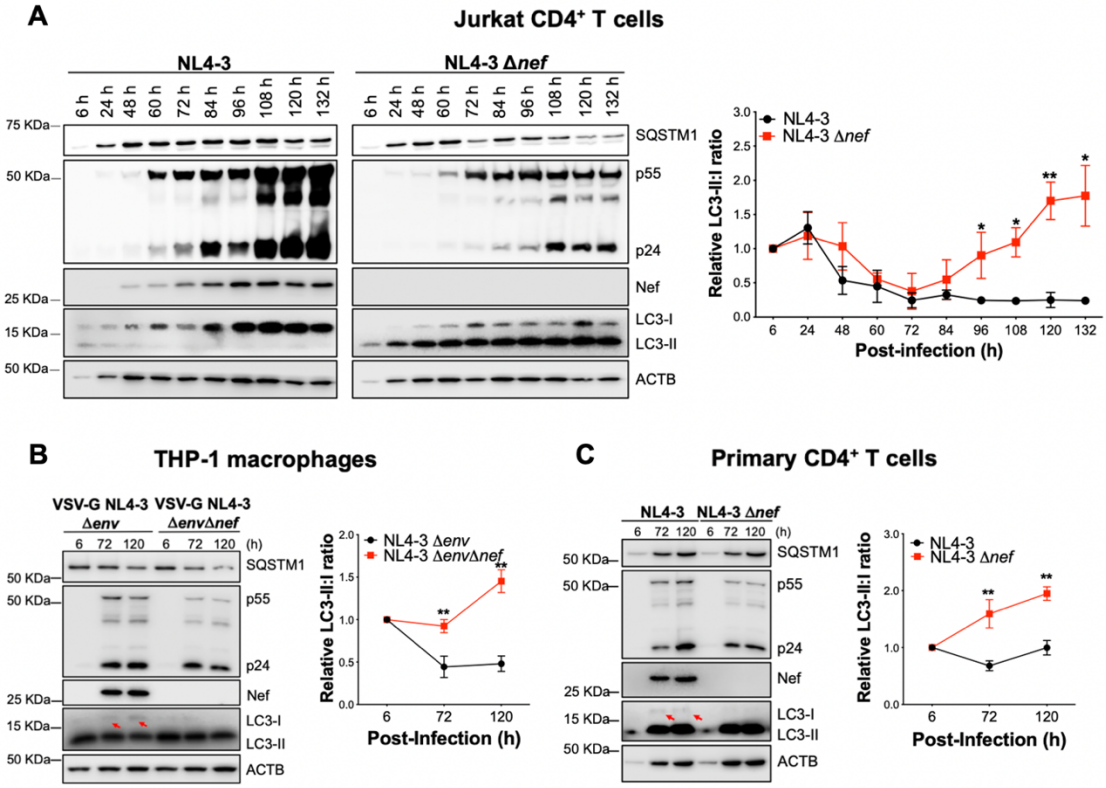

Figure 3.4. Effect of HIV-1 Nef on autophagy progression in target cells. (**A**) Jurkat CD4$^+$ T cells, (**B**) THP-1-derived macrophages and (**C**) primary CD4$^+$ T cells were infected with 100 ng of p24 equivalents of HIV-1 NL4-3 or HIV-1 NL4-3 Δ*nef*. In the case of macrophages, infections were performed with VSV-G pseudotyped HIV-1 NL4-3 Δ*env* or HIV-1 NL4-3 Δ*env*Δ*nef*. Cell lysates were collected at the indicated time intervals and analyzed by western blot for SQSTM1, Gag (p55 and p24), Nef, LC3, and ACTB (left panels). The right panels correspond to the mean and SEM of 3 independent experiments showing the ratios of LC3-II:I over time relative to the first data point, which were calculated by densitometric analyses. *: $p \leq 0.05$; **: $p \leq 0.01$. Red arrows in panels A and B indicate the accumulation of LC3-I.

As indicated earlier, primary $CD4^+$ T cells exhibit high autophagy activation, reflected by elevated LC3-II (**Fig. 3.1B** and **3.4C**). Although the prominent expression of LC3-II complicated the detection of LC3-I, the Nef-mediated impairment in autophagy flux was still noticeable in these cells, since we detected LC3-I in NL4-3-infected cells, but not in cells infected with NL4-3 Δ*nef* (**Fig. 3.4C; red arrows**). In conclusion, by measuring autophagy status through the calculation of the relative ratios of LC3-II:I, we have been able to compare the effects of HIV on this pathway across different cell types. Our data indicate that, although their basal autophagy activation and the threshold to trigger this cascade differ, cells – including primary $CD4^+$ T cells – respond to HIV infection/transfection by inducing autophagy, likely targeting Gag for elimination. However, HIV uses the accessory protein Nef to intersect with this pathway. Altogether these findings allowed us to generate the three working hypotheses that will embody this thesis project.

HYPOTHESIS 1: Autophagy restricts HIV replication by specifically targeting the virus protein Gag for degradation, but HIV uses Nef to counteract this effect.

HYPOTHESIS 2: HIV Nef inhibits the first stages of autophagy, impairing LC3 lipidation and formation of autophagosomes.

HYPOTHESIS 3: HIV Nef's ability to inhibit autophagy is conserved among closely related primate lentiviruses.

CHAPTER 4

HYPOTHESIS 1: AUTOPHAGY RESTRICTS HIV REPLICATION BY SPECIFICALLY TARGETING THE VIRUS PROTEIN GAG FOR DEGRADATION, BUT HIV USES NEF TO COUNTERACT THIS EFFECT

The figures presented in this chapter are derived from the following publication[1] in which I am first author and I have permission from the journal editorial to reproduce the figures in this thesis.

Sergio Castro-Gonzalez, Yuhang Shi, Yuexuan Chen, Marta Colomer-Lluch, Jayc Waller, Ying Song, Anju Bansal, Frank Kirchhoff, Konstantin Sparrer, Chengyu Liang and Ruth Serra-Moreno. HIV-1 Nef counteracts autophagy restriction by enhancing the association between BECN1 and its inhibitor BCL2 in a PRKN-dependent manner. *Autophagy*, 1-25, doi:10.1080/15548627.2020.1725401 (2020).

Results

Autophagy causes a defect in HIV virion production that is countered by the virus protein Nef

Our preliminary studies have indicated that HIV Gag may be an autophagic target. However, the levels of Gag remain steady in the presence of HIV Nef (**Fig. 3.2**), evidencing that Nef's ability to intersect with autophagy restores Gag levels. Since Gag is the major driver of virion assembly and is the precursor of the HIV capsid, the autophagy-mediated clearance of Gag would inevitably impact virus progeny size. In order to test this hypothesis, we assessed the impact of the pharmacological activation of autophagy on Gag and virion assembly and release in the presence and absence of Nef. For this, we transfected HEK293T cells with the wild-type HIV-1 NL4-3 proviral DNA or the mutant HIV Δ*nef*. 24 h later, the cell medium was replaced, and autophagy induced by using increasing doses of rapamycin for 12 h. Next, we collected the cell lysates to analyze them by western blot, and the culture supernatants to measure virion production by ELISA specific to the HIV capsid protein p24. This technique allowed us to quantify the effects of rapamycin-induced autophagy on virion release. We expressed particle release relative to the no-rapamycin treatment as the percentage of maximal virus production for each virus (wild-type and Δ*nef*), as we previously reported[51,113]. By comparing the effect of rapamycin-induced autophagy within viruses – instead of between viruses – we

excluded (a) any differences in transfection efficiencies between these proviral constructs, and (b) any other processes that Nef may be influencing, such as infectivity enhancement through SERINC3 and SERINC5 antagonism[118].

We found that rapamycin-induced autophagy caused a dose-dependent defect in virion release for the *nef*-deleted NL4-3 virus (**Fig. 4.1A; top panel**), which was also associated with a dose-dependent decrease in Gag (**Fig. 4.1A; bottom panel**). By contrast, wild type NL4-3 only exhibited a partial decrease in particle release at the higher concentrations of rapamycin and minimal defects in Gag (**Fig. 4.1A**). Of note, whereas in cells transfected with NL4-3 Δ*nef* autophagy proceeded uninterruptedly (since there was a transition of LC3-I to LC3-II in response to rapamycin), autophagy flux was halted in cells transfected with wild type NL4-3, since there was an impairment in the emergence of LC3-II (**Fig. 4.1A; bottom panel**). These findings confirm that not only rapamycin-induced autophagy poses a significant restriction on HIV replication, but also that the protein Nef exerts a strong protective effect under these conditions. In order to corroborate that the absence of a functional Nef accounts for the susceptibility of *nef*-defective viruses to the rapamycin restriction, we next performed a complementation assay by providing *nef in trans*. As expected, we were able to restore the rapamycin-resistant phenotype previously observed in the wild-type virus (**Fig. 4.1B**).

Once we confirmed the protective role of Nef against the rapamycin-mediated restriction of HIV, we needed to corroborate that this antiviral activity was the result of the specific activation of autophagy and not due to any off-target effects that rapamycin might exert. For this, we challenged once again the rapamycin-susceptible *nef*-deficient virus with increasing doses of rapamycin, but also in the presence of 3-methyladenine (3MA), a drug that specifically inhibits the class III PtdIns3K C1, necessary for phagophore nucleation[192,216]. Whereas rapamycin efficiently caused a defect in virion production for the *nef*-deleted virus, the addition of 3MA rescued particle release to similar levels as the wild type virus (**Fig. 4.1C**). The role of autophagy in the restriction of HIV Gag and virion production was further

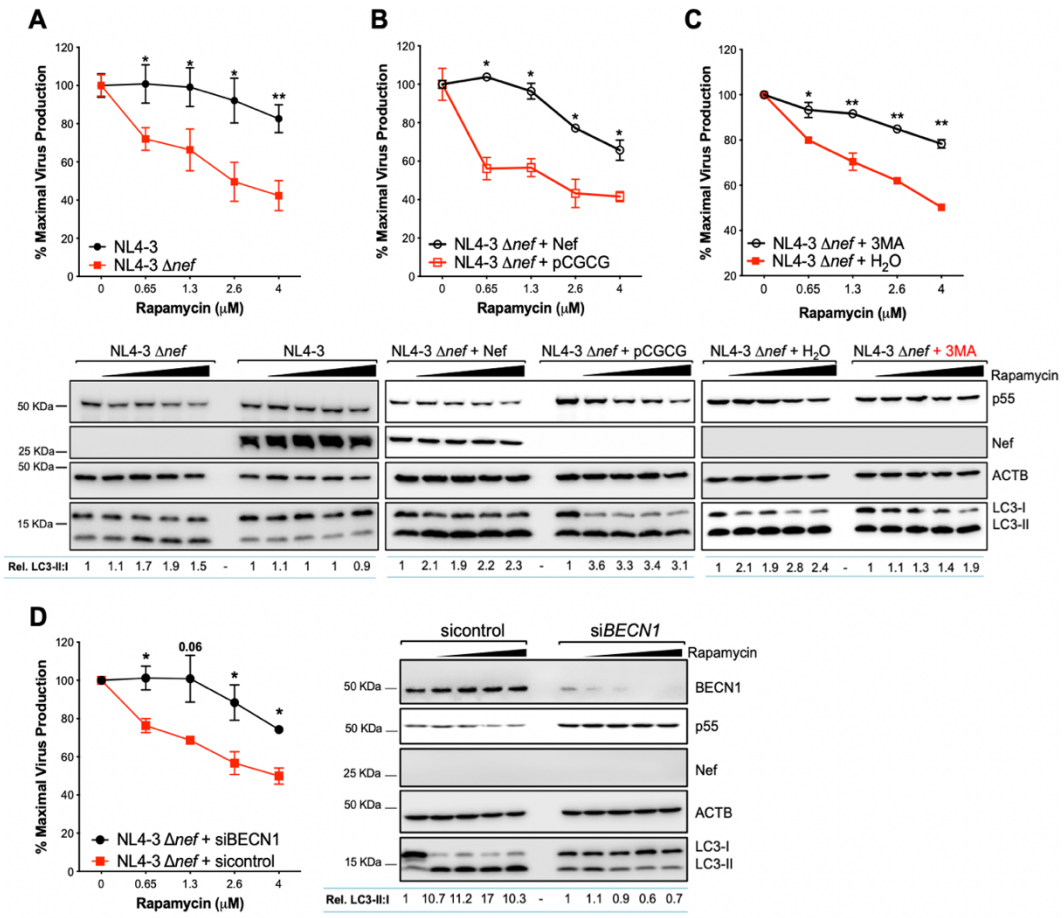

Figure 4.1. Autophagy limits virion production in nef-defective HIV in HEK293T cells. (**A**) Top panel: HEK293T cells were transfected with the full-length proviral DNA of HIV-1 NL4-3 or NL4-3 Δ*nef* and treated with rapamycin for 12 h. The percentage of maximal virus production was then measured by the accumulation of HIV p24 in the supernatant relative to the no-rapamycin treatment. (**B**) Top panel: HEK293T cells were transfected with HIV-1 NL4-3 Δ*nef* and trans-complemented with either NL4-3 *nef* or an empty vector. Cells were treated with rapamycin for 12 h, and the percentage of maximal virus was measured as explained above. (**C**) Top panel: HEK293T cells were transfected with HIV-1 NL4-3 Δ*nef* and stimulated with rapamycin for 12 h. Cells were either treated with 3-MA (3 mM) or water 4 h before measuring particle release. (**A-C**) Bottom panels: Cells were also analyzed by western blot for Gag p55, Nef, ACTB, and LC3. (**D**) Left panel: HEK293T cells were transfected with either siRNA for *BECN1* or a control siRNA. 24 h later, the cells were transfected again with the proviral DNA of HIV-1 NL4-3 Δ*nef* and treated with rapamycin for 12 h. Next, the percentage of maximal virus production was measured as indicated above. Right panel: Cells were also analyzed by western blot as in previous panels. The percentage of maximal virus production is indicated as the mean and SEM from 4 independent biological replicates. *: $p \leq 0.05$; **$p \leq 0.01$. Numbers underneath the blots indicate the ratio of LC3-II:I relative to the no-rapamycin treatment.

corroborated by depleting BECN1, the key component in the class III PtdIns3K C1

that facilitates the isolation of phagophore membranes[146,171]. Consistent with this role, depletion of BECN1 arrested autophagy activation, reflected by retention in LC3-I, since this factor is critical for the biogenesis of LC3-II (**Fig. 4.1D; right panel**).

Accordingly, the overall Gag levels for NL4-3 Δ*nef* were higher than in the si-control cells, affording in turn, significantly higher virion production (**Fig. 4.1D**).

In order to validate these observations, we performed infectivity assays in Jurkat CD4$^+$ T cells. Not only CD4$^+$ T cells are natural targets for HIV replication, but also by infecting them with *nef*-competent and *nef*-defective viruses, instead of transfections, we widened our scope to evaluate the potential effects of autophagy on pre-integration events of the HIV replication cycle. For this analysis, Jurkat cells were infected with either wild-type HIV or HIV Δ*nef* at a MOI of 0.3. 24 h later, cells were washed, and any virions produced removed. Next, cells were treated with increasing concentrations of rapamycin for 12 h and the impact of rapamycin-induced autophagy

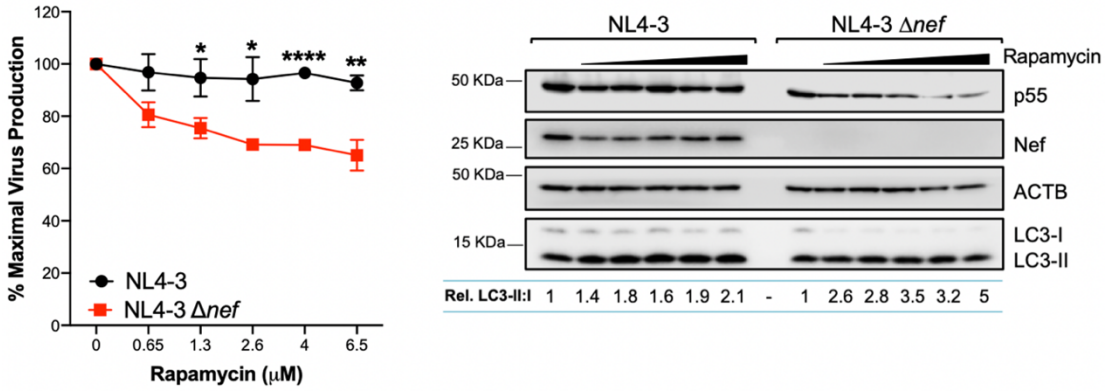

Figure 4.2. Autophagy limits virion production in *nef*-defective HIV target cells. Left panel: Jurkat CD4$^+$ T cells were infected with 100 ng of p24 equivalents of HIV-1 NL4-3 or HIV-1 NL4-3 Δ*nef*. 24 h later, the cell medium was replaced and supplemented with different concentrations of rapamycin. 12 h later, the percentage of maximal virus production was measured as detailed above. Right panel: Cells were also analyzed by western blot for Gag p55, Nef, ACTB, and LC3. The percentage of maximal virus production is indicated as the mean and SEM from 4 independent biological replicates. *: $p \leq 0.05$; **$p \leq 0.01$; ****$p \leq 0.0001$. Numbers underneath the blots indicate the ratio of LC3-II:I relative to the no-rapamycin treatment.

on Gag and virion release was assessed by western blot and p24 ELISA. As shown in **Fig. 4.2**, rapamycin-induced autophagy successfully attenuated HIV replication in Jurkat cells infected with *nef*-defective viruses, whereas the presence of Nef in wild-type HIV completely hampered this restriction (**Fig. 4.2**). Nevertheless, rapamycin seems to have a more modest impact on HIV replication in this cell model. This is in line with our previous observations showing that $CD4^+$ T cells are more resistant to autophagy activation than HEK293T cells (**Fig. 3.1**). In conclusion, these results further corroborate that autophagy poses a hurdle for HIV by affecting Gag levels, but the virus uses Nef to overcome this barrier. Since we observed the autophagy-mediated defect in Gag and particle production in HEK293T cells, in which we provided NL4-3 clones through transfections bypassing any entry and integration steps, we can conclude that the autophagy block takes place at a post-integration event in the HIV replication cycle.

Autophagy specifically targets HIV Gag for lysosomal degradation

Once the detrimental effect of autophagy on HIV has been demonstrated, we next wanted to determine which specific post-integration event in the HIV replication cycle autophagy is intersecting. The studies presented in **Fig. 4.1** and **Fig. 4.2** indicate that autophagy activation is associated with a reduction in Gag levels. Since Gag plays a crucial role in the recruitment of different components for virion assembly[57,217,218], we hypothesized that autophagy causes defects in viral production and release by directly targeting HIV Gag for degradation. Because autophagy maturation involves the fusion between autophagosomes and lysosomes, where the acidic pH and the presence of specialized proteases cause cargo degradation, we first assessed whether the pharmacological inhibition of lysosomes could prevent the rapamycin-associated depletion of Gag. Of note, since we had similar findings on the role of autophagy in Gag levels, as well as the effect of HIV-1 Nef on autophagy progression in all cell types investigated, we decided to stick to HEK293T cells for these mechanistic assays. We transfected HEK293T cells with the HIV Δ*nef* provirus. 24 h later, cells were treated with rapamycin for 12 h in the presence and absence of chloroquine (lysosomal inhibitor). We also included cells treated with Rapamycin and ALLN, a proteasomal

inhibitor, to rule out any potential degradation of Gag through the proteasomal pathway. We chose 12 h of incubation, since our previous studies showed that 12 h were enough to promote the degradation of Gag in these cells (**Fig. 4.3**). Once again, in cells treated with rapamycin only, Gag levels were reduced. As anticipated, the addition of chloroquine blocked autophagy maturation, reflected by a significant accumulation of LC3-II. Under these conditions, the rapamycin-mediated degradation of Gag was also prevented, and so it was the degradation of the autophagic marker SQSTM1 (**Fig. 4.3**). However, the treatment with the proteasomal inhibitor ALLN, did not impede such degradation of Gag or SQSTM1 (**Fig. 4.3**). Therefore, these results confirm that the lysosomal activity of autophagy maturation causes the reduction in Gag levels, most likely by directly targeting Gag to autophagosomes.

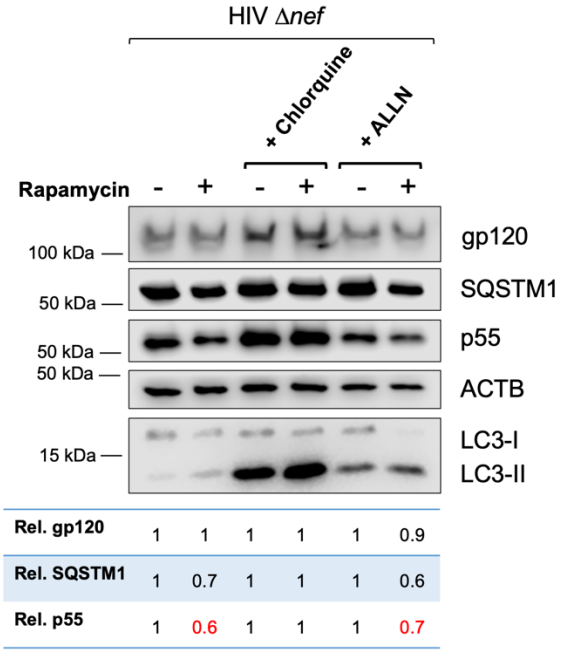

Figure 4.3. Pharmacological activation of autophagy promotes the specific degradation of HIV-1 Gag. (**A**) HEK293T cells were transfected with HIV-1 NL4-3 Δ*nef* and treated with rapamycin (4 μM), chloroquine (60 μM) and/or ALLN (25 μM) for 12 h. Cells were also analyzed by western blot for gp120, SQSTM1, Gag p55, ACTB, and LC3. Images are representative of 3 independent experiments.

HIV Gag is associated to cellular membranes by means of its myristoylated group in the N-terminus. Therefore, it is plausible that the presence of Gag in

autophagosomes may be coincidental, as a consequence of its membrane distribution. To rule this out, we assessed whether rapamycin-induced autophagy had a similar effect on the steady levels of gp120, another HIV protein that associates to cellular membranes. Remarkably, autophagy did not promote the degradation of gp120 (**Fig. 4.3**), corroborating that autophagy targets Gag for degradation in a specific manner.

The role of autophagy in targeting Gag for elimination was further investigated by co-immunoprecipitation (co-IP) as well as fluorescence microscopy analyses. We reasoned that if Gag is redistributed to autophagosomes by means of an autophagy receptor, we should detect a physical interaction –even if it is indirect– between LC3 and HIV Gag. For this, three different types of IPs were performed. On one hand, we co-transfected HEK293T with the fusion proteins Gag-EGFP and EGFP-LC3. 48 h later, cells were processed, and lysates were subjected to immunoprecipitation. In this case Gag-EGFP was pulled down and its association with EGFP-LC3 and SQSTM1 was then analyzed (**Fig. 4.4A**). In order to evaluate if the proteins present in the pulldown fractions were the result of unspecific binding with the magnetic beads employed in these IPs, we included a control containing the cell lysates and the magnetic beads but no antibody. Also, to discriminate between antibody bands (heavy and light chains) detected in the pulldown fraction from the proteins of interest, we included an antibody control consisting on lysis buffer and beads coated with the antibody used in the IP. Our data showed that Gag-EGFP interacts with the autophagosome-associated proteins EGFP-LC3 and SQSTM1(**Fig. 4.4A**). This indicates that Gag is recruited into the LC3-coated autophagosomes, possibly by the adaptor protein SQSTM1. In a similar, although more physiological approach, we immunoprecipitated endogenous LC3 and assessed its association with SQSTM1 and Gag-EGFP; an empty vector control as well as a sample without the anti-LC3 antibodies (beads only) were included in order to exclude unspecific results (**Fig. 4.4B**). As anticipated, the pool of LC3-interacting partners was positive for both the SQSTM1 and the protein Gag-EGFP (**Fig. 4.4B**). In order to corroborate that the interactions between Gag and the autophagosome markers were specific, we reproduced this immunoprecipitation using cells transfected with the full length wild-

type NL4-3 provirus. Whilst Gag was detected, once again in the pulldown fraction as

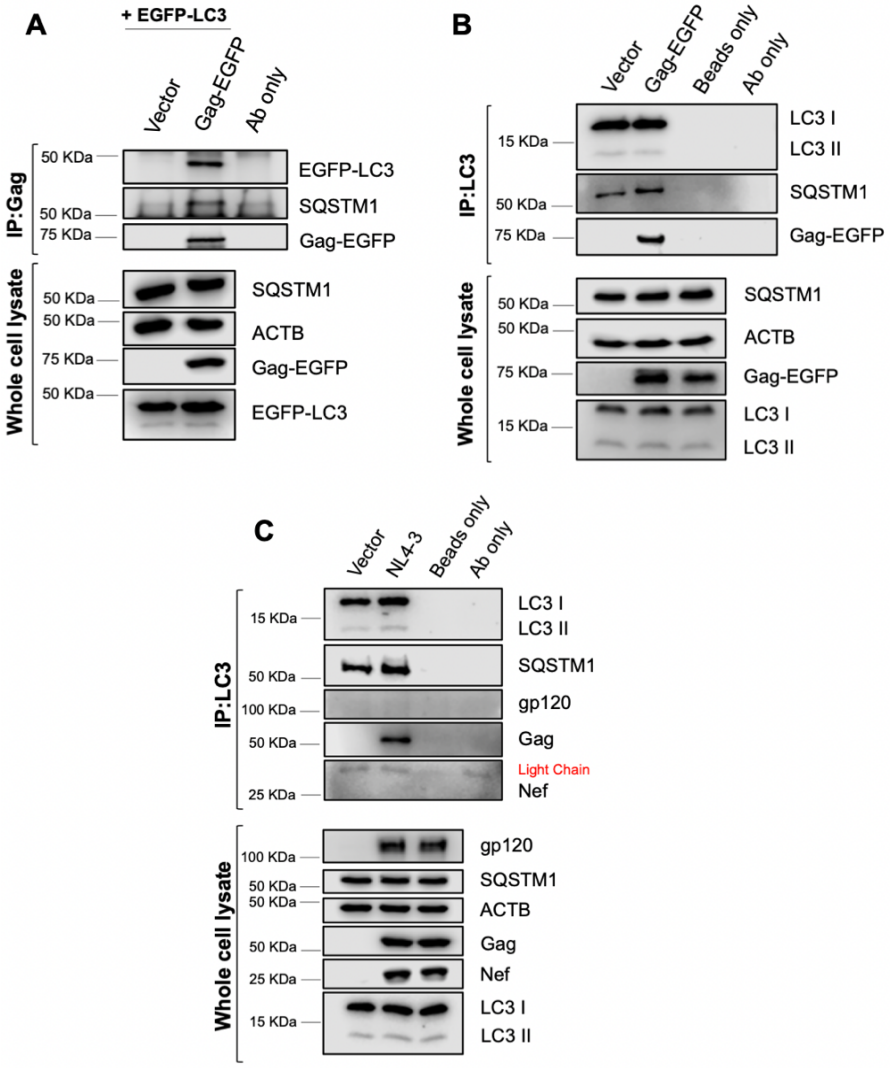

Figure 4.4. HIV-1 Gag co-immunoprecipitates with LC3. (**A**) HEK293T cells were co-transfected with *Gag-EGFP*, *EGFP-LC3* or an empty vector. 48 h later, the cell lysates were subjected to immunoprecipitation for HIV Gag. The pulldown fraction was then examined for the presence of SQSTM1 and LC3. The cell lysates were also analyzed by western blot to assess the cellular levels of SQSTM1, Gag, LC3 and ACTB. (**B**) HEK293T cells were transfected with *Gag-EGFP* or an empty vector. 48 h later, the cell lysates were subjected to immunoprecipitation for LC3. The pulldown fraction was then examined for the presence of SQSTM1 and Gag. The cell lysates were also analyzed by western blot to assess the cellular levels of SQSTM1, Gag, LC3 and ACTB. (**C**) HEK293T cells were transfected with HIV-1 NL4-3 or an empty vector. 48 h later, the cell lysates were subjected to immunoprecipitation for LC3. The pulldown fraction was then examined for the presence of SQSTM1, Gag, gp120 and Nef. The cell lysates were also analyzed by western blot to assess the cellular levels of gp120, SQSTM1, Gag, Nef, LC3 and ACTB. Images are representative of 3 independent experiments.

an LC3-interacting partner, no interactions between LC3 and other membrane-associated HIV proteins such as Nef or gp120 were detected, which demonstrates the specificity of the autophagy-mediated recruitment of the virus protein Gag (**Fig. 4.4C**).

The recruitment of Gag to autophagosomes was further supported by fluorescence microscopy analyses. For this approach, HEK293T cells were co-transfected with the provirus of HIV Δ*nef* along with the autophagosome marker EGFP-LC3, which upon rapamycin stimulation, can be incorporated into the nascent autophagosomes and is subsequently detected as green fluorescent puncta[153]. 48 h post-transfection, cells were processed for imaging. Gag was visualized by using a DyLight-550 (red) secondary antibody and the nuclei was stained with DAPI (blue). Our data confirms that HIV Gag co-localizes with the EGFP-LC3 puncta (autophagosomes) (**Fig. 4.5**). Therefore, altogether these findings indicate that the virus protein Gag is specifically targeted by

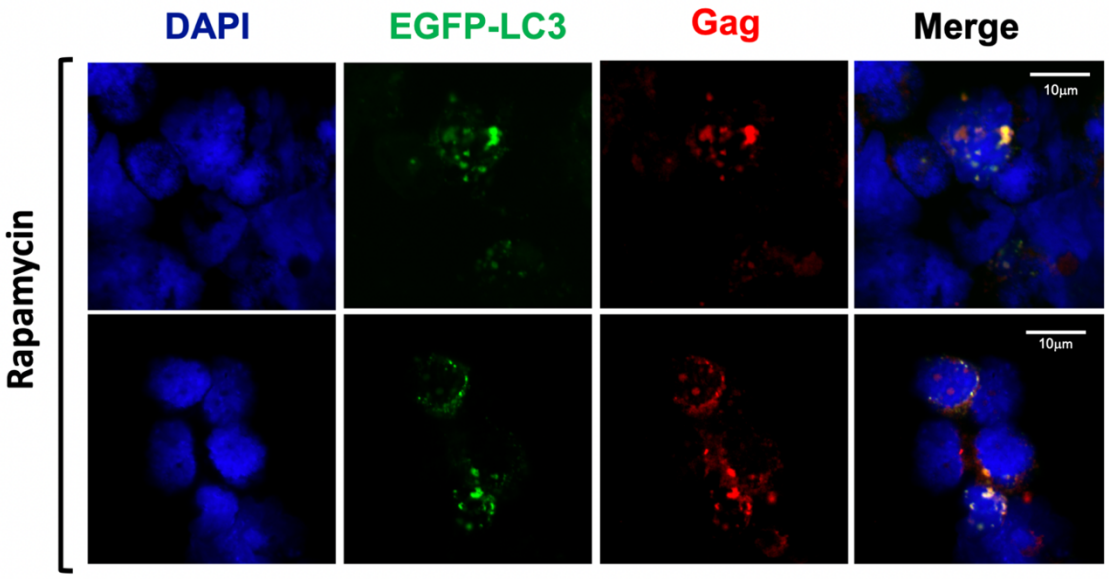

Figure 4.5. HIV-1 Gag co-localizes with LC3. HEK293T cells were co-transfected with EGFP-*LC3B* and HIV-1 NL4-3 Δ*nef*. Cells were exposed for 4 h to rapamycin (4 μM) prior to microscopy visualization. Next, cells were visualized for EGFP-LC3 (GFP; green), Gag (DyLight-550; red) and the nuclei (DAPI; blue). White scale bar: 10 μm. Representative images of 3 independent experiments.

the autophagy machinery for lysosomal degradation, which in turn diminishes virus progeny size.

Discussion

Autophagy is a degradative and highly conserved pathway that serves as a potent mechanism of defense against virus infections. Its efficacy at clearing intracellular pathogens has been extensively investigated[182,219]. Hence, the therapeutic manipulation of this pathway for the successful elimination of viruses such as HIV represents a very attractive approach. However, some viruses have developed strategies to either circumvent autophagy-associated restriction or even exploit this pathway to increase their infectivity[196,199,201-203]. Therefore, in order to consider the exploitation of autophagy in future therapeutic strategies against HIV, we first need to understand the fundamentals of the interplay between HIV and the autophagy machinery.

Despite the fact that multiple studies have tried to elucidate the role of autophagy in HV infection, the conclusions drawn have reached no consensus so far. Whereas the majority of these investigations point to the detrimental potential of this pathway against HIV[207,209-211,220], some studies have shown that autophagy might be assisting in some steps of the virus life cycle, and in consequence, HIV purposely promotes the activation of autophagy to enhance its replication[205,206]. Our results unequivocally indicate that autophagy does restrict HIV replication. This negative effect of autophagy is observed in HEK293T cells and also in $CD4^+$ T cells, which represent the main target of HIV *in vivo* and whose depletion is tightly associated with HIV pathogenesis and AIDS progression. The restrictive effect of autophagy is achieved by specifically targeting the virus protein Gag for lysosomal degradation. This defect in Gag is independent on the trigger employed to induce autophagy; pharmacological stimulation or the activation of the innate sensing system (PRRs stimulation) promoted by proviral transfections or infections. Due to the central role of Gag in the formation of viral particles, the autophagy-mediated elimination of this protein impairs the steps of virion assembly and release and thus, the overall replicative capacity of HIV.

In addition, we found no indication whatsoever about HIV's ability to exploit the activation of autophagy for its own benefits. On the contrary, our findings demonstrate that the virus has developed a defensive strategy in order to prevent autophagy-mediated restriction. In particular, HIV uses the multifunctional immune evading factor Nef to circumvent the antiviral effects of autophagy. Although other virus proteins have been previously linked to the capacity of HIV to counteract autophagy[133,135], our data clearly points to Nef as a primary player in this role, with the ability to completely bypass autophagy-mediated restriction in $CD4^+$ T cells. Rising as a new potential immune evasion mechanism for the enhancement of viral fitness, we need to further explore the molecular mechanism(s) utilized by Nef to antagonize autophagy.

Materials and methods

Plasmid DNA constructs

(i) *HIV-1 proviral clones.* The following full-length proviral constructs were obtained through the NIH AIDS Reagent Program, Division of AIDS, NIAID, NIH. Specifically, full-length constructs for wild type HIV-1 NL4-3 (pNL4-3, 114), NL4-3 Δ*vpu* (pNLU35, 968), NL4-3 Δ*env* (pNL4-3 ΔEnv EGFP, 1110), NL4-3 Δ*nef* (pNL4-3 ΔNef, 12755), and NL4-3 Δ*vpr* (pNL4-3.HSA.R^-, 3417). HIV-1 NL4-3 viruses based on these plasmids were generated by transient transfection in HEK293T cells as previously described[51,113,221].

(ii) *VSV-G construct.* The plasmid for the expression of the Indiana variant of the vesicular stomatitis virus (VSV) glycoprotein was a gift from Dr. David T. Evans (University of Wisconsin, Madison, WI).

(iii) *Plasmids coding for autophagy proteins.* The following construct was obtained through Addgene: pC3-EGFP-LC3B (11546, Dr. Karla Kirkegaard's lab).

(iv) *Plasmids coding for HIV proteins.* The expression vector pCGCG, which harbors EGFP from an internal ribosomal entry site, was used to clone the HIV NL4-3 Nef allele using the XbaI and MluI unique restriction sites. HIV-1 Gag (pGag-EGFP) was obtained through the NIH AIDS Reagent Program, Division of AIDS, NIAID, NIH from Dr. Marilyn Res.

Transfections

6 x 10^5 HEK293T (American Type Culture Collection [ATCC], CRL-11268) cells were transfected using GenJet *in vitro* DNA transfection reagent (SignaGen Laboratories, SL100488), following the manufacturer's suggestions, including total DNA, dish size, incubation time, and the ratio of GenJet:DNA for optimal transfection efficiency. Cell viability was monitored for every transfection to evaluate if the expression of the above-described constructs could cause cellular toxicity or damage. No evidence of toxicity was observed. If viability was below 85%, cells were considered unsuitable for further analyses. Viabilities were usually above 90%.

Infections

(i) *Jurkat cells.* One million Jurkat $CD4^+$ T cells (ATCC, TIB-152) were infected with 100 ng of p24 equivalents of HIV-1 NL4-3 or NL4-3 Δ*nef* for 3 h at 37°C. Cells were then washed and re-suspended in 5 mL of R10: RPMI medium (ThermoFisher Scientific, 11875-119) supplemented with 10% of fetal bovine serum (ThermoFisher Scientific, 26140-079). Cell samples were collected at 6, 24, 48, 60, 72, 84, 96, 108, 120, and 132 h post-infection for their analysis by western blot.

(ii) *$CD4^+$ T cells from PBMCs*. One million naïve $CD4^+$ T cells isolated from PBMCs (Zenbio, Inc., SER-PBCD4 TH-N-F) were activated using Dynabeads coated with anti-CD3 and anti-CD28 antibodies (ThermoFisher Scientific, 111.31D). Cells were also expanded using IL2 (interleukin 2; 30 IU/mL; NIH AIDS Reagent Program, Division of AIDS, NIAID, NIH; 136) for 3 d. Next, cells were infected with 100 ng of p24 equivalents of HIV-1 NL4-3 or NL4-3 Δ*nef* for 3 h at 37°C. Cells were then

washed and re-suspended in 3 mL of R10 medium. Cell lysates were collected at 6, 72, and 120 h post-infection for their analysis by western blotting.

(iii) *THP1-derived Macrophages.* One million THP-1 monocytes (ATCC, TIB-202) were differentiated into macrophages after stimulation with 200 nM of PMA (phorbol 12-myristate 13-acetate; Sigma-Aldrich, P1585) for 3 d. Differentiation to a macrophage phenotype was confirmed by microscopy after the PMA treatment. Next, macrophages were infected with 100 ng of p24 equivalents of VSV-G pseudotyped HIV-1 NL4-3 Δ*env* or NL4-3 Δ*env*Δ*nef* for 3 h at 37°C. Cells were washed and re-suspended in 3 mL of R10 medium. Cell lysates were collected at 6, 72 and 120 h post-infection for their analysis by western blotting.

Virus release assays

6 x 10^5 HEK293T cells were transfected with 2,000 ng of full-length proviral DNA of HIV-1 NL4-3 or NL4-3 Δ*nef*. For the trans-complementation studies, transfections with *nef*-deleted proviruses also included pCGCG-NL4-3 Nef or the empty vector pCGCG. 24 h post-transfection, the cell medium was replaced and rapamycin (Sigma-Aldrich, R8781) was added at different concentrations (0–4 μM). In the competition assays between rapamycin and 3-methyladenine (3-MA; Sigma-Aldrich, M9281), this compound was added at 3 mM (IC_{50}) 8 h after rapamycin stimulation. The culture supernatants were collected and analyzed by p24 antigen-capture ELISA (Advanced Biolabs, 5421), as previously described[113,221-223]. In the case of virus release assays in Jurkat cells, 10^6 Jurkat cells were infected with 100 ng of p24 equivalents of HIV-1 NL4-3 or NL4-3 Δ*nef* for 3 h at 37°C. Cells were then washed and re-suspended in 5 mL of R10 medium. 24 h later, cells were washed and aliquoted into 24-well plates at 150,000 cells per well. Cells were stimulated with rapamycin (0-6.5 μM) for 12 h. Virion release was determined as explain above. In addition, cells were washed, lysed, and harvested for their analysis by western blotting.

Gag degradation assays

6 x 10^5 HEK293T cells were transfected with 2,000 ng of full-length proviral DNA of HIV-1 NL4-3 or NL4-3 Δ*nef*. 24 h post-transfection, the cell medium was replaced and rapamycin (Sigma-Aldrich, R8781) was added at 4 μM for 12 h. When Rapamycin was combined with Chloroquine (Sigma-Aldrich, C6628-256) or ALLN (EMD Millipore, 208750-5MG), these compounds were added at 60 μM and 25 μM, respectively, for 12 h along with rapamycin. Cells were then washed, lysed and harvested for their analysis by western blotting.

Western blotting

Cells including HEK293T, Jurkat, THP-1 monocytes, THP-1-derived macrophages as well as primary $CD4^+$ T cells were harvested after the corresponding time intervals and doses of the rapamycin treatment, in lysis IP buffer (Thermo Scientific, 87787) complemented with protease inhibitors (Roche, 04693116001) and phosphatase inhibitor cocktails 2 and 3 (Sigma-Aldrich, P5726 and P0044). Cell lysates were incubated on ice for 1 h. Samples were then centrifuged at 16,000 x *g* for 8 min. The supernatant was collected, mixed with 2x SDS sample buffer (Sigma-Aldrich, S3401) and boiled for 5 min. Proteins were then separated by electrophoresis on SDS-PAGE polyacrylamide gels (8-12%) and transferred to a polyvinylidene difluoride (PVDF) membrane (BioRad, 1620177) using a Trans-Blot SD transfer cell (BioRad, 1703940). After blocking the membranes for 1 h in blocking buffer (BioRad, 1706404) at room temperature, we proceeded with the incubation with primary antibodies overnight at 4°C (antibody sources and dilutions are detailed in **Table 4.1**). Next, membranes were washed 3 times in PBS-tween (Sigma-Aldrich, P3563) for 15 min at room temperature before being probed for 1 h with the secondary antibody solution at a 1:2,000 dilution. Four different secondary antibodies were used, all conjugated with horseradish peroxidase: goat anti-mouse-HRP, goat anti-rabbit-HRP, donkey anti-rabbit-HRP and donkey anti-goat-HRP (**Table 4.1**). After the incubation with the secondary antibodies, the membranes were washed 3 additional times in PBS-tween, developed using SuperSignal West Femto maximum-sensitivity substrate (Pierce, 34095), and visualized using a Li-Cor Odyssey Fc Imager 2800 (Li-Cor, Lincoln, NE).

Knockdown assays

The esiRNA oligos used to knockdown human *BECN1* were obtained from Sigma-Aldrich (EHU061741), and harbored the following sequence:
GGCTGAGAGACTGGATCAGGAGGAAGCTCAGTATCAGAGAGAATACAGTGAAT TTAAACGACAGCAGCTGGAGCTGGATGATGAGCTGAAGAGTGTTGAAAACCAGA TGCGTTATGCCCAGACGCAGCTGGATAAGCTGAAGAAAACCAACGTCTTTAATG CAACCTTCCACATCTGGCACAGTGGACAGTTTGGCACAATCAATAACTTCAGGC TGGGTCGCCTGCCCAGTGTTCCCGTGGAATGGAATGAGATTAATGCTGCTTGG GGCCAGACTGTGTTGCTGCTCCATGCTCTGGCCAATAAGATGGGTCTGAAATTT CAGAGATACCGACTTGTTCCTTACGGAAACCATTCATATCTGGAGTCTCTGACAG ACAAATCTAAGGAGCTGCCGTTATACTGTTCTGGGGGGTTGCGGTTTTTCTGGG ACAACAAGTTTGACCATGCAATGGTGGCTTTCCTGGACTGTGTGCAG.

BECN1 depletion was achieved by transient transfection of the esiRNAs in 6 x 10^5 HEK293T cells, using Lipofectamine 3000 *in vitro* transfection reagent following the manufacturer's instructions (ThermoFisher Scientific, L3000015). Knockdown was verified by western blot 3-5 days post-transfection.

RT-qPCR assays

(i) *RNA extraction and cDNA synthesis.* 6 x 10^5 HEK293T cells were transfected with 2,000 ng of HIV-1 NL4-3 or NL4-3 Δ*nef* proviral DNA. RNA was then isolated and purified at 6 and 18 h post-transfection, using a Qiagen RNeasy Minikit (74104) following the manufacturer's instructions. Total RNA integrity and purity was verified using a bioanalyzer (Genomics Unit, Center for Biotechnology, Texas Tech University). Only RNA samples with RIN values above 8 were used for subsequent analyses. cDNA was synthesized from 1 μg of purified RNA using an iScript cDNA synthesis kit (BioRad, 1725037). cDNA samples were subsequently used for qPCR analysis.

(ii) *qPCR.* In order to calculate *gag* relative levels of expression, the SYBR green-based real-time qPCR method was used. For each reaction, SsoAdvanced universal SYBR green supermix (BioRad, 1725271) was used, together with different PrimePCR primers (BioRad, Hercules, CA) to measure RNA quality (PrimePCR RNA assay RQ1 and RQ2 primers, 10025694), genomic DNA contamination (PrimePCR gDNA, 10025352), housekeeping genes (PrimePCR human *GAPDH*). For the *gag* qPCR assays, the following primers were used Gag FW: TATCAGAAGGAGCCACCCCA and Gag RV: CCCATTCTGCAGCTTCCTCA, which generate an amplicon of 114 bp. A melting curve analysis was then performed, and mRNA levels were normalized to *GAPDH* to obtain the relative expression levels of *gag* for each time point and treatment condition. A fold change of >2.0 was considered biologically relevant.

Immunoprecipitation assays

One million HEK293T cells were transfected with 2,000 ng of pGag-EGFP, pC3-EGFP-LC3B or HIV-1 NL4-3. 48 h post-transfection, cells were washed and lysed using lysis IP buffer supplemented with phosphatase and protease inhibitor cocktails, as detailed above. The whole cell lysates were then pre-incubated for 1 h at room temperature with Protein A magnetic beads (New England Biolabs, S1425S) to remove unspecific binding proteins. Protein A magnetic beads were then coated with the antibody of interest (anti-HIV-1 Gagp55/p24 or anti-LC3 clone D11) (**Table 4.1**) for 1 h at room temperature. Next, cell lysates were subjected to immunoprecipitation by adding antibody-coated beads to the pre-cleared samples. The immunoprecipitation proceeded overnight at 4°C. Next, beads were washed in lysis IP buffer 4 times with the assistance of a magnet. Finally, washed beads were resuspended in 2x SDS sample buffer and the pulldown samples were analyzed by western blot. The relative binding between our proteins of interest was calculated by densitometric analyses using the Image Studio software (Li-Cor), where the positive bands were normalized to the levels of the immunoprecipitated protein.

Fluorescence microscopy

20,000 HEK293T cells were co-transfected in sterile tissue culture-treated 8-well slides with 100 ng of *EGFP-LC3B* and 100 ng of HIV Δ*nef*. 48 h post-transfection, cells were treated for 4 h with rapamycin at 4 μM. Cells were then washed with DPBS (Invitrogen, 14190-144). Permeabilization and fixation of the samples was achieved by incubating the cells for 10 min in acetone-methanol (1:1) at -30ºC. Next, cells were blocked for 1 h with the antibody diluent solution (2% fish skin gelatin + 0.1% triton X-100 1x DPBS with 10% goat serum) and incubated 1 more hour with the mouse monoclonal anti-Gag p55/p24 primary antibody (**Table 4.1**) at a dilution of 1:200. Subsequently, cells were washed and incubated for another hour with a goat anti-mouse IgG2a secondary antibody conjugated with an Alexa-568 fluorophore (**Table 4.1**) at a dilution 1:500. Afterwards, cells were incubated for 5 min with DAPI (1:5,000; Invitrogen, 62248) to visualize cell nuclei. After staining, the slides were washed and mounted using anti-quenching mounting medium (Vector Laboratories, 3304770). The samples were visualized by confocal microscopy on an Olympus FV3000 instrument using the 60x objective and the lasers 405, 488, and 561nm in order to excite DAPI, GFP and Alexa 568, respectively. After collection, images were merged for the 405, 488 and 561 nm channels, processed and analyzed using ImageJ and Photoshop (Adobe). Proportional adjustments of brightness/contrast were applied.

Statistical analysis

All statistical calculations were performed with a two-tailed unpaired Student T test using Graph Pad Prism version 8.0.1. *P* values ≤ 0.05 were considered statistically significant.

Table 4.1. Antibody sources and conditions (hypothesis 1).

Protein	Primary antibody	Dilution	Source
ACTB/β-actin	Mouse monoclonal (C4) to ACTB/β-actin	1:1000	Sigma-Aldrich, MAB1501

Table 4.1. Continued

BECN1	Rabbit monoclonal (D40C5) to BECN1	1:1000	Cell Signaling Technology, 3495S
GFP	Mouse monoclonal (LGB-1) to GFP	1:1000	Abcam, ab291
LC3	Rabbit polyclonal and Rabbit monoclonal (D11) to LC3B	1:1000	Cell Signaling Technology, 2775S and 3868S
HIV Nef	Mouse monoclonal (2H12(01-007)) to HIV-1 Nef	1:1000	ThermoFisher Scientific, MA1-71505
HIV-1 Gag p55/p24	Mouse monoclonal (183-H12-5C) to HIV p24	1:1000	NIH AIDS Reagent Program, 3537
HIV-1 gp120	Goat polyclonal to HIV-1 gp120	1:1000	Abcam, ab21179
SQSTM1/p62	Mouse monoclonal to SQSTM1/p62	1:1000	Abcam, ab56416
Mouse IgG	Goat polyclonal (HRP-conjugated)	1:2000	Pierce, 31430
Mouse IgG2a	Goat polyclonal (Alexa-568 conjugated)	1:500	ThermoFisher Scientific, A21134
Rabbit IgG	Goat polyclonal (HRP-conjugated)	1:2000	Abcam, ab97051
Rabbit IgG	Donkey polyclonal (HRP-conjugated)	1:2000	Abcam, ab16284

Table 4.1. Continued

Rabbit IgG1	Goat polyclonal (Alexa-633 conjugated)	1:500	ThermoFisher Scientific, A21070
Goat IgG	Donkey polyclonal (HRP-conjugated)	1:2000	Abcam, ab6885

CHAPTER 5

HYPOTHESIS 2: HIV NEF INHIBITS THE FIRST STAGES OF AUTOPHAGY, IMPAIRING LC3 LIPIDATION AND FORMATION OF AUTOPHAGOSOMES

The figures presented in this chapter are derived from the following publication[1] in which I am first author and I have permission from the journal editorial to reproduce the figures in this thesis.

Sergio Castro-Gonzalez, Yuhang Shi, Yuexuan Chen, Marta Colomer-Lluch, Jayc Waller, Ying Song, Anju Bansal, Frank Kirchhoff, Konstantin Sparrer, Chengyu Liang and Ruth Serra-Moreno. HIV-1 Nef counteracts autophagy restriction by enhancing the association between BECN1 and its inhibitor BCL2 in a PRKN-dependent manner. *Autophagy*, 1-25, doi:10.1080/15548627.2020.1725401 (2020).

The pleiotropic impact of the protein Nef on general cell physiology and, in particular, on innate host immune responses, makes this molecule a pivotal player in AIDS pathogenesis. There is an extensive literature on Nef's abilities to promote immune evasion through the downregulation of various immune receptors by intercepting with multiple trafficking pathways[119,122,126,129]. Importantly, a few studies have recently revealed the unprecedented potential of Nef to intercept autophagy by either, preventing the late stages of the pathway[130,132], or by promoting the cytoplasmic sequestration of the transcription factor EB (TFEB) – a master regulator of autophagy involved in the regulation of different autophagy-related genes[131]. In this study, however, our preliminary data suggested that Nef also possesses the capacity to intersect with the first stages of autophagy by preventing the lipidation of the protein LC3 and therefore, the subsequent formation of autophagosome structures (**Fig. 3.2**, **3.4**). In this chapter, we are testing this hypothesis and characterizing the molecular mechanism(s) employed by Nef to achieve this novel strategy to counteract autophagy.

Results

Nef inhibits LC3 lipidation and autophagosome formation

To investigate the mechanism(s) by which Nef antagonizes autophagy, we first confirmed that the relative increase in LC3-I detected in the presence of *nef*-competent NL4-3 is also observed in Nef-only expressing cells, in the absence of the rest of the

NL4-3 genome. For this, we monitored autophagy in HEK293T cells transfected with pCGCG-EGFP, an expression vector that codes for EGFP from an internal ribosomal entry site (IRES), and pCGCG-NL4-3-Nef-EGFP [51,113]. We replaced the cell medium 8 h post-transfection, and we either (a) treated the cells with increasing concentrations of rapamycin for 4 h (48 h post-transfection), or (b) starved the cells for 4 days. We harvested the cells after these treatments and analyzed autophagy by assessing the levels of SQSTM1 as well as LC3-II:I by western blot. Consistent with our observations with the full-length NL4-3 provirus, Nef, but not the empty vector control, arrested autophagy progression reflected by low LC3-II:I ratios and more steady SQSTM1 levels. We observed this obstruction in all three biological replicates under rapamycin and starvation-induced autophagy (**Fig. 5.1A, 5.1B**; bar graphs). These data clearly show that the presence of Nef promotes the accumulation of LC3-I, which might be the result of an impairment in its lipidation. However, this phenotype may also be caused by an indirect effect of Nef on the induction of *LC3B*. To test this, we monitored the mRNA levels of *LC3B* in the presence and absence of Nef by RT-qPCR. Since previous studies reported that Nef blocks autophagy through the sequestration of TFEB, and *LC3B* is regulated by TFEB[131,224-226]– amongst other transcription factors – we also assessed the expression of another TFEB-regulated gene to rule out if any effects of Nef on autophagy and LC3 lipidation can be attributed to its reported role in the sequestration of this transcription factor. For this, we chose *ATG16L1*, the only enzyme from the E3-like complex that catalyzes the lipidation of LC3 that is also regulated by TFEB[138,225,226]. We transfected HEK293T cells with an empty vector (pCGCG) or NL4-3 *nef*. We examined *LC3B* and *ATG16L1* mRNA levels at 6, 24, and 48 h post-transfection, and we indicated their expression relative to the 6 h data point as mRNA fold change after normalization to *GAPDH* and *GFP* (to correct for transfection efficiencies). As mentioned earlier, cytosolic DNA triggered autophagy, since we detected a peak in *LC3B* and *ATG16L1* mRNAs 6 h post-transfection in both the empty vector and NL4-3 *nef*-transfected cells. Accordingly, this effect slowly disappeared upon replacing the cell medium, indicated by a steady decline in the mRNA levels of *ATG16L1* and *LC3B* (**Fig. 5.1C**; lines with open symbols). However, while we detected no differences in the expression of

ATG16L1 (**Fig. 5.1C**; blue lines), we found a ~2-fold reduction in *LC3B* mRNA in Nef-expressing cells, although it did not reach statistical significance (**Fig. 5.1C,** green lines). Hence, these observations rule out a role for Nef in the upregulation of *LC3B.* On the contrary, it seems that Nef downregulates *LC3B* as an additional mechanism to

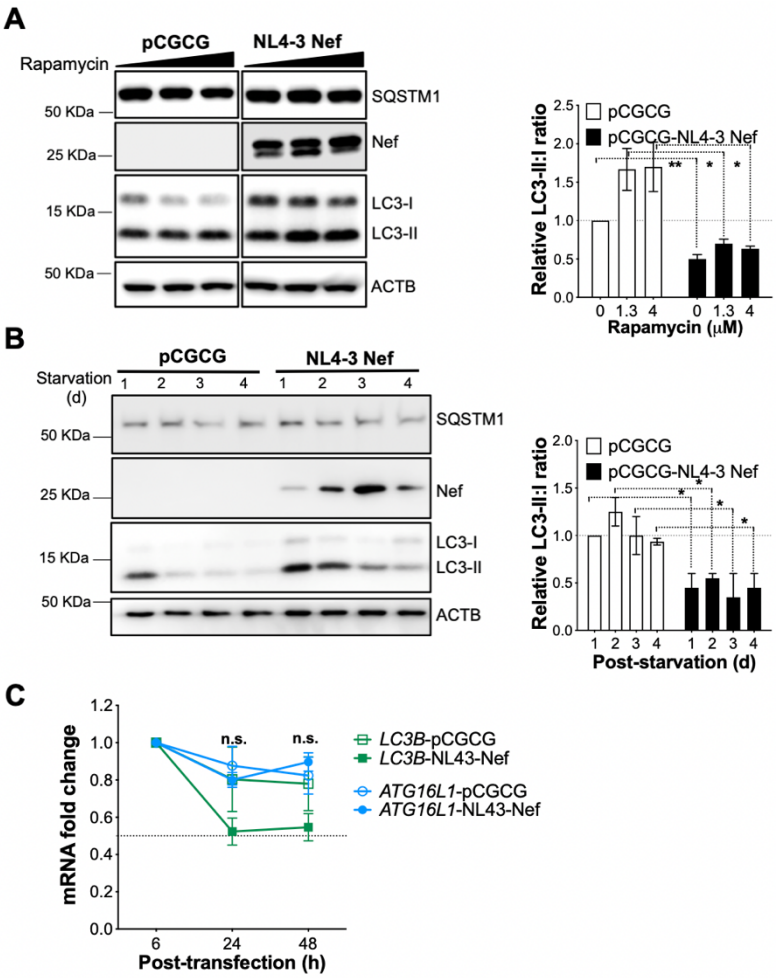

Figure 5.1. Nef impairs the lipidation of LC3. (**A, B**) HEK293T cells were transfected with NL4-3 *nef* or an empty vector. 48 h later, cells were (A) exposed to the indicated concentrations of rapamycin, or (B) starved for the selected times. Left panels: Cells were analyzed by western blot for SQSTM1, Nef, LC3, and ACTB. Right panels: Data represent the mean and SEM of the ratios of LC3-II over LC3-I relative to the empty vector control (without rapamycin or at 1 d post-starvation, respectively) from 3 independent biological replicates. (**C**) HEK293T cells were transfected with NL4-3 *nef* or an empty vector. Next, the mRNA levels of *LC3B* and *ATG16L1* were assessed at the selected time points by RT-qPCR and expressed as fold change after normalization to *GAPDH* and *GFP*. Data represent the mean and SEM from 3 independent biological replicates. The dashed line represents cutoff for biologically relevant differences. *: $p \leq 0.05$; **: $p \leq 0.01$; n.s. not significant.

block autophagy, but likely in a TFEB-independent manner. Therefore, the relatively high levels of LC3-I detected in Nef-expressing cells illustrated in **Fig. 5.1A** and **5.1B** are the result of the inhibitory effect of Nef on the lipidation of LC3-I, causing a defect in the emergence of LC3-II, which again, occurs independently of Nef's ability to hamper TFEB.

Our data show that HIV Nef is able to prevent LC3 lipidation regardless the stimuli used to activate autophagy, since the relatively low ratio of LC3-II:I associated with the presence of Nef is observed when autophagy is triggered by rapamycin stimulation (**Fig. 5.1A**), starvation (**Fig. 5.1B**), transfection (**Fig. 3.2**) or infections (**Fig. 3.4**). The common denominator of all these stress triggers is the inactivation of the mechanistic target of rapamycin complex 1 (MTORC1) and downstream events[142,144,227]. Therefore, our findings indicate that Nef must intersect with the first stages of autophagy at a step between MTORC1 inactivation and the lipidation of LC3.

The Nef-mediated obstruction in LC3 lipidation should inevitably impact autophagosome formation. To corroborate that this is the case, we performed flow cytometry assays. For this, we employed the fluorescent protein EGFP-LC3, widely used by others in the autophagy field[152,154]. Upon autophagy activation, the fusion protein EGFP-LC3 is associated to phagophores and autophagosomes rather than distributed in the cytosol. This membrane association makes autophagosome bound EGFP-LC3 resistant to saponin elimination. In consequence, upon saponin treatment, cytosolic EGFP-LC3-I is washed out, so any EGFP signal detected corresponds to phagophore- and autophagosome-bound EGFP-LC3-II. To avoid any interference in the EGFP signal between pCGCG and EGFP-LC3B, we used pcDNA5 instead of pCGCG-EGFP as the empty vector control and pCI-NL4-3-Nef-HA instead of pCGCG-NL4-3-Nef-EGFP in our transfections. As expected, the inhibitory effect that 3-MA exerts on autophagy led to considerably lower EGFP signal than in rapamycin-treated cells. Consistent with the data in **Fig. 5.1A, 5.1B** and **5.1C**, showing that Nef halts the lipidation of LC3, Nef reduced autophagosome biogenesis, reflected by

significantly lower levels of membrane-associated EGFP-LC3 in comparison with the other treatments (**Fig. 5.2A**).

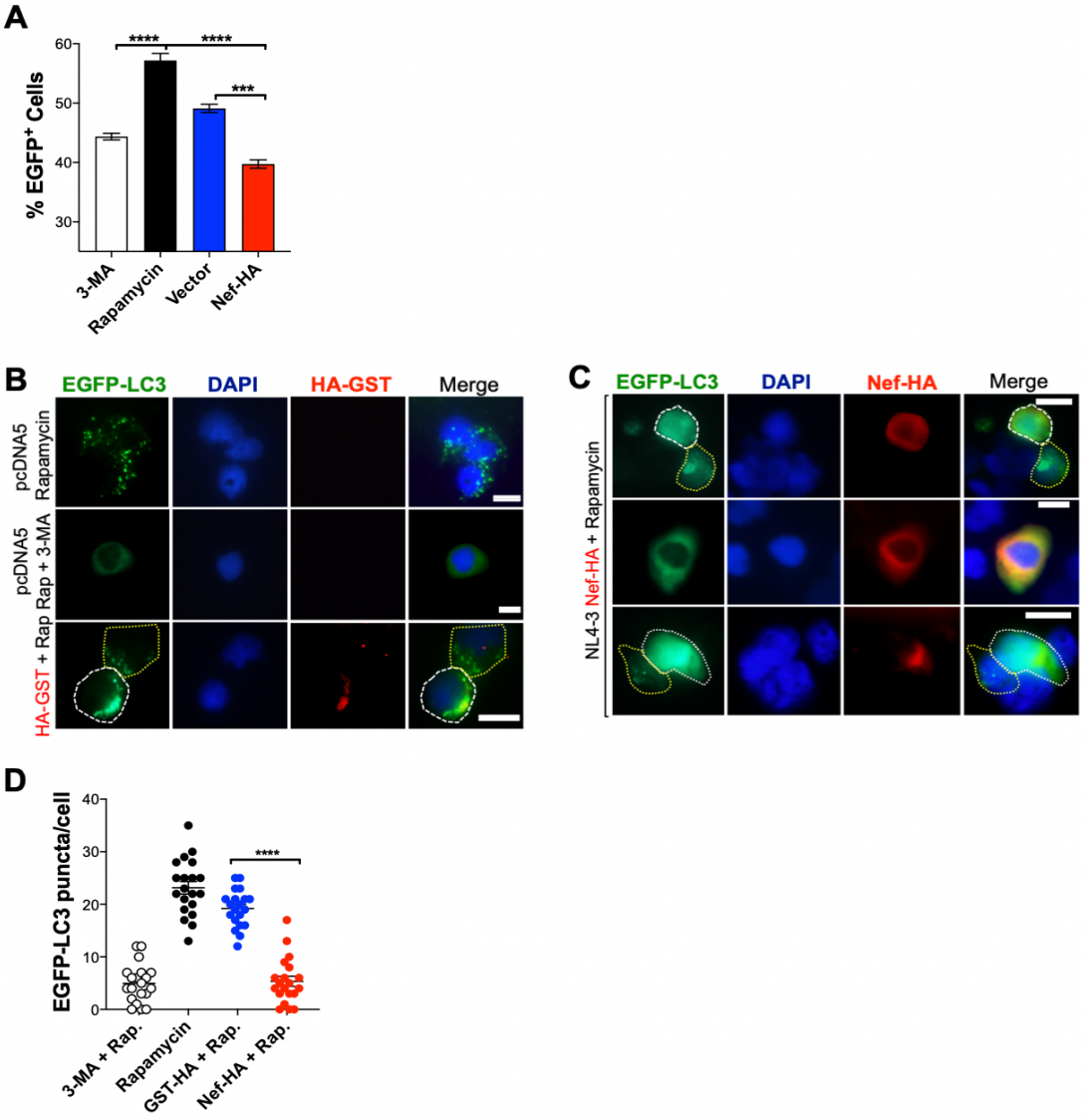

Figure 5.2. Nef impairs autophagosome formation. (**A**) HEK293T cells were co-transfected with EGFP-*LC3B* and an empty vector or NL4-3 *nef*-HA. As controls, cells were also treated with rapamycin (4 μM) and 3-MA (3 mM). 48 h post-transfection, cells were analyzed by flow cytometry for autophagosome-associated EGFP-LC3B. Data correspond to the mean and SEM of the percentage of $EGFP^+$ cells from 3 independent experiments. (**B, C**) HEK293T cells were co-transfected with EGFP-*LC3B* and either an empty vector, *GST*-HA (B) or NL4-3 *nef*-HA (C). Cells were exposed for 4 h to rapamycin (4 μM) in the presence and absence of 3-MA (3 mM) prior to microscopy visualization. Next, cells were stained for GFP (green), HA (DyLight-550; red) and the nuclei (DAPI; blue). (**D**) Data correspond to the mean and SEM of EGFP-LC3B puncta present in 20 randomly selected cells for each experimental condition. *: $p \leq 0.05$; **: $p \leq 0.01$; ***: $p \leq 0.001$; ****: $p \leq 0.0001$; n.s. not significant. White scale bar: 10 μm. Cells surrounded by white borders are HA^+.

We further confirmed these findings by fluorescence microscopy. As for **Fig. 4.5**, we used EGFP-LC3 to visualize autophagosome structures through EGFP-LC3 puncta. For this, we co-transfected HEK293T cells with EGFP-*LC3B* and either an empty vector (pcDNA5), an irrelevant gene (HA-*GST*), or NL4-3 *nef*-HA. 48 h post-transfection, we treated cells with rapamycin (4 μM) for 4 h, and subsequently imaged them for HA (DyLight-550; red), EGFP-LC3 (green) and the nuclei (DAPI; blue) (**Fig. 5.2B, C**). As a negative control, we treated rapamycin-stimulated cells with 3-MA (3 mM) for 4 h. Consistent with its role in autophagy activation, rapamycin potently triggered the formation of autophagosomes reflected by multiple EGFP-LC3 puncta (**Fig. 5.2B;** top panel). By contrast, treatment with 3-MA prevented the lipidation of LC3, and in consequence, we observed LC3-I distributed throughout the cytosol (**Fig. 5.2B;** middle panel). As expected, HA-GST had no impact on the progression of autophagy, since we readily detected LC3 puncta (**Fig. 5.2B;** bottom panel). Consistent with the data in **Fig. 5.2A**, expression of Nef caused a similar phenotype as 3-MA, since we mainly found EGFP-LC3 dispersed in the cytosol with only a few puncta (**Fig. 5.2C;** cells with white borders**)**. Quantification of puncta in 20 randomly selected cells confirmed a significant reduction of autophagosomes by Nef (**Fig. 5.2D**). Accordingly, ZFYVE1/DFCP1 puncta – a marker associated with the nucleation of the phagophores– was also significantly diminished in Nef-expressing cells, even under conditions of rapamycin-induced autophagy (**Fig. 5.3**). ZFYVE1 shuttles from Golgi to the ER upon autophagy activation and facilitates the creation of a membrane hub for the accumulation of autophagy proteins. Remarkably, its translocation to phagophore structures depends on class III PtdIns3K complex I function[228]. In the presence of an irrelevant protein such as GST, ZFYVE1 was able to accumulate to promote the formation of phagophores (**Fig. 5.3A)**. However, the formation of ZFYVE1 puncta was drastically reduced in cells expressing Nef (**Fig. 5.3B**). Quantification of puncta in 20 randomly selected cells confirmed a significant reduction in the accumulation of the early autophagic marker ZFYVE1 in the presence of Nef (**Fig. 5.3C**). Hence, these results support that Nef interferes with autophagy

initiation, impairing efficient conversion of LC3-I into LC3-II, and in turn, autophagosome biogenesis.

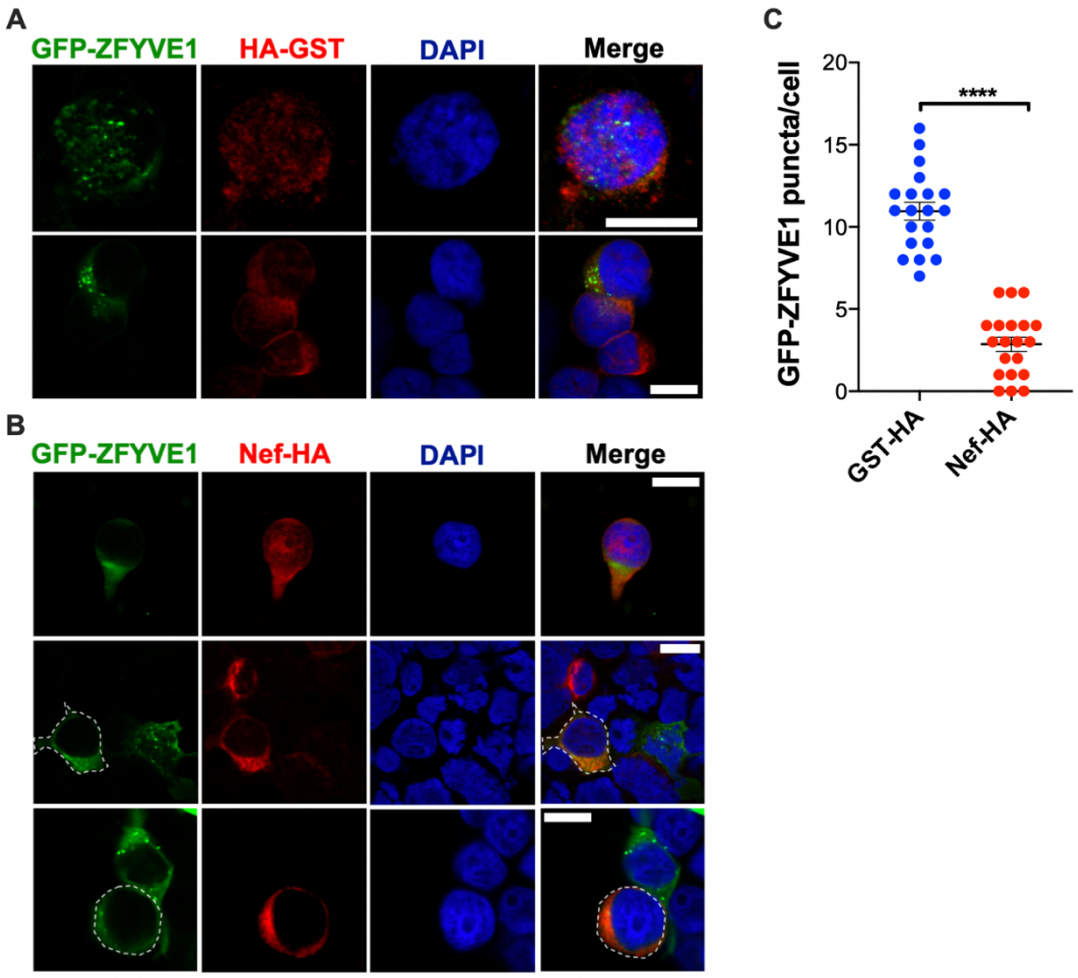

Figure 5.3. Nef reduces ZFYVE1 puncta formation. (**A, B**) HEK293T cells were co-transfected with GFP-*ZFYVE1* and either *GST*-HA (A) or NL4-3 *nef*-HA (B) and treated with 4 μM of rapamycin for 4 h. 48 h later, cells were stained for GFP (green), HA (DyLight-550; red) and the nuclei (DAPI; blue). (**C**) Data correspond to the mean and SEM of GFP-ZFYVE1 puncta present in 20 randomly selected cells expressing GST-HA or NL4-3 Nef-HA. ****: $p \leq 0.0001$. White scale bar: 10 μm. Cells

Nef enhances the association between BECN1 and BCL2 to prevent autophagy initiation

Our data consistently show that Nef impacts autophagy initiation, affecting the transition of LC3-I into LC3-II. To elucidate the mechanism by which Nef achieves this, we explored the following hypotheses: (a) Nef interacts with LC3, physically preventing its lipidation; (b) Nef interferes with the enzymatic complex involved in the lipidation of LC3 (E1: ATG7, E2: ATG3 and E3: ATG12–ATG5-ATG16L1), either through direct interaction or by affecting their expression or subcellular localization; or (c) Nef blocks steps before LC3 lipidation in the autophagy cascade, such as enhancement of the autophagy inhibitory activity of BCL2 or blocking ULK1 (unc-51 like autophagy activating kinase 1) or BECN1. To investigate these possible scenarios, we assessed the ability of NL4-3 Nef to physically interact with any of these proteins in HEK293T cells by co-immunoprecipitation, and we monitored any changes in their expression pattern by western blot. We observed no evident interactions between Nef and any of these autophagy molecules (**Fig. 5.4A**). Likewise, we detected no evident fluctuations in their steady-state levels either, even under rapamycin stimulation (**Fig. 5.4B**). However, we observed a change in the migration pattern of BCL2 in cells expressing Nef, reflecting changes in BCL2's post-translational modifications (PTMs) (**Fig. 5.4B;** red asterisks).

BCL2, as explained earlier, is an inhibitor of autophagy that by associating with the BH3 domain of BECN1, facilitates BECN1 homodimerization and, in consequence, prevents BECN1 from forming the class III PtdIns3K complex I[156,157]. This enzymatic complex is essential for the formation of phagophore structures and the recruitment of the E3-like complex required for the lipidation of LC3[151](**Fig. 5.5A**). Therefore, the release of BECN1 from BECN1-BCL2 is essential for the initiation of the autophagic response. This association is regulated by a myriad of PTMs, among them those that regulate BCL2[146]. For instance, phosphorylation of BCL2 at Ser70 causes its dissociation from BECN1, allowing BECN1 to form the PtdIns3K complex I[147,229] (**Fig. 5.5A**; top). Conversely, BCL2 mono-ubiquitination by

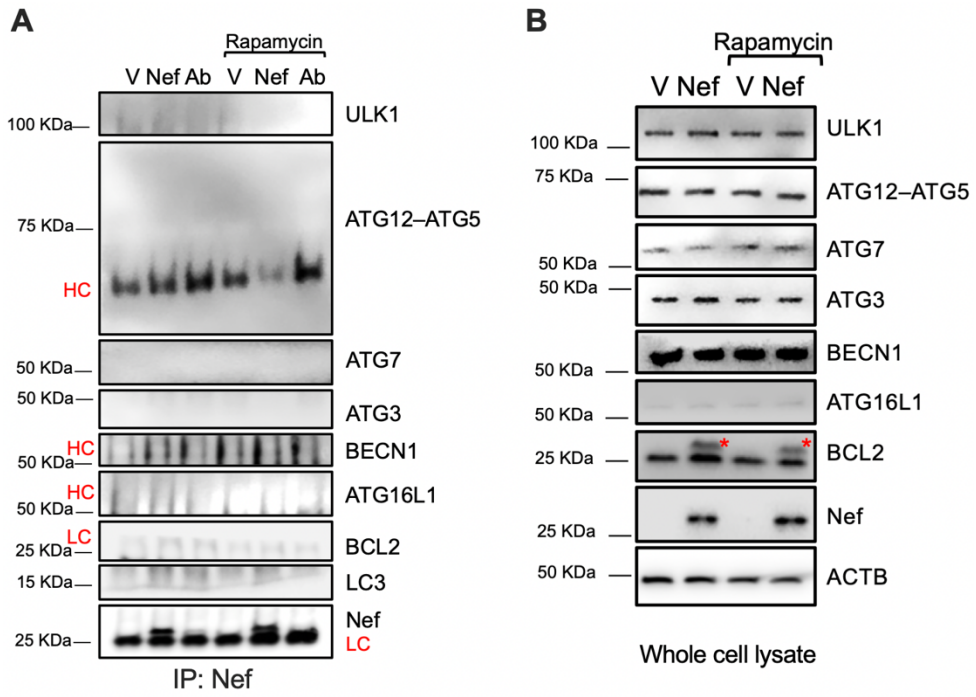

Figure 5.4. Nef promotes a posttranslational modification on BCL2. HEK293T cells were transfected with NL4-3 *nef* or an empty vector. 48 h later, cells were exposed to rapamycin (4 μM) for 4 h. (**A**) The cell lysates were subjected to immunoprecipitation for Nef, and the pulldown fraction was evaluated by western blot for ULK1, ATG12–ATG5, ATG7, ATG3, BECN1, ATG16L1, BCL2, LC3 and Nef. (**B**) The cell lysates were also analyzed by western blot to assess the expression levels of the proteins ULK1, ATG12–ATG5, ATG7, ATG3, BECN1, ATG16L1, BCL2, Nef, and ACTB. V: vector; HC: heavy chain; LC: light chain. Ab ctr: antibody control. Asterisk: differential migration pattern of BCL2. Images representative of 3 independent experiments.

the cellular E3 ligase PRKN/Parkin enhances its interaction with BECN1[158], inhibits autophagy initiation and, in consequence, leads to a defect in the lipidation of LC3 (**Fig. 5.5A**; bottom). To investigate how Nef affects BCL2 PTMs, we immunoprecipitated BCL2 from Nef-expressing HEK293T cells or transfected with a vector control, and assessed BCL2 ubiquitination levels by probing membranes with a ubiquitin-specific antibody. As a negative control, we also probed membranes with anti-SUMO antibodies, since BCL2 has not been reported to harbor SUMO target sequences. We analyzed the phosphorylation status of BCL2 from the whole cell lysates using a p-Ser70-specific antibody. Consistent with our observations in **Fig. 5.4B**, we found a different pattern in the migration of BCL2 between cells expressing Nef and the empty vector (**Fig. 5.5B**; bottom blots). We also detected an

intensification in p-BCL2 in the presence of Nef. However, we only noticed BCL2 mono-ubiquitination in Nef-expressing cells (**Fig. 5.5B**, top blots). Although our ubiquitin-specific antibody did not discriminate between mono- and poly-ubiquitination, the relative size of the ubiquitin-containing band fitted with mono-ubiquitinated BCL2 (**Fig. 5.5B**; red pound symbol). Since phosphorylation and mono-ubiquitination of BCL2 have opposing effects on the association between BECN1 and BCL2, and thus on autophagy, we next investigated if Nef affected the interaction between these two proteins. Consistent with the Nef-dependent mono-ubiquitination of BCL2, we found >2-fold enhancement in the BECN1-BCL2 interaction in Nef-expressing HEK293T cells (**Fig. 5.5C** and **5.5D**). Remarkably, we consistently observed this phenomenon regardless of what molecule was pulled down, even when we overexpressed BECN1. Quantifications of the relative BECN1-BCL2 binding from 6 independent experiments supported these findings (**Fig. 5.5D**; graph).

After confirming that Nef blocks autophagy through BCL2, we wanted to further corroborate that this activity is essential for the counteraction of the restrictive effect of autophagy on virion release (**Fig. 4.1**). For this, we assessed autophagy activation status, as well as its effect on virion production, under conditions of BCL2 inhibition (**Fig. 5.6A** and **5.6B**). We transfected HEK293T cells with the proviral HIV-1 NL4-3 and Δ*nef* constructs. 24 h later, we replaced the cell medium, and treated the cells with increasing concentrations of rapamycin (0–4 μM) for 12 h, as described above, in the presence and absence of the BCL2 inhibitor GX15-070 at its IC_{50} (3 μM). GX15-070 specifically mimics the BH3 domain in BECN1 required for its interaction with BCL2[157,230], and therefore, impairs BECN1-BCL2 association. As expected, the presence of Nef from wild-type HIV successfully impaired autophagy progression in cells treated with rapamycin (**Fig. 5.6A** and **5.6B**). However, in the presence of GX15-070, we observed a significant increase in autophagy flux and a concomitant reduction in Gag and virion production, even in the absence of rapamycin stimulation (**Fig. 5.6B**, compare lanes 1 and 6), reflecting Nef's inability to block autophagy flux (**Fig. 5.6B**; see LC3 levels in the blots). Moreover, the fact that GX15-070 similarly restricted both wild type and *nef*-defective NL4-3, rather than causing

additive effects for NL4-3 Δ*nef*, supports that Nef uses BCL2 through its association with BECN1 to counteract the autophagy-mediated restriction on viral replication (**Fig. 5.6A**)

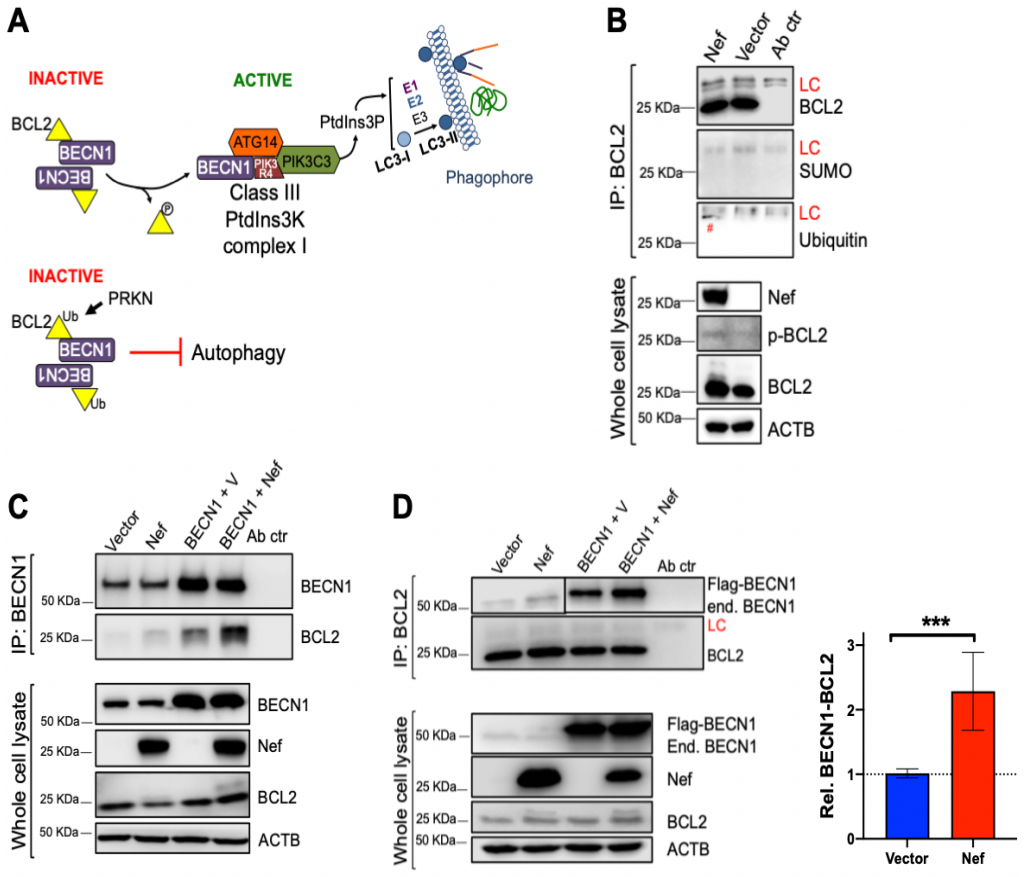

Figure 5.5. Nef enhances the association between BECN1 and BCL2. (**A**) Schematic diagram of the regulatory effect of BCL2 on the BECN1-dependent initiation of autophagy. (**B**) HEK293T cells were transfected with NL4-3 *nef* or an empty vector. 48 h later, BCL2 was immunoprecipitated from the cell lysates to assess its levels of ubiquitination and SUMOylation. The cell lysates were also analyzed by western blot to evaluate the levels of Nef, p-BCL2, BCL2, and ACTB. (**C,D**) HEK293T cells were co-transfected with *BECN1*-Flag and NL4-3 *nef* or an empty vector. 48 h later, the cell lysates were subjected to immunoprecipitation for (C) BECN1 or (D) BCL2. The pulldown fraction was then examined for the presence of both proteins. The cell lysates were also analyzed by western blot to assess the cellular levels of BECN1, Nef, BCL2, and ACTB. Graph: Data represent the mean and SEM of 6 independent biological replicates to calculate the relative binding between BECN1 and BCL2 obtained by densitometry analyses. V: vector. Rel: relative. Ab ctr: Antibody control. HC and LC: Heavy and Light chain of the antibodies from the target proteins. Pound sign: ubiquitinated BCL2.

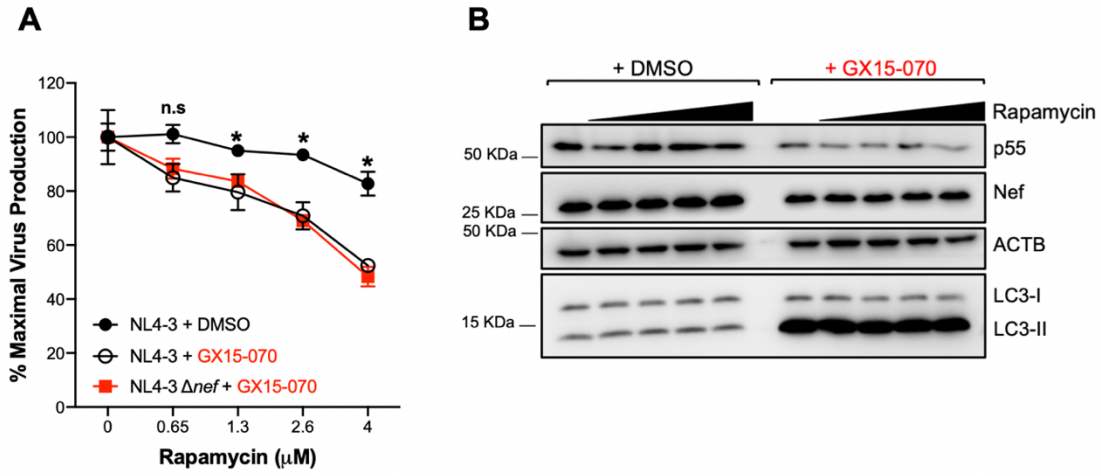

Figure 5.6. Nef uses BCL2 to arrest autophagy initiation. HEK293T cells were transfected with the full-length proviral DNA of HIV-1 NL4-3 or NL4-3 Δ*nef*. 24 h later, the cell medium was replaced, and cells were treated for 12 h with either the indicated concentrations of rapamycin and DMSO or a combination of rapamycin and GX15-070 at its IC_{50} (3 μM), an inhibitor of BCL2. (**A**) The percentage of maximal virus production relative to the no-rapamycin treatment was then measured for each virus and condition by the accumulation of HIV p24 in the culture supernatant. Data represent the mean and SEM of 3 independent biological replicates. (**B**) Cell lysates for samples transfected with the HIV-1 NL4-3 proviral construct were also analyzed for Gag p55, Nef, ACTB, and LC3. *: $p \leq 0.05$; *** $p \leq 0.001$; n.s. not significant.

The Nef-mediated enhancement of BECN1-BCL2 interaction is PRKN-dependent

Since PRKN is the primary E3 ligase known to mediate BCL2 mono-ubiquitination [158], we investigated whether this molecule is necessary for the Nef-dependent enhancement of the association between BCL2 and BECN1. For this, we took advantage of the fact that HeLa cells are PRKN negative[231-233]. Specifically, we performed additional co-immunoprecipitation assays for BCL2 and BECN1 in HEK293T cells, parental HeLa cells, and HeLa cells expressing ectopic PRKN-myc. These experiments were performed in the presence and absence of NL4-3 Nef.

Consistent with our previous data, Nef enhanced the association between BECN1 and BCL2 by >2-fold in HEK293T cells. As expected, we observed no enhancement in this interaction in parental HeLa cells. However, providing PRKN-myc *in trans* to HeLa cells expressing Nef restored the enrichment in the BECN1-BCL2 interaction (**Fig. 5.7A**; top blots), and reduced the relative LC3-II:I ratios (**Fig. 5.7A**; bottom blots), indicating that PRKN is part of the mechanism by which Nef intersects with the autophagy machinery. We consistently observed these results in four independent experiments where we calculated the relative binding levels between BECN1 and BCL2 for each cellular scenario (**Fig. 5.7A**; graph). Additionally, in order to

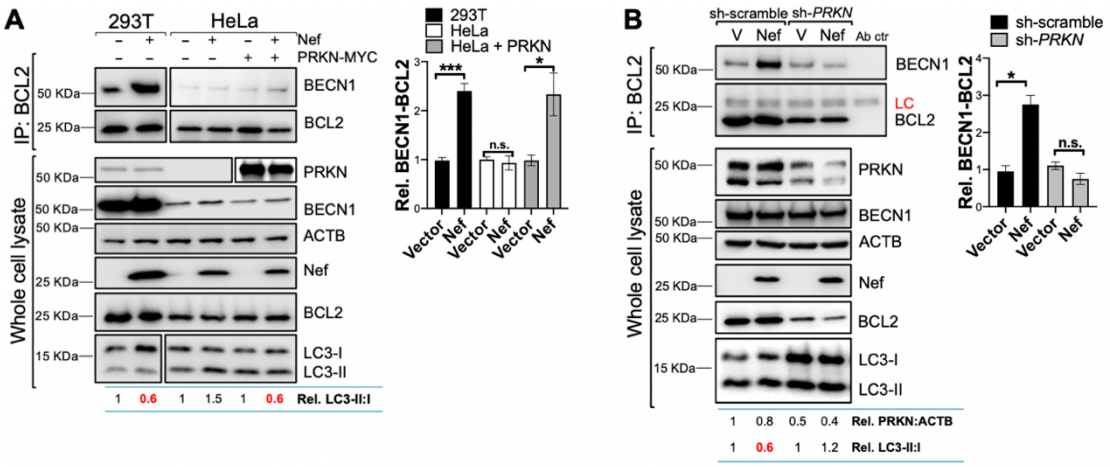

Figure 5.7. The Nef-enhanced association between BECN1 and BCL2 is PRKN-dependent. (**A**) HEK293T and HeLa cells were co-transfected with *BECN1*-Flag and either NL4-3 *nef* or an empty vector. In addition, HeLa cells were trans-complemented with *PRKN*-myc. 48 h post-transfection, the cell lysates were immunoprecipitated for BCL2, and the pulldown fraction was examined for the presence of BECN1 and BCL2. The cell lysates were also subjected to western blot to assess the cellular levels of the proteins PRKN, BECN1, ACTB, Nef, BCL2, and LC3. The ratios of LC3-II over LC3-I relative to the empty vector are provided underneath the blots. Graph: Densitometric analyses were used to determine the relative levels of interaction between BECN1 and BCL2. Data represent the mean and SEM of 4 independent biological replicates. (**B**) HEK293T cells were depleted of PRKN by shRNA and subsequently co-transfected with *BECN1*-Flag and NL4-3 *nef* or an empty vector. Cell lysates were analyzed for the BECN1-BCL2 interaction by immunoprecipitation and western blot. Similar to panel A, the relative PRKN expression levels normalized to ACTB as well as the ratios of LC3-II over LC3-I are provided underneath the blots. Graph: Densitometric analyses were used to determine the relative levels of interaction between BECN1 and BCL2. Data represent the mean and SEM of 4 independent biological replicates. V: vector. Rel: relative. Ab ctr: antibody control. *: $p \leq 0.05$; *** $p \leq 0.001$; n.s. not significant.

corroborate these findings, we performed loss-of-function studies in HEK293T cells by knocking down *PRKN* using sh-RNA. Under these conditions, Nef no longer enhanced the association between BECN1 and BCL2 and, in consequence, autophagy progression became restored, reflected by higher relative LC3-II:I ratios (**Fig. 5.7B**; blots and graph). In agreement with these results, depletion of PRKN in rapamycin-stimulated cells caused a significant restriction in Gag levels and HIV-1 production (**Fig. 5.8**). These findings confirm that HIV-1 requires PRKN in order to promote the Nef-associated mono-ubiquitination of BCL2 and subsequent circumvention of autophagy.

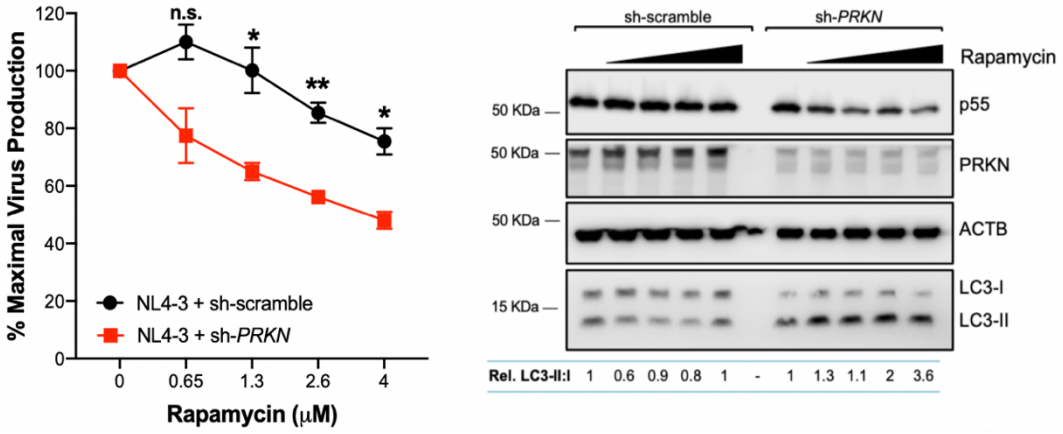

Figure 5.8. Nef requires PRKN to counteract autophagy. Left panel: HEK293T cells were depleted of PRKN by shRNA followed by transfection with the full-length proviral DNA of HIV-1 NL4-3. Cells were treated with the indicated concentrations (0–4 μM) of rapamycin for 12 h. The percentage of maximal virus production relative to the no-rapamycin treatment was then measured by the accumulation of HIV p24 in the culture supernatant. Data represent the mean and SEM of 3 independent biological replicates. Right panel: Cell lysates were also analyzed for Gag p55, PRKN, ACTB, and LC3. The ratios of LC3-II over LC3-I relative to the respective no-rapamycin treatments are provided underneath. *: $p \leq 0.05$; ** $p \leq 0.01$; *** $p \leq 0.001$; n.s. not significant.

To understand how Nef exploits PRKN to inhibit autophagy, we investigated whether Nef recruits this protein to facilitate BCL2 mono-ubiquitination. For this, we performed co-immunoprecipitation assays in HEK293T cells co-expressing PRKN-myc and NL4-3 Nef-HA. We included CD4 (cluster of differentiation 4), as a positive control, since it is a well-known interacting partner of Nef [234-241]. As expected, we

found CD4 in the Nef pulldown fraction. Remarkably, PRKN also co-immunoprecipitated with Nef, indicating that either directly or indirectly, these two proteins interact (**Fig. 5.9**). Thus, the association of Nef with PRKN is consistent with the requirement of this protein to facilitate the mono-ubiquitination of BCL2 and, in consequence, increase BCL2 association with BECN1, obstructing in turn autophagy initiation.

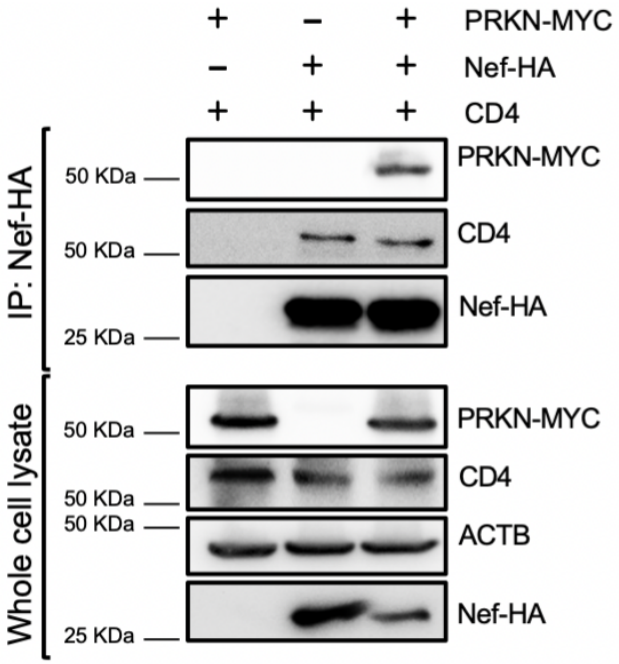

Figure 5.9. PRNK interacts with Nef. HEK293T cells were co-transfected with NL4-3 *nef*-HA and *PRKN*-myc or an empty vector. Human CD4 was included as a positive control for Nef binding. 48 h later, cells were lysed and immunoprecipitated for HA. The affinity-isolated fraction was examined for the presence of PRKN-myc, CD4 and Nef-HA. The cell lysates were also analyzed for the expression of PRKN-myc, CD4, ACTB, and Nef-HA. Representative image of 3 independent experiments.

Nef increases BECN1-BCL2 binding in the endoplasmic reticulum

Besides its role in regulating autophagy, BCL2 plays an important role in eliciting pro-survival responses, and these two distinct functions depend on BCL2's subcellular localization. Whereas mitochondrial BCL2 is associated with anti-apoptotic responses, ER-bound BCL2 is involved in the regulation of autophagy through its association with BECN1[146,155-157,242-246]. The E3 ligase PRKN is primarily associated with mitochondrial quality control, playing a critical role in cell survival by promoting the elimination of damaged mitochondria through autophagy (mitophagy)[247,248]. Therefore, we wanted to investigate whether Nef increases BCL2 ubiquitination and association with BECN1 in the mitochondria or the ER. To answer this question, we monitored how NL4-3 Nef affects BCL2's PTMs and BECN1-BCL2

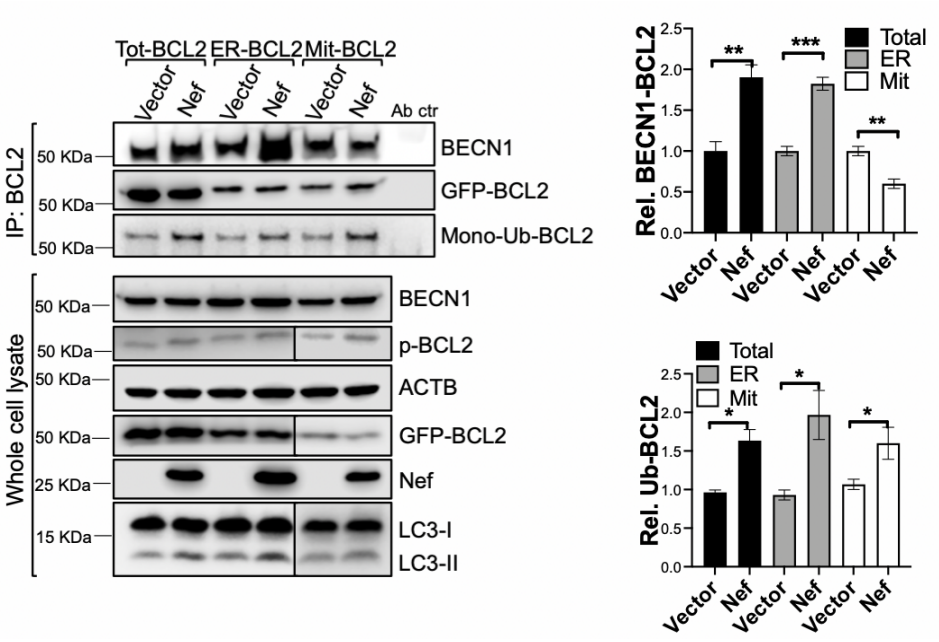

Figure 5.10. Nef promotes BECN1-BCL2 binding in the ER. HEK293T cells were co-transfected with *BECN1*-Flag and Tot-GFP-*BCL2* (total BCL2), ER-GFP-*BCL2* (Endoplasmic Reticulum-associated BCL2) or Mit-GFP-*BCL2* (Mitochondrial BCL2). In addition, cells were transfected with NL4-3 *nef* or an empty vector. 48 h later, the cell lysates were immunoprecipitated for BCL2. The pulldown fraction was examined for the presence of BECN1, GFP-BCL2 and Ub-BCL2. The cell lysates were also analyzed by western blot to assess the cellular levels of BECN1, p-BCL2, ACTB, GFP-BCL2, Nef, and LC3. Graphs: Densitometric analyses were used to determine the relative interaction between BECN1 and BCL2 and the relative levels of ubiquitinated BCL2. Data represent the mean and SEM of 5 independent biological replicates. *: $p \leq 0.05$; **: $p \leq 0.01$; ***: $p \leq 0.001$.

binding in each subcellular localization by immunoprecipitation. For this, we transfected HEK293T cells with GFP-tagged BCL2 constructs fused with ER CYB5A (cytochrome B5) or mitochondrial MAOB (monoamine oxidase B) target sequences to drive their distinct subcellular localization[246,249-251]. Consistent with the data in **Fig. 5.5B**, we found that Nef enhanced the ubiquitination and phosphorylation levels of the total GFP-BCL2 control – which can associate with both the ER and the mitochondria – as well as the ER-BCL2 and Mit-BCL2 isoforms (**Fig. 5.10**). However, the effect of Nef on BECN1-BCL2 binding differed when we analyzed the subcellular variants. Whereas the presence of Nef caused an overall increase in BECN1-BCL2 binding for

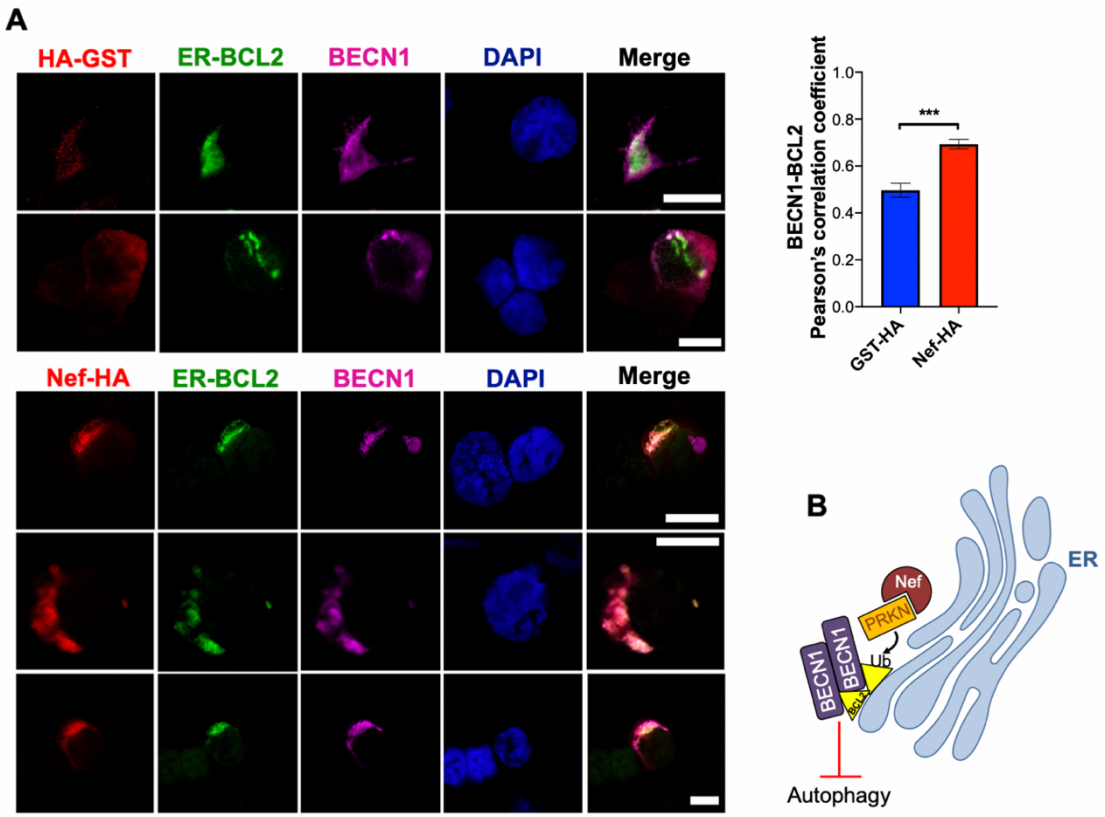

Figure 5.11. Nef sequesters BECN1-BCL2 at the ER. (**A**) HEK293T cells were co-transfected with *BECN1*-Flag, ER-GFP-*BCL2* and either *GST*-HA or NL4-3 *nef*-HA. 48 h later, cells were stained for HA (DyLight-550; red), ER-GFP-BCL2 (green), BECN1-Flag (Alexa-633; magenta) and nuclei (DAPI; blue). Merge of HA, ER-GFP-BCL2 and BECN1-Flag is provided. The Pearson's correlation coefficient for the colocalization of BECN1 and BCL2 is provided in a graph from 15 independent events for each experimental condition. (**B**) Proposed mechanism by which Nef arrests autophagy initiation. ***: $p \leq 0.001$. White scale bar: 10 μm.

total GFP-BCL2 and more strikingly for ER-BCL2, Nef did not enhance the interaction between BECN1 and Mit-BCL2 (**Fig. 5.10**; graphs). This result is consistent with the fact that the ER-bound variant is the main isoform involved in the regulation of autophagy[155-157]. Immunofluorescence images of HEK293T cells co-expressing ER-BCL2, BECN1-Flag, and either HA-GST (as an irrelevant protein) or NL4-3 Nef-HA supported this mechanism (**Fig. 5.11A**). As expected, we found colocalization between BECN1 and ER-bound BCL2 in the presence of HA-GST. However, Nef significantly increased the colocalization of BECN1 and ER-BCL2 (**Fig. 5.11A**). Therefore, these findings suggest a model in which Nef enhances PRKN-mediated ubiquitination of BCL2 in the ER, consequently arresting autophagy through the sequestration of BECN1 (**Fig. 5.11B**).

The Nef-mediated enhancement in the BECN1-BCL2 interaction also affects the functionality of the class III PtdIns3K complex II

Throughout the variety of assays performed for the characterization of Nef's mechanisms to downregulate autophagy, we observed that, besides causing considerable retention of LC3-I, Nef also increased the overall levels of LC3-II, particularly in the presence of total GFP-BCL2 and ER-associated GFP-BCL2 (**Fig. 5.10**; bottom blots). This phenomenon has already been described by others and reflects an additional mechanism by which Nef blocks autophagy at the maturation level by preventing the fusion between autophagosomes and lysosomes[130]. In addition to phagophore nucleation, BECN1 also participates in the maturation stages of autophagy by being part of the class III PtdIns3K complex II[132,171,252]. Therefore, to investigate whether the Nef-mediated enrichment in BECN1-BCL2 also affects the biogenesis of class III PtdIns3K complex II, we explored changes in the interaction patterns between BECN1 and UVRAG, a molecule that is exclusively found in class III PtdIns3K complex II[171,252]. For this, we immunoprecipitated UVRAG from HEK293T cells co-expressing BECN1-Flag and either an empty vector, ER-BCL2, NL4-3 Nef, or both (ER-BCL2 and Nef). We then analyzed the pulldown fraction for UVRAG and BECN1. Overexpression of ER-BCL2 caused a significant reduction in BECN1-UVRAG binding, suggesting that the BCL2-mediated sequestration of

BECN1 affected both PtdIns3K complexes. Since Nef increases the association between ER-BCL2 and BECN1, we found a similar phenotype in cells expressing Nef.

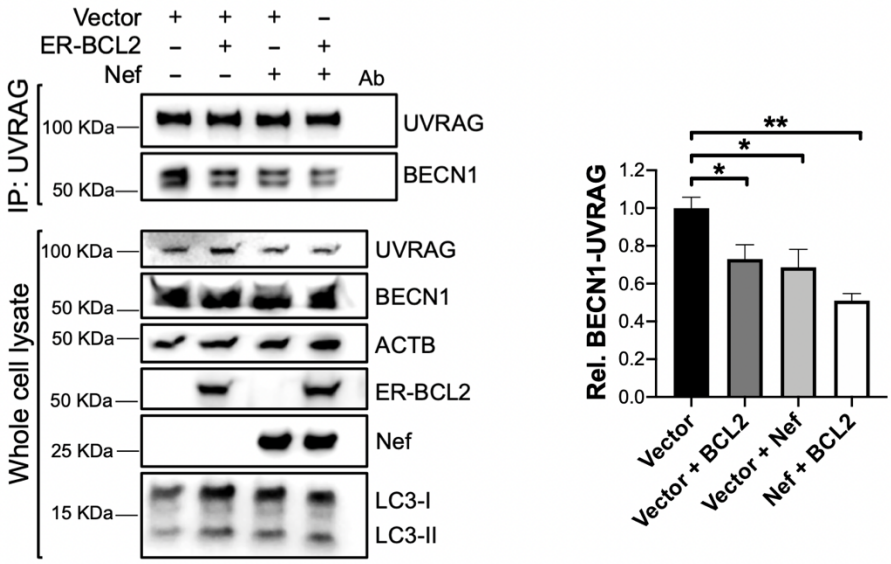

Figure 5.12. The Nef-enhanced sequestration of BECN1 by BCL2 also affects autophagy maturation. HEK293T cells were co-transfected with *BECN1*-Flag and an empty vector, NL4-3 *nef* and/or ER-GFP-*BCL2*. 48 h later, cells were immunoprecipitated for UVRAG and the pulldown fraction was analyzed for the presence of UVRAG and BECN1-Flag. The cell lysates were also examined for UVRAG, BECN1, ACTB, ER-GFP-BCL2, Nef, and LC3. Graph: Densitometric analyses were used to determine the relative interaction between BECN1 and UVRAG. Data represent the mean and SEM of 3 independent biological replicates. *: $p \leq 0.05$; **: $p \leq 0.01$.

Accordingly, co-expression of ER-BCL2 and Nef reduced even further binding between UVRAG and BECN1 (**Fig. 5.12**; blots and graph). Remarkably, either through overexpression of ER-BCL2, Nef or both, we detected a marked retention in LC3-I, accompanied by accumulation of LC3-II (**Fig. 5.12**; blots), confirming that Nef's ability to increase the interaction between BCL2 and BECN1, not only arrests autophagy at the initiation stages but also in the maturation level.

Discussion

Previous studies have reported the capacity of HIV Nef to inhibit autophagy either by blocking the maturation stages (preventing the fusion between autophagosomes and

lysosomes) or by blocking the nuclear translocation of the autophagy-regulating transcription factor TFEB[130-132]. Interestingly, our studies revealed that Nef additionally intersects with autophagy at the initiation steps through a previously unrecognized mechanism. Our binding assays indicate that Nef enhances the association between the autophagy initiator BECN1 and its inhibitor BCL2, which thereby prevents the formation of phagophore structures early in the autophagy cascade[156,157,159,253]. Under normal conditions, BECN1 enables these early stages by forming the class III PtdIns3K complex I, a multimolecular complex that mediates the synthesis of PtdIns3P[148,156,254]. PtdIns3P is an essential element for phagophore biogenesis and the lipidation of LC3, and thus, autophagy initiation. Consistent with this role of BECN1, our observations confirm that the Nef-mediated enrichment in the interaction between BECN1 and BCL2 obstructs the lipidation of LC3, consequently causing an accumulation of the cytosolic variant LC3-I. However, this phenotype might also be the result of indirect effects of Nef on the expression of *LC3B*. To rule this out, we monitored the transcription levels of this gene, which is regulated by several transcription factors, among them TFEB[224]. As anticipated, no increase in the expression of *LC3B* was detected. On the contrary, Nef downmodulates its transcription. Although these results may be in line with Campbell *et al.* observations in macrophages, where they reported that Nef blocks autophagy by sequestering TFEB in the cytoplasm[131], our transcriptional assays also examined fluctuations in the expression levels of another TFEB target: *ATG16L1*[224]. Unlike the effects of Nef on *LC3B*, we found no significant changes in *ATG16L1* expression. Therefore, these results confirm that the accumulation of LC3-I observed in the presence of Nef is not the result of the upregulation of this gene, but rather a TFEB-independent inhibition in the lipidation of LC3-I. In agreement with these findings, our flow cytometry and fluorescence microscopy studies confirmed that the Nef-mediated inhibition of LC3 lipidation is associated with a severe impairment in autophagosome formation.

In order to characterize the underlying molecular mechanism by which HIV Nef enhances the sequestration of BECN1 by BCL2, we examined changes in the PTMs of BCL2. We found that Nef achieves this goal by promoting the mono-ubiquitination of

BCL2. As previously described, when phosphorylated, BCL2 tends to dissociate from BECN1, enabling autophagy progression, whereas its mono-ubiquitination increases BCL2 stability and therefore, its inhibitory effect on BECN1[158-160]. Even though our studies indicate that Nef can promote both PTMs, the mono-ubiquitination of BCL2 certainly outcompetes the effect of the phosphorylation and therefore, reinforces BCL2's ability to bind to BECN1. Our studies also show that Nef-induced mono-ubiquitination of BCL2 is mediated by the ubiquitin E3 ligase PRKN, which in addition to its association with mitochondrial quality control[231,232], it can also regulate autophagy through the ubiquitination of BCL2[158]. The role of PRKN in the Nef-mediated inhibition of autophagy is unprecedented and was verified in our loss of function and complementation experiments in $PRKN^+$ (HEK293T) and $PRKN^-$ (HeLa) cells. In fact, when PRKN is provided *in trans* to $PRKN^-$ cells, Nef enhances the association between BECN1 and BCL2, which is accompanied by an impairment in the transition of LC3-I to LC3-II. Conversely, the selective depletion of PRKN in HEK293T cells causes a loss-of-function phenotype in which Nef cannot enhance the BECN1-BCL2 interaction nor prevent the lipidation of LC3, and this consequently impacts Gag levels and virion production.

The subcellular distribution of BCL2 is another factor that strongly determines the role of this molecule. Whereas BCL2 can be found on the outer membrane of the mitochondria, where it acts as an anti-apoptotic agent, its anti-autophagic function through the association with BECN1 takes place at the ER[155-157]. Our binding analyses and imaging studies confirm that despite the fact that Nef is able to promote the mono-ubiquitination of BCL2 at both subcellular localizations, only the mono-ubiquitination of the ER-BCL2 is able to strengthen the sequestration of BECN1 and consequently, to impede the progression of the early stages of autophagy. In accordance with these findings, the pharmacological inhibition of BCL2, as well as the depletion of PRKN, rendered HIV susceptible to autophagy restriction, confirming that Nef requires and exploits the cellular factors PRKN and BCL2 in order to counteract the detrimental effect of autophagy. However, a few questions are yet to be answered in this regard. First, is Nef recruiting PRKN? If so, what is the underlying mechanism? And second,

what are the consequences of the Nef-dependent mono-ubiquitination of BCL2 in the mitochondria? Therefore, further studies need to be pursued to evaluate the potential impact of Nef-mediated mono-ubiquitination of BCL2 on apoptosis, and its implication on viral pathogenesis.

All together, these results demonstrate that HIV Nef promotes the PRKN-dependent mono-ubiquitination of BCL2 in order to antagonize early events of autophagy through the sequestration of the initiator BECN1 at the ER. Interestingly, not only is BECN1 involved in the initiation of autophagy, as a member of the class III PtdIns3K complex I, but also in autophagy maturation, as a key component of the class III PtdIns3K complex II [171,172,252]. In agreement with this, our results indicate that the enhanced interaction between BECN1 and BCL2 promoted by Nef additionally impairs the biogenesis of this UVRAG-containing class III PtdIns3K complex II and, thus, it causes defects in autophagy maturation. Therefore, this unprecedented ability of Nef to intersect with autophagy through the mono-ubiquitination of BCL2, might be partially responsible for some observations previously reported in regard to the effect of Nef at the maturation stages[132]. Nevertheless, while posing a secondary effect on maturation, our findings indicate that the main impact of Nef over the autophagic system occurs at the earlier steps, preventing the lipidation of LC3 and subsequent formation of autophagosomes. Moreover, Campbell *et al.* reported that Nef-associated cytoplasmic sequestration of TFEB also occur in a BECN1-dependent manner and, therefore, this phenomenon might be yet another consequence derived from this newly characterized capacity of Nef to enhance the interaction between BCL2 and BECN1.

Noteworthy, previous studies have already pointed to the potential of manipulating the association/dissociation between BCL2 and BECN1 as an approach to treat different pathologies with promising results[190,192,255]. Hence, in addition to the pharmacological inhibition of the virus protein Nef, modulating the association between BCL2 and BECN1 could represent an interesting therapeutic strategy in the fight against HIV.

Materials and methods

Plasmid DNA constructs

(i) *HIV-1 proviral clones.* The following full-length proviral constructs were obtained through the NIH AIDS Reagent Program, Division of AIDS, NIAID, NIH, from Drs. Malcolm Martin and Olivier Schwartz, respectively[256-260]. Specifically, full-length constructs for wild type HIV-1 NL4-3 (pNL4-3, 114) and NL4-3 Δ*nef* (pNL4-3 ΔNef, 12755). HIV-1 NL4-3 viruses based on these plasmids were generated by transient transfection in HEK293T cells, as previously described[51,113,221].

(ii) *HIV Nef expression vectors.* The expression vector pCGCG (a gift from Dr. Jacek Skowronski [Case Western Reserve University, Cleveland, OH]), which harbors EGFP from an internal ribosomal entry site, was used to clone different NL4-3 Nef using the XbaI and MluI unique restriction sites[51,107,116]. In addition, an HA-tagged version of NL4-3 Nef was obtained from Addgene: pCI-NL4-3 Nef-HA-WT (24162, Dr. Warner Greene's lab).

(iii) *Plasmids coding for autophagy proteins.* The following constructs were obtained through Addgene: pEMD-C1-GFP-BCL2 fusion genes (GFP-BCL2, 17999; GFP-BCL2-Cb5, 18000; and GFP-BCL2-Maob, 18001; all obtained from Dr. Clark Distelhorst's lab), pRK5-PRKN-myc (7612, Dr. David Root's lab), pC3-EGFP-LC3B (11546, Dr. Karla Kirkegaard's lab), pMX-GFP-ZFYVE1 (38269, Dr. Noboru Mizushima's lab), and pcDNA4-BECN1-Flag (24388, Dr. Qing Zhong's lab). The protein GST was HA-tagged and cloned into pcDNA5 (ThermoFisher Scientific, V601020), as previously described[222].

Transfections

6 x 10^5 HEK293T (American Type Culture Collection [ATCC], CRL-11268) and HeLa (NIH AIDS Reagent Program, Division of AIDS, NIAID, NIH from Dr. Richard Axel; 153) cells were transfected using GenJet *in vitro* DNA transfection reagent (SignaGen Laboratories, SL100488), following the manufacturer's suggestions, including total DNA, dish size, incubation time, and the ratio of GenJet:DNA for

optimal transfection efficiency. Cell viability was monitored for every transfection to evaluate if the expression of the above-described constructs could cause cellular toxicity or damage. No evidence of toxicity was observed. If viability was below 85%, cells were considered unsuitable for further analyses. Viabilities were usually above 90%.

Virus release assays

6 x 10^5 HEK293T cells were transfected with 2,000 ng of full-length proviral DNA of HIV-1 NL4-3. 24 h post-transfection, the cell medium was replaced, and rapamycin (Sigma-Aldrich, R8781) was added at different concentrations (0–4 μM). In the experiments with the BCL2 inhibitor GX15-070 (AdooQ, A10665), this compound was added along with rapamycin at 3 μM, which corresponds to its IC_{50}. 48 h post-transfection, the culture supernatants were collected and analyzed by p24 antigen-capture ELISA (Advanced Biolabs, 5421 and 5436), as previously described[51,113,221-223].

Western blotting

Cells, including HEK293T and HeLa were harvested in lysis IP buffer (ThermoFisher Scientific, 87787) complemented with protease inhibitors (Roche, 04693116001) and phosphatase inhibitor cocktails 2 and 3 (Sigma-Aldrich, P5726 and P0044). Cell lysates were incubated on ice for 1 h. Samples were then centrifuged at 16,000 x *g* for 8 min. The supernatant was collected, mixed with 2x SDS sample buffer (Sigma-Aldrich, S3401) and boiled for 5 min. Proteins were then separated by electrophoresis on SDS-PAGE polyacrylamide gels (8-12%) and transferred to a polyvinylidene difluoride (PVDF) membrane (BioRad, 1620177) using a Trans-Blot SD transfer cell (BioRad, 1703940). After blocking the membranes for 1 h in blocking buffer (BioRad, 1706404) at room temperature, we proceeded with the incubation with primary antibodies overnight at 4°C (antibody sources and dilutions are detailed in **Table 5.1**). Next, membranes were washed 3 times in PBS-tween (Sigma-Aldrich, P3563) for 15 min at room temperature before being probed for 1 h with the secondary antibody solution at a 1:2,000 dilution. Three different secondary antibodies were used, all

conjugated with horseradish peroxidase: goat anti-mouse-HRP, goat anti-rabbit-HRP and donkey anti-rabbit-HRP (**Table 5.1**). After the incubation with the secondary antibodies, the membranes were washed 3 additional times in PBS-tween, developed using SuperSignal West Femto maximum sensitivity substrate (Pierce, 34095), and visualized using a Li-Cor Odyssey Fc Imager 2800 (Li-Cor, Lincoln, NE).

Knockdown assays

Human *PRKN* was silenced using the following Dharmacon shRNA constructs: *TRCN0000000281*, *TRCN0000000282*, *TRCN0000000283*, *TRCN0000000284*, *TRCN0000000285*. Protein depletion was achieved by transient transfection of a combination of the different shRNAs, following the same transfection protocols described above. PRKN knockdown was verified by western blot 3-5 d post-transfection.

RT-qPCR assays

(i) *RNA extraction and cDNA synthesis.* 6 x 10^5 HEK293T cells were transfected with 2,000 ng of NL4-3 *nef* or the empty vector pCGCG. RNA was then isolated and purified at 6, 24 and 48 h post-transfection, using a Qiagen Rneasy Minikit (74104) following the manufacturer's instructions. Total RNA integrity and purity was verified using a bioanalyzer (Genomics Unit, Center for Biotechnology, Texas Tech University). Only RNA samples with RIN values above 8 were used for subsequent analyses. cDNA was synthesized from 1 μg of purified RNA using an iScript cDNA synthesis kit (BioRad, 1725037). cDNA samples were subsequently used for qPCR analysis.

(ii) *qPCR.* In order to calculate *LC3B,* and *ATG16L1* relative levels of expression, the SYBR green-based real-time qPCR method was used. For each reaction, SsoAdvanced universal SYBR green supermix (BioRad, 1725271) was used, together with different PrimePCR primers (BioRad, Hercules, CA) to measure RNA quality (PrimePCR RNA assay RQ1 and RQ2 primers, 10025694), genomic DNA contamination (PrimePCR gDNA, 10025352), housekeeping genes (PrimePCR human *GAPDH*) and autophagy

genes (PrimePCR human *MAP1LC3B* and human *ATG16L1*). In addition, corrections for differences in transfection efficiencies were performed by quantifying *GFP* expression using the following primer pair GFP FW: 5' CAAACTGCCTGTTCCATGGC3' and GFP RV: 5' CCTTCGGGCATGACACTCTT3', which gives a 120 bp amplicon. A melting curve analysis was then performed, and mRNA levels were normalized to *GAPDH* and/or *GFP* mRNAs to obtain the relative expression levels of *LC3B* and *ATG16L1* for each time point and treatment condition. A fold change of >2.0 was considered biologically relevant.

Immunoprecipitation assays

One million HEK293T or HeLa cells were transfected with 2,000 ng of *BECN1*-Flag, *PRKN*-myc, NL4-3 *nef*, NL4-3 *nef*-HA, human *CD4*, the empty vector pCGCG and/or the GFP-*BCL2* constructs. 48 h post-transfection, cells were washed and lysed using lysis IP buffer supplemented with phosphatase and protease inhibitor cocktails, as detailed above. The whole-cell lysates were then pre-incubated for 1 h at room temperature with Protein A or G magnetic beads (New England Biolabs, S1425S and S1430S) to remove unspecific binding proteins. Protein A or G magnetic beads were then coated with the antibody of interest (HIV-1 Nef, BCL2, Flag, UVRAG or BECN1; **Table 5.1**) for 1 h at room temperature. Next, cell lysates were subjected to immunoprecipitation by adding antibody-coated beads to the pre-cleared samples. The immunoprecipitation proceeded overnight at 4°C. Next, beads were washed in lysis IP buffer 4 times with the assistance of a magnet. Finally, washed beads were resuspended in 2x SDS sample buffer and the pulldown samples were analyzed by western blot. The relative binding between our proteins of interest was calculated by densitometric analyses using the Image Studio software (Li-Cor), where the positive bands were normalized to the levels of the immunoprecipitated protein.

Fluorescence microscopy

(i) *LC3 and ZFYVE1 puncta.* 20,000 HEK293T cells were co-transfected in sterile tissue culture-treated 8-well slides with 100 ng of *EGFP-LC3B* or *GFP-ZFYVE1* and

either 100 ng of HA-*GST* or NL4-3 *nef*-HA. 48 h post-transfection, cells were treated for 4 h with rapamycin at 4 μM with or without the autophagy inhibitor 3-MA at 3 mM. Cells were then washed with DPBS (ThermoFisher Scientific, 14190-144). Permeabilization and fixation of the samples were achieved by incubating the cells for 10 min in acetone-methanol (1:1) at -30ºC. Next, cells were blocked for 1 h with the antibody diluent solution (2% fish skin gelatin [Sigma-Aldrich, 67765] + 0.1% Triton X-100 [Sigma-Aldrich, X100] 1x DPBS with 10% goat serum [ThermoFisher Scientific, 500062Z]) and incubated 1 more hour with the mouse monoclonal anti-HA antibody conjugated with DyLight-550 (**Table 5.1**) at a dilution of 1:200. Afterwards, cells were incubated for 5 min with DAPI (1:5,000; ThermoFisher Scientific, 62248) to visualize cell nuclei. After staining, the slides were washed and mounted using the anti-quenching mounting medium (Vector Laboratories, 3304770). EGFP-LC3B-expressing cells were visualized by epifluorescence on an Olympus BX41 fluorescence microscope, using DAPI, TexasRed and GFP filter cubes and the 60x objective. Cells expressing GFP-ZFYVE1 were visualized by confocal microscopy on an Olympus FV3000 microscope using the 60x objective and the lasers 405, 488, and 561 nm in order to excite DAPI, GFP, and DyLight-550, respectively. After collection, images were processed and analyzed using the ImageJ software (National Institutes of Health) and Photoshop (Adobe), and proportional adjustments of brightness/contrast were applied.

(ii) *ER-BCL2 and BECN1 colocalization.* 20,000 HEK293T cells were co-transfected in sterile tissue culture-treated 8-well slides with 100 ng of *BECN1*-Flag, 100 ng of GFP-*BCL2*-Cb5 (ER-bound isoform) and either 100 ng of HA-*GST* or NL4-3 *nef*-HA. 48 h post-transfection, cells were washed with DPBS, permeabilized and fixed by incubating them for 10 min in acetone-methanol (1:1) at -30ºC. Next, cells were incubated for 1 h with the antibody diluent solution (2% fish skin gelatin + 0.1% Triton X-100 1x DPBS with 10% goat serum) and 1 more hour with the following primary antibody cocktail: mouse monoclonal anti-HA primary antibody conjugated with DyLight-550 (**Table 5.1**) at a dilution of 1:200, and rabbit monoclonal anti-Flag (**Table 5.1**) at a dilution 1:400. Subsequently, cells were washed and incubated for

another hour with a goat anti-rabbit IgG1 secondary antibody conjugated with an Alexa 633 fluorophore (**Table 5.1**) at a dilution 1:500. Finally, samples were incubated for 5 min with DAPI (1:5,000) to visualize cell nuclei. After staining, the slides were washed and mounted using anti-quenching mounting medium. The samples were visualized by confocal microscopy on an Olympus FV3000 instrument using the 60x objective and the lasers 405, 488, 561, and 640 nm in order to excite DAPI, GFP, DyLight-550 and Alexa 633, respectively. After collection, images were merged for the 488, 561, and 640 nm channels, processed and analyzed using ImageJ and Photoshop. Proportional adjustments of brightness/contrast were applied. Colocalization between ER-BCL2 and BECN1 was evaluated in ImageJ (JACoP plugin) by calculating Pearson's correlation coefficient.

Flow cytometry

300,000 HEK293T cells were co-transfected with 2,000 ng of *EGFP-LC3B* and 2,000 ng of either NL4-3 *nef*-HA or empty vector control. 48 h post-transfection, cells were treated with rapamycin (4 μM) and/or 3-MA (3 mM) for 4 h before collection for analysis. Cells were then washed with DPBS, trypsinized (ThermoFisher Scientific, 25200) and centrifuged at 600 *x g* for 5 min, followed by an additional wash of 10 min at 4ºC with 0.05% saponin (Sigma-Aldrich, 47036) in DPBS. Cells were subsequently washed 2 additional times in DPBS. Finally, samples were fixed with 1% paraformaldehyde in DPBS. Cells were analyzed using an Attune instrument (ThermoFisher Scientific, Waltham, MA). Data were processed with the FlowJo software (version 10.5.3) using 50,000 events. Debris and doublets were excluded using FSC and SSC gating, and the percentage of EGFP-positive single cells was calculated for every sample and treatment condition.

Statistical analysis

All statistical calculations were performed with a two-tailed unpaired Student T test using Graph Pad Prism version 8.3.0. P values ≤ 0.05 were considered statistically significant.

Table 5.1. Antibody sources and conditions (hypothesis 2).

Protein	Primary antibody	Dilution	Source
ATG3	Rabbit polyclonal to ATG3	1:1000	Cell Signaling Technology, 3415S
ATG5	Rabbit polyclonal to ATG5	1:500	Cell Signaling Technology, 2630S
ATG7	Rabbit monoclonal (D12B11) to ATG7	1:500	Cell Signaling Technology, 8558S
ATG12	Rabbit monoclonal (D88H11) to ATG12	1:1000	Cell Signaling Technology, 4180S
ATG16L1	Rabbit monoclonal (D6D5) to ATG16L1	1:1000	Cell Signaling Technology, 8089S
ACTB/β-actin	Mouse monoclonal (C4) to ACTB/β-actin	1:1000	Sigma-Aldrich, MAB1501
BCL2	Mouse monoclonal (124) to BCL2	1:1000	Cell Signaling Technology, 15071S
phospho-BCL2	Rabbit monoclonal (5H2) to Phospho-BCL2/Bcl-2 (Ser70)	1:500	Cell Signaling Technology, 2827S

Table 5.1. Continued

BECN1	Rabbit monoclonal (D40C5) to BECN1	1:1000	Cell Signaling Technology, 3495S
CD4	Rabbit polyclonal	1:500	Abcam, ab203034
Flag	Rabbit monoclonal (D6W5B)	1:400	Cell Signaling Technology, 14793
GFP	Mouse monoclonal (4B10B2) and Rabbit monoclonal (E385) to GFP	1:1000 1:1000	Sigma-Aldrich, SAB5300167 Abcam, ab32146
HA	Mouse monoclonal (16B12) to HA (Dylight-550 conjugated)	1:200	Abcam, ab117502
HA	Mouse monoclonal	1:1000	Covance, 901502
LC3	Rabbit polyclonal to LC3B	1:1000	Cell Signaling Technology, 2775S
MYC	Mouse monoclonal	1:1000	Abcam, ab18185

Table 5.1. Continued

HIV Nef	Mouse monoclonal (2H12(01-007)) to HIV-1 Nef	1:1000	ThermoFisher Scientific, MA1-71505
PRKN	Mouse monoclonal (PRK8) to PRKN	1:1000	Abcam, ab77924
HIV-1 Gag p55/p24	Mouse monoclonal (183-H12-5C) to HIV p24	1:1000	NIH AIDS Reagent Program, 3537
SQSTM1/p62	Mouse monoclonal to SQSTM1/p62	1:1000	Abcam, ab56416
SUMO	Rabbit polyclonal to SUMO 2+3	1:1000	Abcam, ab139470
Ubiquitin	Rabbit monoclonal (E4I2) to Ubiquitin	1:1000	Cell Signaling Technology, 43124S
ULK1	Rabbit monoclonal (D8H5) to Ulk1	1:500	Cell Signaling Technology, 8054
UVRAG	(D2Q1Z) Rabbit monoclonal to UVRAG	1: 1000	Cell Signaling Technology, 13115S

Table 5.1. Continued

Mouse IgG	Goat polyclonal (HRP-conjugated)	1:2000	Pierce, 31430
Mouse IgG2a	Goat polyclonal (Alexa-568 conjugated)	1:500	ThermoFisher Scientific, A21134
Rabbit IgG	Goat polyclonal (HRP-conjugated)	1:2000	Abcam, ab97051
Rabbit IgG	Donkey polyclonal (HRP-conjugated)	1:2000	Abcam, ab16284

CHAPTER 6

HYPOTHESIS 3: HIV NEF'S ABILITY TO INHIBIT AUTOPHAGY IS CONSERVED AMONG CLOSELY RELATED PRIMATE LENTIVIRUSES

The figures presented in this chapter are derived from the following publication[1] in which I am first author and I have permission from the journal editorial to reproduce the figures in this thesis.

Sergio Castro-Gonzalez, Yuhang Shi, Yuexuan Chen, Marta Colomer-Lluch, Jayc Waller, Ying Song, Anju Bansal, Frank Kirchhoff, Konstantin Sparrer, Chengyu Liang and Ruth Serra-Moreno. HIV-1 Nef counteracts autophagy restriction by enhancing the association between BECN1 and its inhibitor BCL2 in a PRKN-dependent manner. *Autophagy*, 1-25, doi:10.1080/15548627.2020.1725401 (2020).

Studies on the conservation patterns of virus genes have contributed to our understanding of viral phylogenetical relationships, adaptation and their evolution. These studies have also identified virus genes that are under negative or purifying selection, meaning that they are highly conserved within a genus or even a family. Such conservation highlights the relevance of those genes for viral infectivity and fitness. With no doubt, HIV *nef* is a critical gene for infectivity and pathogenesis. Contrary to what one would expect, this gene is very variable across the primate lentiviruses, yet its functional activities remain conserved for the most part. Specifically, Nef promotes the downregulation of the immune receptors CD4, CD28, major histocompatibility complexes, and the restriction factors SERINC3 and SERINC5, offering HIV mechanisms for immune evasion[118,120,121,261,262]. Since Nef is a key virulence factor, and its ability to counteract autophagy restriction represents another mechanism to evade the innate immune response, we hypothesized that similar to its other roles, the ability of Nef to block autophagy is conserved across the primate lentiviruses.

Results

The ability of Nef to block autophagy is mainly observed in HIV-1/SIV$_{cpz}$

To investigate if Nef's ability to prevent the initiation of autophagy is conserved in other primate lentiviral species, we analyzed a set of 23 *nef* genes from primary isolates of pandemic HIV-1 as well as representative HIV-2 variants and the

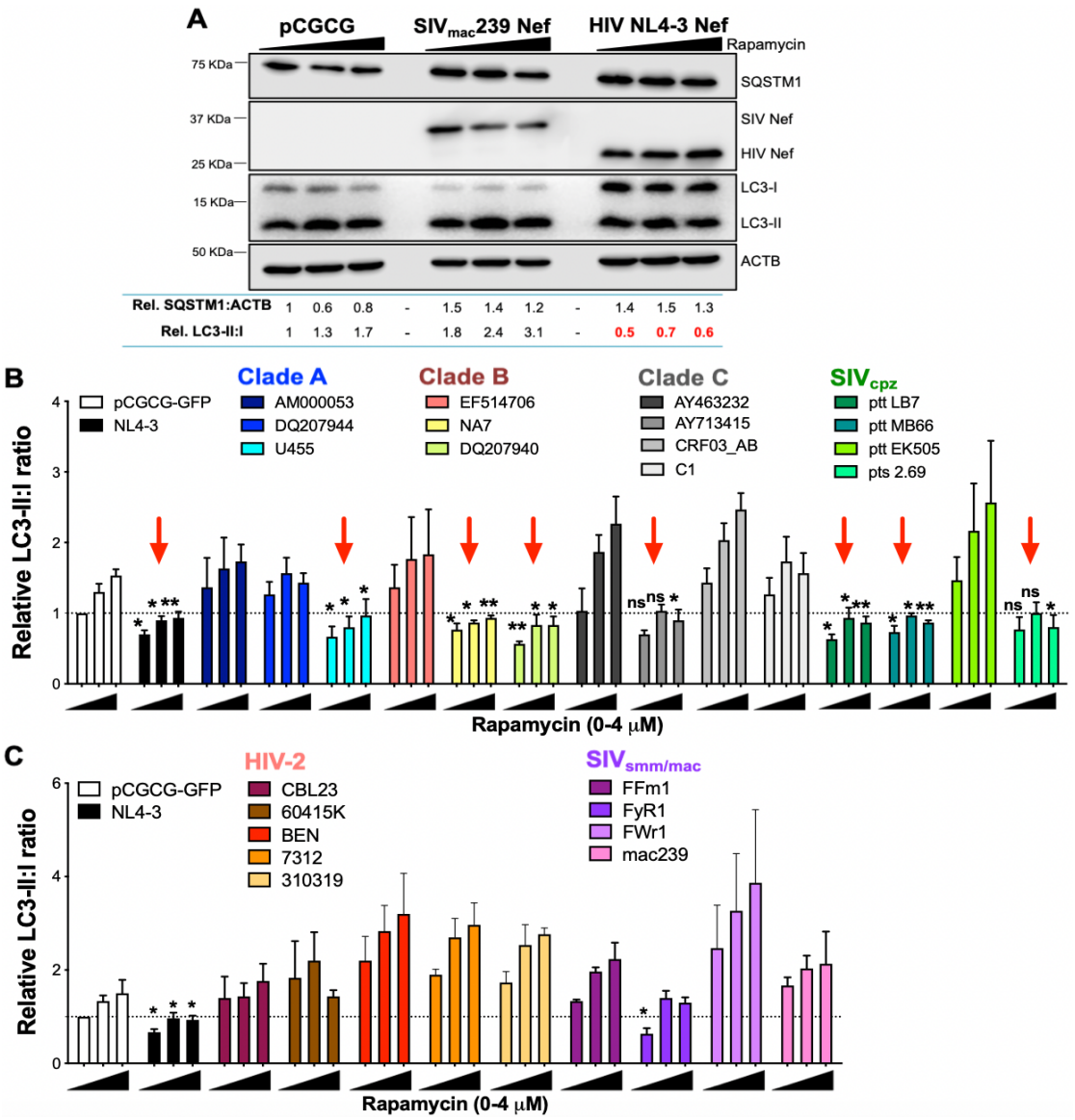

Figure 6.1. Nef's ability to inhibit autophagy is mainly observed in HIV-1/SIV$_{cpz}$. (**A**) Representative data of the analyses of the anti-autophagic properties of lentiviral Nef proteins. HEK293T cells were transfected with NL4-3 *nef*, an empty vector and SIV$_{mac}$239 *nef*. 48 h later, cells were exposed for 4 h to increasing concentrations of rapamycin (0–4 μM). Next, cells were analyzed by western blot for the levels of SQSTM1, Nef, LC3, and ACTB. Densitometric analyses were performed to determine the levels of SQSTM1:ACTB and the ratio of LC3-II over LC3-I relative to the empty vector control under no rapamycin treatment. (**B, C**) Data correspond to the mean and SEM of the relative LC3-II:I ratios from 3 independent biological replicates of different lentiviral *nef* alleles of the HIV-1/SIV$_{cpz}$ lineage (B) and HIV-2/SIV$_{smm}$ lineage (C). *: $p \leq 0.05$; **: $p \leq 0.01$; n.s. not significant. Red arrows indicate Nef alleles active against autophagy.

simian precursors of both of these human viruses (SIV$_{cpz}$ and SIV$_{smm}$). Specifically,

we assessed their ability to block autophagy by examining SQSTM1 levels and the conversion of LC3-I into LC3-II and under conditions of rapamycin stimulation. As controls, we used the empty vector (pCGCG) and NL4-3 Nef. **Fig. 6.1A** illustrates the representative results for one Nef allele; $SIV_{mac}239$ *nef*. Unlike the positive control NL4-3 Nef, the expression of $SIV_{mac}239$ Nef did not impede LC3 lipidation nor prevented SQSTM1 degradation upon rapamycin stimulation (**Fig. 6.1A**). We performed these experiments 3 independent times for each Nef allele, always together with the negative (pCGCG) and positive (NL4-3 Nef) controls, to calculate the relative LC3-II:I ratios as well as any statistical differences with the vector control under no rapamycin treatment. As previously described, relative LC3-II:I ratios <1 represent conditions of autophagy inhibition (**Fig. 6.1B**; alleles with red arrows). We found that the ability of Nef to block autophagy was mainly observed in the HIV-1/SIV_{cpz} lineage (**Fig. 6.1B** and **Fig. 6.2**; red arrows and colored squares), while this activity was

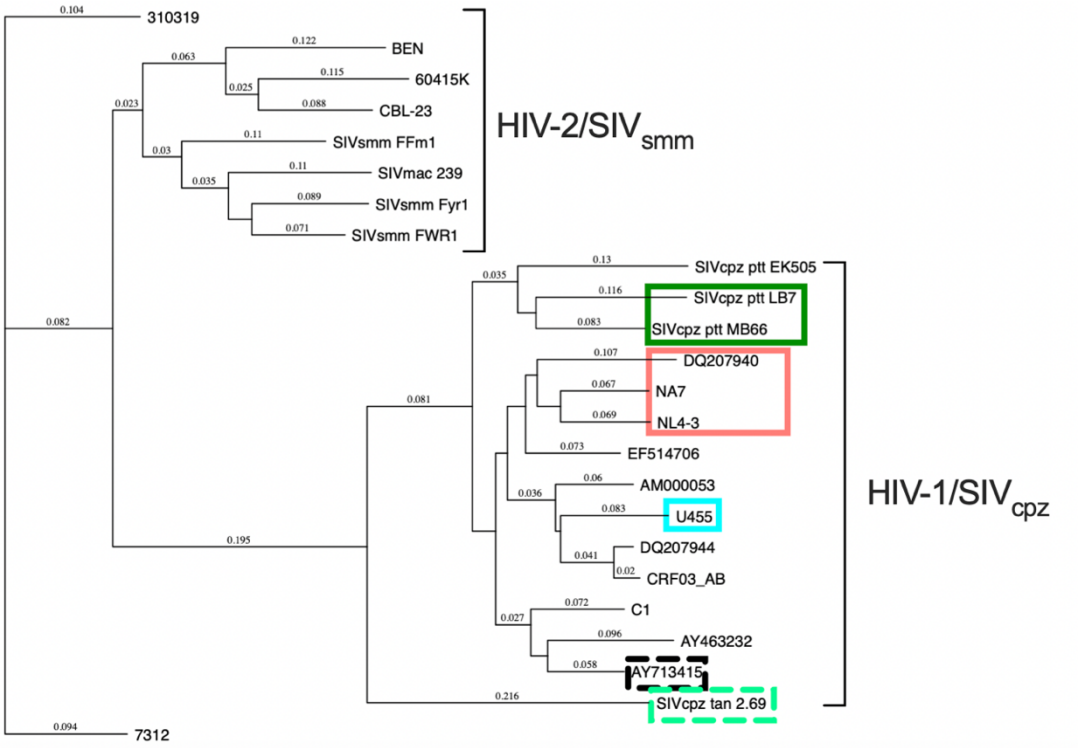

Figure 6.2. Phylogenetic profile of Nef's ability to inhibit autophagy. The amino acid sequence of Nef from the different lentiviral species was compared and clustered in a cladogram where the relative evolutionary distance between each variant is shown. Color-coded squares are used to identify species in which Nef is able to inhibit autophagy (solid line) or exhibit partial activity (dashed line).

largely missing in the HIV-2/SIV$_{smm}$ panel (**Fig. 6.1C** and **Fig. 6.2**). We confirmed these findings by flow cytometry analysis. Similar to our previous observations with NL4-3 Nef, alleles exhibiting an impact on LC3 lipidation were also associated with a decrease in autophagosome formation, illustrated in **Fig. 6.3** by relatively lower levels of the autophagosome-associated fluorescent protein EGFP-LC3B.

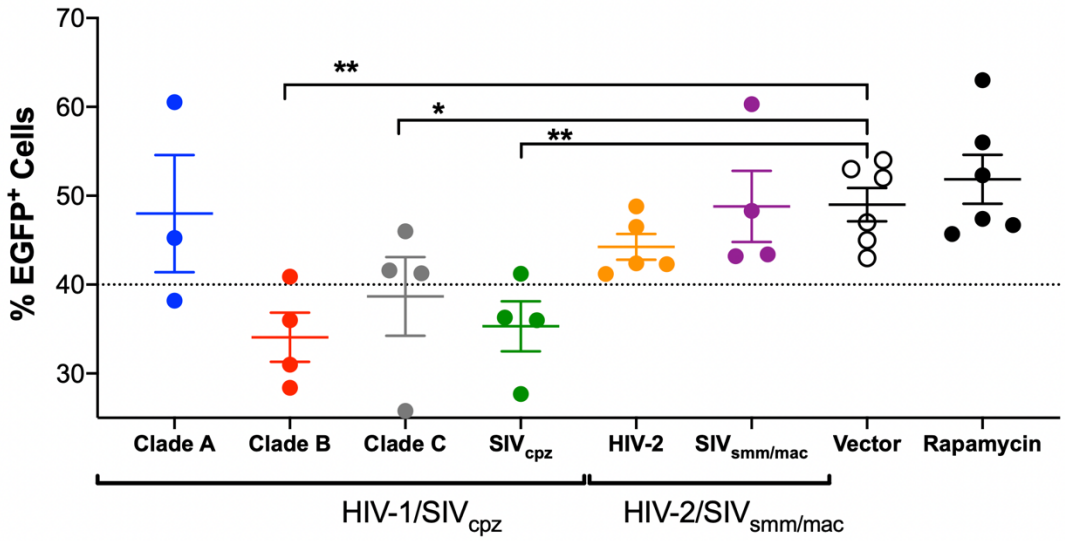

Figure 6.3. Nef alleles from SIV$_{cpz}$ and the pandemic clades of HIV-1 inhibit autophagosome formation. HEK293T cells were co-transfected with EGFP-*LC3B* and an empty vector or the different *nef* alleles belonging to the HIV-1/SIV$_{cpz}$ lineage and the HIV-2/SIV$_{smm}$ lineage. As a positive control, a set of cells was treated with rapamycin (4 μM). 48 h post-transfection, cells were analyzed by flow cytometry for autophagosome-associated EGFP-LC3B. Data correspond to the mean and SEM of the percentage of EGFP$^+$ cells from 3 independent experiments. Each point represents the mean of 3 independent experiments for each Nef isolate. *: $p \leq 0.05$; **: $p \leq 0.01$.

Primate lentiviruses exhibit high plasticity in the use of their accessory proteins to overcome restriction factors. This plasticity is particularly evident for Tetherin/BST-2. Whereas HIV-1 primarily uses Vpu as a BST-2 countermeasure, HIV-2 uses Env, and the majority of SIVs use Nef [51,95,111,114,263-266]. Therefore, it would not be surprising if HIV-1/SIV$_{cpz}$ use Nef as their primary autophagy antagonist, while members of the HIV-2/SIV$_{smm}$ lineage devote a different protein for this task. To test this hypothesis, we transfected HEK293T cells with the full-length

proviral DNA of $SIV_{mac}239$, the viral isolate whose Nef allele is a poor autophagy antagonist (**Fig. 6.1A**). $SIV_{mac}239$ was originated after the cross-species transmission of SIV_{smm} from sooty mangabeys to rhesus macaques. In addition to the wild-type virus, we also included $SIV_{mac}239$ mutants harboring deletions in *nef* and *env* as well as the molecular clone of SIV Δ*nef*P, a virus that regained virulence after serial passage in rhesus macaques by accumulating compensatory mutations in $gp41^{223,267}$. As controls, we included an empty retroviral vector, and the proviral DNA of wild type NL4-3 and NL4-3 Δ*nef* . Compared to HIV-1 NL4-3, none of the $SIV_{mac}239$ clones tested were able to overcome autophagy, since they did not affect the conversion of LC3-I into LC3-II, and the relative levels of SQSTM1 were considerably lower than NL4-3, reflecting normal autophagy flux (**Fig. 6.4**; left panel). Once again, the relative LC3-II:I ratios were quantified and normalized to the empty vector control. Accordingly, the ratios corresponding to the $SIV_{mac}239$ clones were significantly higher than wild-type NL4-3, indicating the absence of any alternative protein encoded by this SIV isolate with the potential to intersect with autophagy progression (**Fig. 6.4A**; right panel). Consistent with these findings, when we challenged HEK293T cells transfected with $SIV_{mac}239$ or $SIV_{mac}239$ Δ*nef* to rapamycin stimulation, we observed a similar dramatic reduction in particle release, which indicates that autophagy poses a hurdle for SIV, but unlike HIV-1, $SIV_{mac}239$ does not seem to have evolved any mechanism to counteract this restriction (**Fig. 6.4B**).

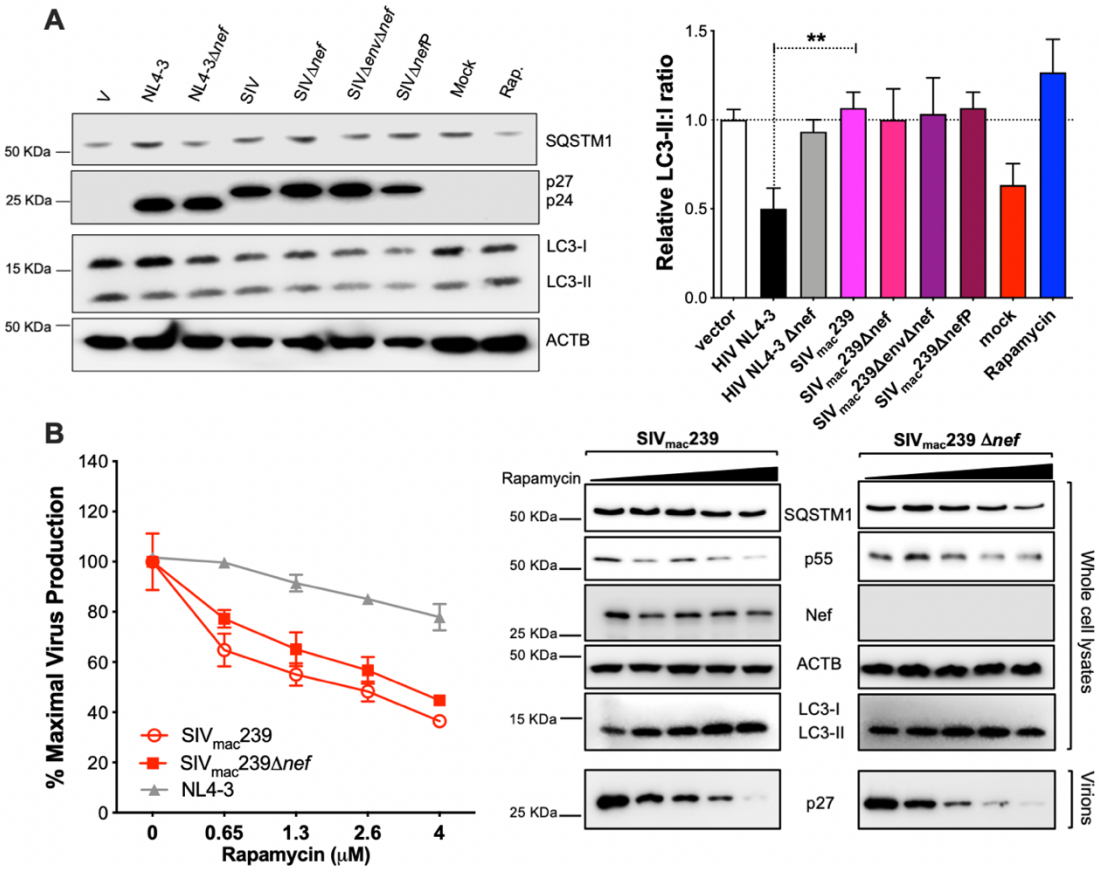

Figure 6.4. SIV$_{mac}$239 is sensitive to autophagy restriction. (**A**) Left panel: HEK293T cells were transfected with the full-length proviral DNA of SIV$_{mac}$239 or mutants of this molecular clone, such as Δ*nef*, Δ*env*Δ*nef* and Δ*nefP*. As controls, the proviral DNA of full-length HIV-1 NL4-3, NL4-3 Δ*nef* and an empty retroviral vector were included, in addition to mock treated cells and cells treated with rapamycin. 48 h later, cell lysates were analyzed by western blot showing the levels of SQSTM1, capsid p27 and p24, LC3, and ACTB. Right panel: The ratio of LC3-II:I relative to the vector control was calculated from 3 biological experiments. (**B**) Left panel: HEK293T cells were transfected with the proviral DNA of SIV$_{mac}$239, SIV$_{mac}$239 Δ*nef* and HIV-1 NL4-3, as a control. Cells were then exposed to rapamycin at the selected concentrations for 12 h and the percentage of maximal virus production was measured by the amounts of SIV p27 or HIV p24 accumulated in the culture supernatant, as described previously. Data correspond to the mean and SEM of 3 independent experiments. Right panel: Representative western blot for SQSTM1, Gag p55, Nef, ACTB , and LC3. Capsid p27 from pelleted virions is also provided. V: vector. **: $p \leq 0.01$.

The N-terminal domain of HIV Nef is required to counteract autophagy

As stated earlier, the primary sequence of Nef differs significantly across the primate lentiviruses. For instance, a comparison between $SIV_{mac}239$ Nef and NL4-3 Nef evidences such disparities, not only in amino acid composition, but also in protein size[126]. Despite these differences, four functional domains can be found in Nef, and these domains harbor motifs that show some degree of conservation. Since unlike NL4-3 Nef, $SIV_{mac}239$ Nef lacks any capacity to inhibit autophagy, we generated chimeras of these two proteins by swapping individual functional domains with the goal to perform a loss-of-function assay and reveal the specific residues in NL4-3 Nef responsible for autophagy antagonism. For this, we replaced the four individual domains in NL4-3 Nef (N-terminus, globular core, flexible loop and C-terminus) by the 'inactive' domains from $SIV_{mac}239$ Nef (**Fig. 6.5**), generating the chimeras I, II, II and IV.

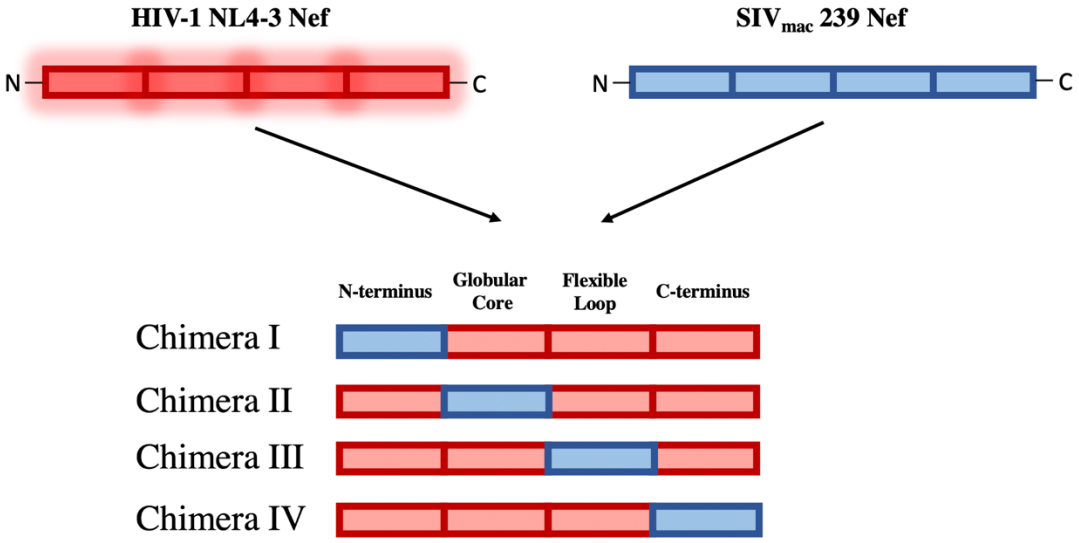

Figure 6.5. SIV/HIV Nef chimeras. Schematic representation of the domain substitution for the generation of the four chimeras between HIV-1 NL4-3 and $SIV_{mac}239$ Nef.

In order to determine whether these chimeras were able to intersect with autophagy, we first analyzed by western blot the relative levels of LC3 lipidation in cells expressing the chimeric proteins. $SIV_{mac}239$ Nef and NL4-3 Nef were used as

negative and positive controls, respectively (**Fig. 6.6A**). All Nef alleles, including these chimeras, were cloned using the vector pCGCG, which harbors EGFP from an internal ribosomal entry site. This feature was especially useful for these assays, since in some instances the modification of the native proteins modified the epitope where the anti-HIV Nef antibodies binds. Therefore, we analyzed transfection efficiency and the expression of our constructs by monitoring the levels of EGFP. In addition, we measured the relative LC3-II:I ratios by densitometry analysis from three independent replicates, which we normalized to $SIV_{mac}239$ Nef transfected cells with no rapamycin stimulation (**Fig. 6.6B**). Our results indicate that NL4-3 Nef, together with the

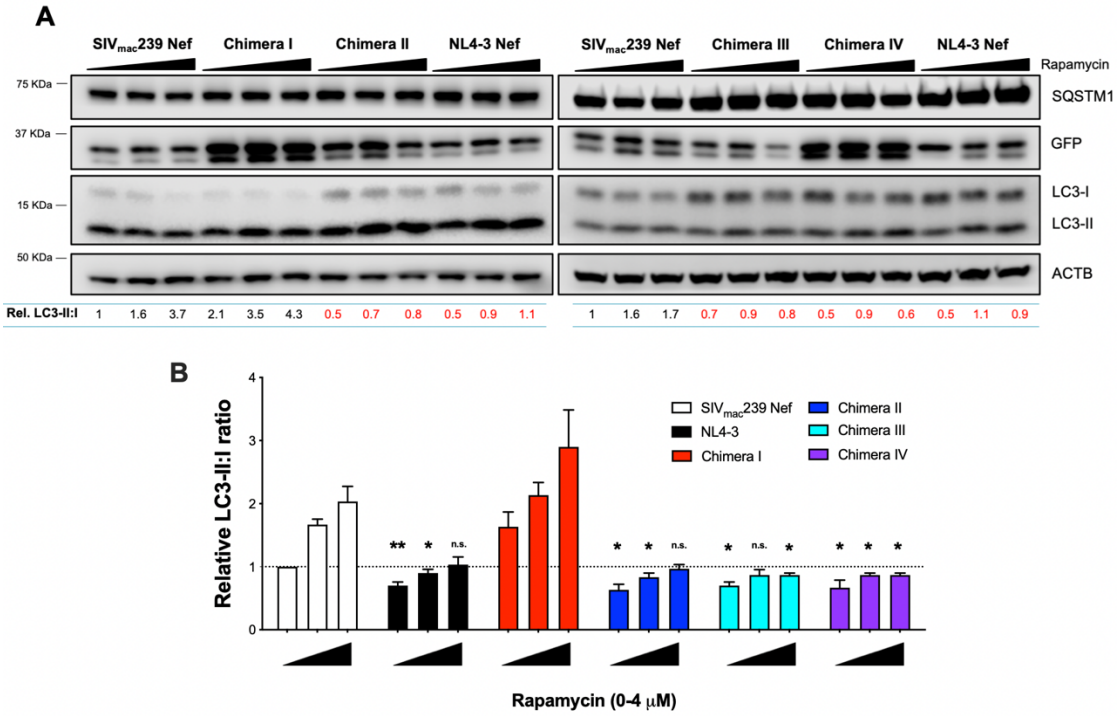

Figure 6.6. The N-terminus of HIV Nef is required to inhibit LC3 lipidation. (**A**) Representative data of the analyses of the anti-autophagic properties of the chimeric Nef proteins. HEK293T cells were transfected with NL4-3 *nef*, the Chimeras I-IV and $SIV_{mac}239$ *nef*. 48 h later, cells were exposed for 4 h to increasing concentrations of rapamycin (0–4 μM). Next, cells were analyzed by western blot for the levels of SQSTM1, GFP, LC3, and ACTB. Densitometric analyses were performed to determine the ratio of LC3-II over LC3-I relative to the $SIV_{mac}239$ *nef* no rapamycin treatment. (**B**) Data correspond to the mean and SEM of the relative LC3-II:I ratios from 3 independent biological replicates. *: $p \leq 0.05$; **: $p \leq 0.01$; n.s. not significant.

chimeras II, III, and IV, were able to reduced LC3 lipidation, whilst the chimera I, as well as the negative control $SIV_{mac}239$ Nef, showed significantly higher ratios of LC3-II:I and thus, normal autophagy progression (**Fig. 6.6B**). Hence, these findings indicate that the capacity of NL4-3 Nef to block LC3 lipidation resides somewhere along the N-terminal domain of the protein, which is the domain that was replaced to generate the chimera I. To corroborate these observations, we next evaluated the subsequent impact of the chimeras on autophagosome formation by flow cytometry assays, employing the fluorescence protein EGFP-LC3, as previously described. In this case, we detected lower levels of autophagosome-associated EGFP-LC3 in cells expressing the chimeras II, III and IV, in opposition to the chimera I, which lacked the capacity to prevent autophagosome formation (**Fig. 6.7**). Therefore, we can conclude that the N-terminal domain of the protein NL4-3 Nef is required for its ability to inhibit the lipidation of LC3 and formation of autophagosomes. However, further analyses are necessary in order to determine the specific residues within the N-terminus involved in such inhibitory activity.

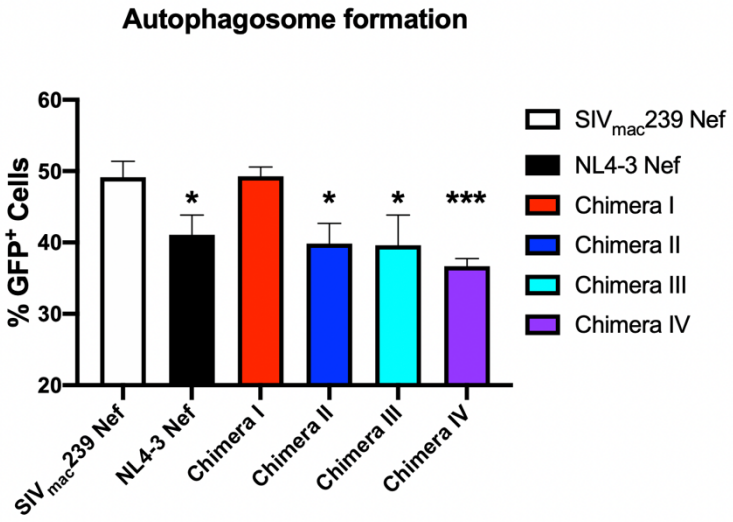

Figure 6.7. The N-terminus of HIV Nef is required to inhibit the formation of autophagosomes. HEK293T cells were co-transfected with EGFP-*LC3B* and an the different *nef* constructs: $SIV_{mac}239$ *nef*, NL4-3 *nef* and the Chimeras I-IV. 48 h post-transfection, cells were analyzed by flow cytometry for autophagosome-associated EGFP-LC3B. Data correspond to the mean and SEM of the percentage of $EGFP^+$ cells from 3 independent experiments. *: $p \leq 0.05$; **: $p \leq 0.01$; ***: $p \leq 0.001$; ****: $p \leq 0.0001$.

The inhibition of autophagy initiation is independent of the class III PtdIns3K complex II binding domain in Nef

Previous studies have pointed to a region in the N-terminus of Nef as being responsible for blocking autophagy maturation. Specifically, amino acids $D_{36}LEK_{39}$ in NL4-3 Nef mimic sequences used by RUBCN/Rubicon, an autophagy inhibitor that affects the functionality of class III PtdIns3K complex II[132]. These amino acids constitute a PI3KC3-binding domain (PIKBD) for both Nef and RUBCN, and it has been reported that both proteins use these residues to directly bind to the class III PtdIns3K complex II and preclude autophagy maturation. To explore if Nef also uses this domain to intersect with the initiation stages of autophagy, we introduced alanine substitutions in this region of Nef ($Nef^{A36\text{-}A39}$) and examined autophagosome formation by flow cytometry and western blotting, as explained above (**Fig. 6.8**). Remarkably, the $Nef^{A36\text{-}A39}$ mutant exhibited a different western blot migration pattern compared to wild type NL4-3 Nef, although their expression levels remained similar (**Fig. 6.8B** and **Fig. 6.8C**). Sequencing verification analyses indicated that our mutagenesis protocol did not incorporate additional nucleotide changes in the expression vector or the Nef coding region. Therefore, we concluded that the hydrophobic residues introduced in the RUBCN-like motif were responsible for this phenotype. Despite this unusual migration profile, $Nef^{A36\text{-}A39}$ retained the ability to block autophagosome formation, depicted by significantly lower membrane-associated EGFP-LC3B than the vector control (**Fig. 6.8A**). Accordingly, $Nef^{A36\text{-}A39}$ caused substantial retention in LC3-I, even greater than wild type Nef (**Fig. 6.8B**), indicating that this domain is dispensable to block autophagy initiation. In fact, $Nef^{A36\text{-}A39}$ still increased the association between BECN1 and BCL2 (**Fig. 6.8C**). By contrast, expression of this mutant significantly reduced the accumulation of LC3-II (**Fig. 6.8B**), which is consistent with previous reports showing that this motif is necessary to prevent autophagy maturation[132]. Therefore, despite being required for the inhibitory effect on autophagy maturation, the PIKBD in Nef is not responsible for hindering the early stages of the pathway, indicating that Nef uses two different mechanisms on separate domains to repress both autophagy initiation and maturation.

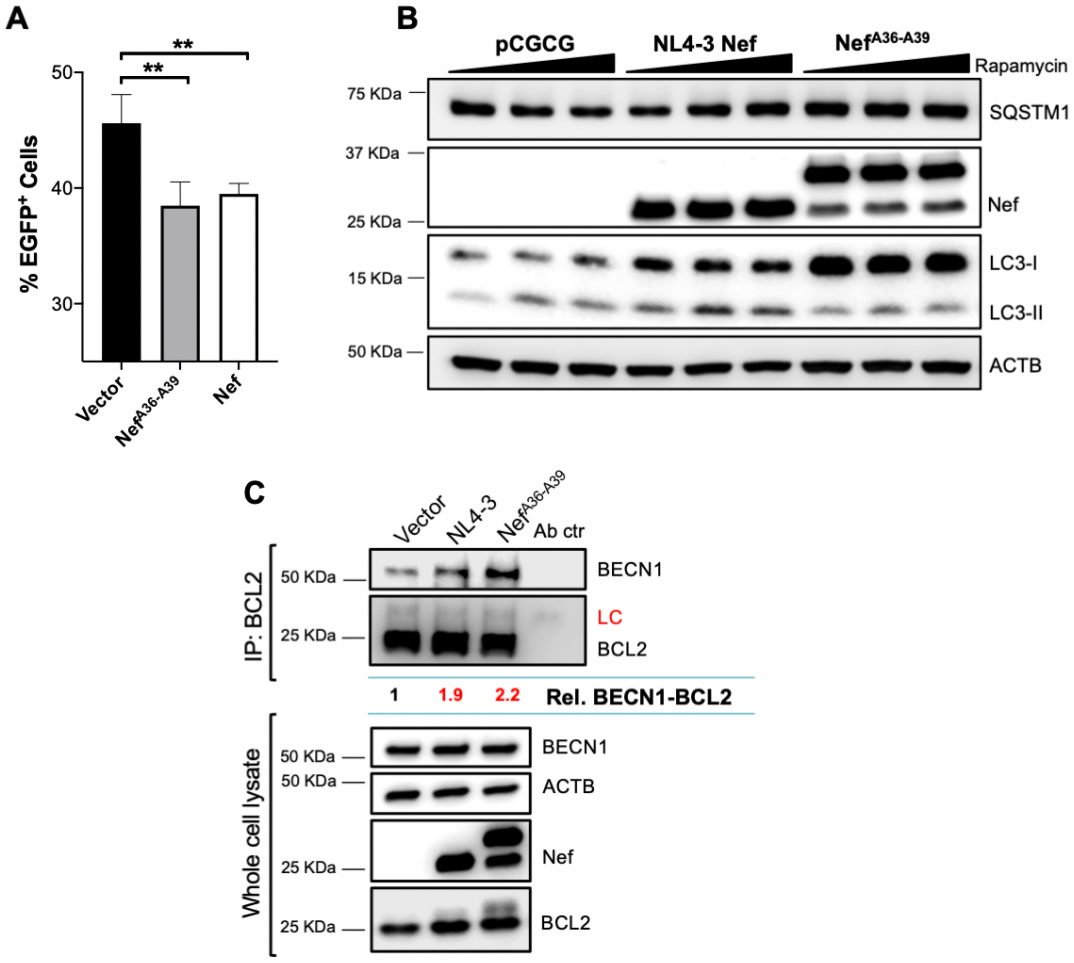

Figure 6.8. Nef's ability to inhibit autophagy initiation is independent of its PIKBD motif. HEK293T cells were transfected with pCGCG-EGFP or pcDNA5 (as vector controls), NL4-3 *nef* or NL4-3 *nef*-HA (used to express the wild-type HIV-1 Nef) and Nef$^{A36\text{-}A39}$ to evaluate (**A**) the ability of this mutant to block autophagosome formation by flow cytometry, through the accumulation of autophagosome-associated EGFP-LC3B; (**B**) its ability to prevent the lipidation of LC3 by western blot; and (**C**) its ability to enhance the BECN1-BCL2 interaction by co-immunoprecipitation. Data correspond to the mean and SEM of 4 independent experiments. Rel: relative. Ab ctr: antibody control. LC: light chain. *: $p \leq 0.05$; **: $p \leq 0.01$.

HIV-1 transmitted/founder viruses derived from pandemic clades B and C conserve the ability to counteract autophagy

As explained above, pandemic HIV-1 is further classified into different clades or subtypes. Individuals that are chronically infected with these HIV-1 subtypes do not carry a single genetic variant, but a highly diverse population of clones with various phenotypic traits. Among these viral clones, there is a particular set constituted by the so-called transmitted/founder viruses (T/F), which play a very important role in mucosal transmission between individuals and are considered highly infectious. Due to the selective forces acting during these transmissions, not all viral variants are fit enough to cross the innate immune barriers present in the new host, which causes a bottleneck effect. In this regard, only the T/F viruses, which possess a relatively higher infectivity and resistance to innate immune-related responses, are capable to successfully infect and establish a chronic infection in the new individual[268-271]. Once the chronic infection is established and the HIV-associated $CD4^+$ cell dysfunction effects emerge, the subsequent reduction of the selective pressure allows other viral clones to thrive (**Fig. 6.9**). Therefore, studies on particular properties within T/F

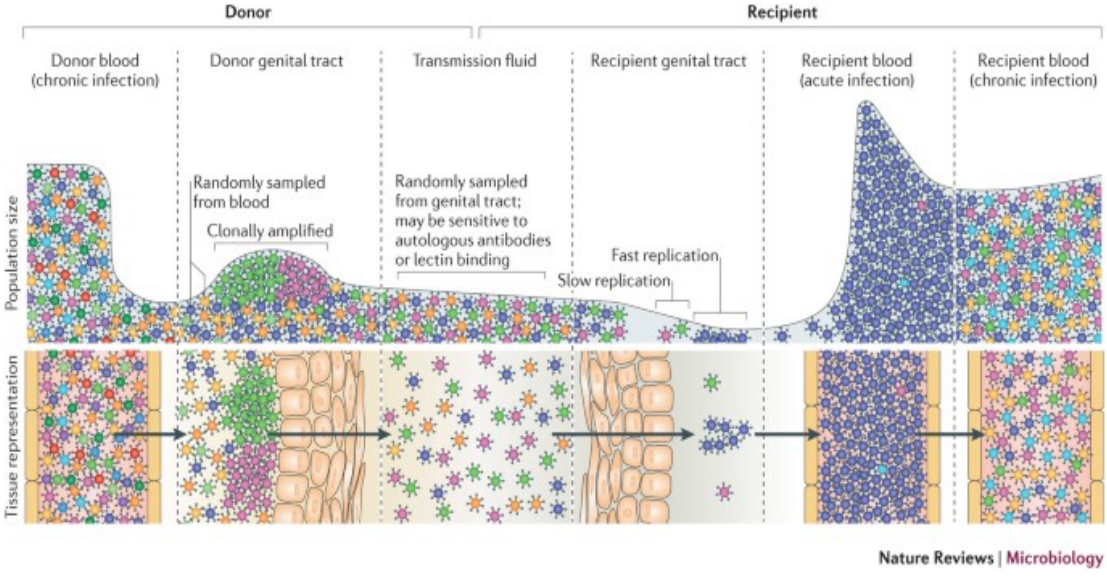

Figure 6.9. Representation of the bottleneck on HIV clone variability during mucosal transmission. Figure adapted from Joseph *et al.*, 2015.

viruses are not only important for the identification of features associated with pathogenicity or infectivity, but also for the design of future therapeutic and preventive strategies, which would be benefited from the bottleneck impact on viral diversity.

As a first approach to investigate whether autophagy counteraction is important for infectivity and pathogenesis, we assessed if this activity is a common feature among pandemic HIV-1 T/F viruses. For this, we evaluated the endurance of ten different T/F viruses to rapamycin treatment. For this, we selected T/F clones that belong to the pandemic subtypes B and C. Importantly, the combination of these two HIV-1 clades represent more than 60% of all current infections worldwide[29,272]. For this study, we transfected HEK293T cells with the proviral DNA of the different viral clones, using wild-type NL4-3 and NL4-3 Δ*nef* as positive and negative controls, respectively. 36 h later, autophagy was induced by treating the cells with rapamycin at a concentration of 4 μM for 18 h. Finally, the cell lysates were collected and analyzed by western blot, and the culture supernatants were used to measure virion production by p24 ELISA (**Fig. 6.10A, Fig. 6.10B**). Remarkably, all T/F viruses showed little reduction on both viral release and intracellular levels of HIV Gag upon rapamycin treatment, in contrast to the great impact observed on the autophagy-sensitive mutant NL4-3 Δ*nef* (**Fig. 6.10A, Fig. 6.10B**). Notably, the ability to circumvent autophagy was especially obvious for the T/F clones that belong to the subtype C, which constitute the most prevalent clade worldwide. Next, we evaluated the effect of these viruses on autophagosome formation by flow cytometry. In agreement with previous observations, most T/F viruses, regardless of the pandemic clade they belong to, were able to prevent autophagosome formation, even more efficiently than the prototype NL4-3 clone, indicated by the relatively lower levels of autophagosome-bound EGFP-LC3B (**Fig. 6.10B** and **6.10C**). Hence, altogether our data suggest that all the pandemic T/F viruses analyzed potently intersect with the generation of autophagosome structures, and therefore, counteract autophagy-mediated restriction. Since this activity was observed in all primary isolates, we conclude that autophagy antagonism is critical for the successful spread of HIV-1.

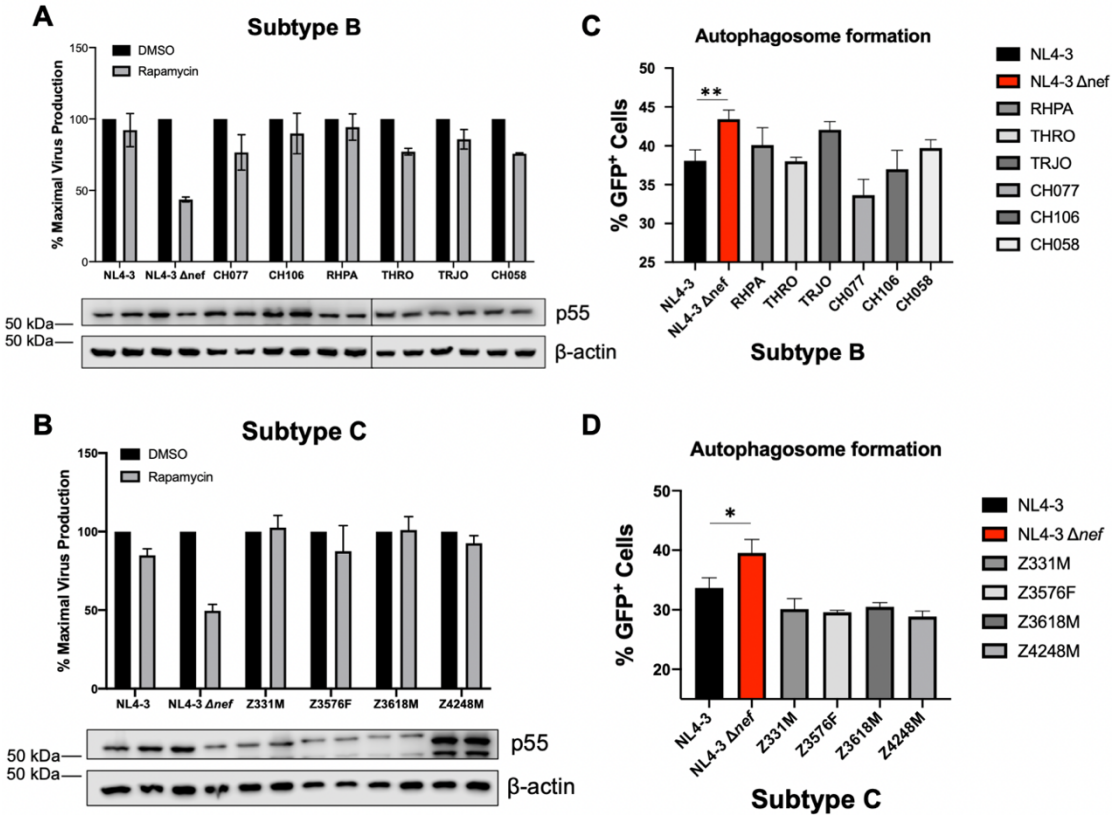

Figure 6.10. Transmitted/founder (T/F) viruses from clades B and C conserve the ability to antagonize autophagy. (**A, B**) HEK293T cells were transfected with HIV-1 NL4-3 or HIV-1 NL4-3 Δ*nef* and 10 different T/F clones that belong to the pandemic HIV-1 subtype B (A) or subtype C (B). 24 h later, the cell medium was replaced and supplemented with rapamycin (4 μM) or DMSO. 18 h later, the percentage of maximal virus production was measured by the accumulation of HIV p24 in the culture supernatant relative to the DMSO treatment. Bottom panels: Cells lysates were also analyzed by western blot for Gag/p55 and ACTB. In each case, the percentage of maximal virus production is indicated as the mean and SEM from 3 independent biological replicates. (**C, D**) HEK293T cells were co-transfected with EGFP-*LC3B* and HIV-1 NL4-3, HIV-1 NL4-3Δ*nef* or the 10 different T/F clones that belong to the pandemic HIV-1 subtype B (C) and subtype C (D). 48 h post-transfection, cells were analyzed by flow cytometry for autophagosome-associated EGFP-LC3. Data correspond to the mean and SEM of the percentage of $EGFP^+$ cells from 3 independent experiments. *: $p \leq 0.05$; **: $p \leq 0.01$.

Discussion

The virus protein Nef is well-known for its ability to facilitate immune evasion through multiple mechanisms, and most of these activities are conserved among primate lentiviruses [261,262,273,274]. Unlike these well-preserved functions, our screens of primary Nef alleles from HIVs and SIVs indicate that the ability to counteract autophagy restriction is mainly found in the HIV-1/SIV_{cpz} lineage. Specifically, pandemic HIV-1 clade B Nef alleles are potent autophagy antagonists. Although clade C isolates are most prevalent due to their high incidence in Africa and Asia, isolates belonging to clade B are ubiquitously found around the globe and have become the most widespread isolates in the Western world, suggesting that autophagy antagonism may be influencing the spread and pathogenesis of HIV-1.

The fact that some Nef alleles from primary SIV isolates are poor autophagy antagonists suggests that these viruses are either unable to antagonize the autophagy block or that they have evolved other genes for this purpose. To test this hypothesis, we tested $SIV_{mac}239$, a virus we have extensively studied due to its plasticity to overcome restriction factors [51,113,222,223], for its ability to antagonize autophagy. Unlike HIV-1 NL4-3, $SIV_{mac}239$ failed at impairing autophagy flux, and thus, was highly susceptible to autophagy restriction, indicating that $SIV_{mac}239$ has not evolved alternative mechanisms to counteract the autophagy block. However, since species-specific differences have dictated the adaptation and evolution of the primate lentiviruses in their respective hosts, we cannot fully rule out that the inability of $SIV_{mac}239$ to counteract autophagy in the context of HEK293T cells (of human origin) is due to species-specific differences in the autophagy proteins targeted by Nef between humans and non-human primates. Although autophagy is highly conserved in mammals, we found that the C-terminus of BCL2 is highly divergent between humans and macaques. Of note, the C-terminus harbors the lysine residues susceptible to mono-ubiquitination. We have cloned the rhesus macaque BCL2 ortholog and are currently assessing its functionality as a BECN1 inhibitor in macaque cells. We are also investigating this potential scenario by reproducing some of these experimental approaches in the context of Rhesus Macaque $CD4^+$ T cells.

Although we cannot fully rule out the inability of $SIV_{mac}239$ to counteract autophagy, we were still able to take advantage of the fact that $SIV_{mac}239$ Nef possesses no inhibitory effect over autophagy progression in a human cellular context. For this, we created four chimeric Nef proteins by swapping the individual structural domains in NL4-3 Nef by the corresponding domains in $SIV_{mac}239$ Nef. These assays allowed us to identify the N-terminus of NL4-3 as accountable for the inhibition of autophagy initiation. Interestingly, the Hurley lab recently identified a region within the N-terminal domain of Nef with the potential to bind to the Class III PtdIns3K C2 and 'switch off' autophagy maturation[132]. However, our results clearly indicate that this domain in Nef is dispensable for its ability to prevent the initial steps of autophagy. Consequently, we conclude that NL4-3 Nef uses two different motifs/mechanisms to block both autophagy initiation and maturation.

To date, no study has addressed yet what the role of autophagy antagonism is in HIV infectivity and pathogenesis. One way to investigate this is by generating HIV-1 NL4-3 clones harboring mutations in the residues that account for this activity, infect $CD4^+$ T cells and assess how the lack of anti-autophagy activity affects virus replication. In order to perform these experiments, we need to know the exact residues in Nef responsible for this activity. As stated above, these mapping studies are still in process. To complement that work, we evaluated the susceptibility of various primary pandemic HIV-1 T/F viruses to autophagy restriction. As detailed earlier, T/F isolates are considered highly infectious. Strikingly, all primary T/F clones tested displayed high levels of autophagy antagonism as well as the capacity to prevent autophagosome formation, suggesting that HIV's ability to circumvent autophagy is partially responsible for the distinctive viral fitness that characterizes these exceptionally infectious and pathogenic isolates. Furthermore, whilst Nef from chronic primary isolates belonging to the subtype C failed to inhibit autophagy (**Fig. 6.1B** and **6.3**), T/F viruses (full-length) derived from this same subtype were successful at eluding the detrimental effect of autophagy. Of note, since for the T/F virus experiments we used the full-length proviral DNA of these isolates, these results suggest that either subtype

C isolates tested in figures 6.1 and 6.3 use proteins other than Nef to counteract autophagy restriction or that distinct genetic variations in *nef* between chronic and T/F isolates account for this difference in phenotype. We are currently in the process of cloning individual subtype C T/F virus genes to answer this question.

In conclusion, the ability of Nef to counteract autophagy is not widely conserved across all primate lentiviruses as we anticipated. Instead, whilst preserved among the pandemic clades of HIV-1, Nef alleles of the HIV-2 and SIV_{sm} lineage are poor autophagy antagonists. These results could explain the relatively lower pathogenicity observed in HIV-2 viruses in comparison to the pandemic HIV-1. However, since HIVs and SIVs are well known for their plasticity to circumvent restriction factors, it is also possible that whereas HIV-1/SIV_{cpz} use to Nef as the primary autophagy countermeasure, HIV-2/SIV_{sm} utilize another gene for this particular purpose. Further genetic analyses are required in order to provide an absolute answer to this question.

Materials and methods

Plasmid DNA constructs

(i) *HIV-1 proviral clones.* The following full-length proviral constructs were obtained through the NIH AIDS Reagent Program, Division of AIDS, NIAID, NIH. Specifically, full-length constructs for wild type HIV-1 NL4-3 (pNL4-3, 114) from Dr. Malcolm Martin[260], NL4-3 Δ*nef* (pNL4-3 ΔNef, 12755) from Dr. Olivier Schwartz[259], the subtype B transmitted founders clones CH077 (pCH077.t/2627, 11742), CH106 (pCH106.c/2633, 11743), RHPA (pRHPA.c/2635, 11744), THRO (pTHRO.c/2626, 11745), TRJO (pTRJO.c/2851, 11747), CH058 (pCH058.c/2960, 11856) were obtained from Dr. John Kappes and Dr. Christina Ochsenbauer, and the subtype C transmitted founder clones Z331M (pZ331M, 13248), Z3576 (pZ3576F, 13256), Z3618 (pZ3618M, 13262), Z4248 (pZ4248M, 13277) were obtained from Dr. Eric Hunter[270,275-277]. HIV-1 viruses based on these plasmids were generated by transient transfection in HEK293T cells, as previously described[51,113,221].

(ii) *SIV_{mac} 239 proviral clones.* Full-length SIV_{mac} 239 proviral DNA as well as mutants of this molecular clone, Δ*nef*, Δ*env*Δ*nef* and Δ*nef*P, were a gift from Dr. David T. Evans (University of Wisconsin, Madison, WI). These constructs were assembled from p239SpSp5', pSP72-239-3', pSP72-239-3'Δ*nef*, pSP72-239-3'Δ*env* and p3'ITMΔ*nef*ΔUS138, as previously described[51,113,267,278,279].

(iv) *HIV and SIV Nef expression vectors.* The expression vector pCGCG (a gift from Dr. Jacek Skowronski; Case Western Reserve University, Cleveland, OH), which harbors EGFP from an internal ribosomal entry site, was used to clone different Nef alleles using the XbaI and MluI unique restriction sites. The following Nef alleles were cloned into this vector: HIV-1 NL4-3 Nef, HIV-1 CRF03_AB Nef, HIV-1 C1 Nef, HIV-1 U455 Nef, HIV-1 AY713415 Nef, HIV-1 AY463232 Nef, HIV-1 AM000053 Nef, HIV-1 DQ207940 Nef, HIV-1 DQ207944, HIV-1 EF514706, HIV-1 NA7 Nef, HIV-2 CBL-23 Nef, HIV-2 60415K Nef, HIV-2 BEN Nef, HIV-2 7312 Nef, HIV-2 310319 Nef, SIV_{cpz} ptt LB7 Nef, SIV_{cpz} ptt MB66 Nef, SIV_{cpz} ptt EK505 Nef, SIV_{cpz} pts 2.69 Nef, SIV_{sm} FFm1 Nef, SIV_{sm} FyR1 Nef, SIV_{sm} FwR1 Nef, and SIV_{mac} 239 Nef[51,107,116,262,265]. NL4-3 $Nef^{A36\text{-}A39}$ was generated by site-directed mutagenesis and cloned into pCGCG. The four chimeric proteins between NL4-3 Nef and SIV_{mac}239 Nef (I, II, III, IV) were obtained by substituting the 4 domains (N-terminus, globular core, flexible loop and C-terminus) in NL4-3 Nef by the corresponding domains in SIV_{mac}239 Nef using overlapping PCR.

(v) *Plasmids coding for autophagy proteins.* The following construct was obtained through Addgene: pC3-EGFP-LC3B (11546, Dr. Karla Kirkegaard's lab).

Transfections

6 x 10^5 HEK293T (American Type Culture Collection [ATCC], CRL-11268) (NIH AIDS Reagent Program, Division of AIDS, NIAID, NIH from Dr. Richard Axel; 153) cells were transfected using GenJet *in vitro* DNA transfection reagent (SignaGen Laboratories, SL100488), following the manufacturer's suggestions, including total DNA, dish size, incubation time, and the ratio of GenJet:DNA for optimal transfection

efficiency. Cell viability was monitored for every transfection to evaluate if the expression of the above-described constructs could cause cellular toxicity or damage. No evidence of toxicity was observed. If viability was below 85%, cells were considered unsuitable for further analyses. Viabilities were usually above 90%.

Virus release assays

6 x 10^5 HEK293T cells were transfected with 2,000 ng of full-length proviral DNA of HIV-1 NL4-3 and NL4-3 Δ*nef*; SIV_{mac} 239, and SIV_{mac} 239 Δ*nef*; HIV-1 transmitted/founder viruses CH077 (pCH077.t/2627), CH106 (pCH106.c/2633), RHPA (pRHPA.c/2635), THRO (pTHRO.c/2626), TRJO (pTRJO.c/2851), CH058 (pCH058.c/2960), Z331M (pZ331M), Z3576 (pZ3576F), 3618 (pZ3618M), and Z4248 (pZ4248M). 36 h post-transfection, the cell medium was replaced, and rapamycin (Sigma-Aldrich, R8781) was added at different concentrations (0–4 μM). 48 h post-transfection, the culture supernatants were collected and analyzed by p24 or p27 antigen-capture ELISA (Advanced Biolabs, 5421 and 5436), as previously described[51,113,221-223]. In addition, cells were washed, lysed, and harvested for their analysis by western blotting.

Immunoprecipitation assays

One million HEK293T cells were transfected with 2,000 ng of *BECN1*-Flag and NL4-3 *nef* , the mutant NL4-3 $Nef^{A36-A39}$ or the empty vector pCGCG. 48 h post-transfection, cells were washed and lysed using lysis IP buffer supplemented with phosphatase and protease inhibitor cocktails, as detailed above. The whole-cell lysates were then pre-incubated for 1 h at room temperature with Protein A or G magnetic beads (New England Biolabs, S1425S and S1430S) to remove unspecific binding proteins. Protein A or G magnetic beads were then coated with the antibody specific for BCL2 (**Table 6.1**) for 1 h at room temperature. Next, cell lysates were subjected to immunoprecipitation by adding antibody-coated beads to the pre-cleared samples. The immunoprecipitation proceeded overnight at 4°C. Next, beads were washed in lysis IP buffer 4 times with the assistance of a magnet. Finally, washed beads were resuspended in 2x SDS sample buffer and the pulldown samples were analyzed by

western blot. The relative binding between our proteins of interest was calculated by densitometric analyses using the Image Studio software (Li-Cor), where the positive bands were normalized to the levels of the immunoprecipitated protein.

Western blotting

Cells, including HEK293T were harvested 48h post-transfection in lysis IP buffer (ThermoFisher Scientific, 87787) complemented with protease inhibitors (Roche, 04693116001) and phosphatase inhibitor cocktails 2 and 3 (Sigma-Aldrich, P5726 and P0044). For the rapamycin assays, cells were treated with Rapamycin at different concentrations (0–4 μM) for 4h before being harvested and lysed. Cell lysates were incubated on ice for 1 h. Samples were then centrifuged at 16,000 x *g* for 8 min. The supernatant was collected, mixed with 2x SDS sample buffer (Sigma-Aldrich, S3401) and boiled for 5 min. Proteins were then separated by electrophoresis on SDS-PAGE polyacrylamide gels (8-12%) and transferred to a polyvinylidene difluoride (PVDF) membrane (BioRad, 1620177) using a Trans-Blot SD transfer cell (BioRad, 1703940). After blocking the membranes for 1 h in blocking buffer (BioRad, 1706404) at room temperature, we proceeded with the incubation with primary antibodies overnight at 4°C (antibody sources and dilutions are detailed in **Table 6.1**). Next, membranes were washed 3 times in PBS-tween (Sigma-Aldrich, P3563) for 15 min at room temperature before being probed for 1 h with the secondary antibody solution at a 1:2,000 dilution. Three different secondary antibodies were used, all conjugated with horseradish peroxidase: goat anti-mouse-HRP, goat anti-rabbit-HRP and donkey anti-rabbit-HRP (**Table 6.1**). After the incubation with the secondary antibodies, the membranes were washed 3 additional times in PBS-tween, developed using SuperSignal West Femto maximum sensitivity substrate (Pierce, 34095), and visualized using a Li-Cor Odyssey Fc Imager 2800 (Li-Cor, Lincoln, NE).

Flow cytometry

300,000 HEK293T cells were co-transfected with 2,000 ng of *EGFP-LC3B* and 2,000 ng of either pCGCG-NL4-3 *nef* , SIV_{mac} 239 *nef* and Chimeras I, II, III, IV; HIV-1 transmitted/founder viruses CH077 (pCH077.t/2627), CH106 (pCH106.c/2633),

RHPA (pRHPA.c/2635), THRO (pTHRO.c/2626), TRJO (pTRJO.c/2851, CH058 (pCH058.c/2960), Z331M (pZ331M), Z3576 (pZ3576F), 3618 (pZ3618M), and Z4248 (pZ4248M). 48 h post-transfection, cells were collected for analysis. Cells were then washed with DPBS, trypsinized (ThermoFisher Scientific, 25200) and centrifuged at 600 *x g* for 5 min, followed by an additional wash of 10 min at 4ºC with 0.05% saponin (Sigma-Aldrich, 47036) in DPBS. Cells were subsequently washed 2 additional times in DPBS. Finally, samples were fixed with 1% paraformaldehyde in DPBS. Cells were analyzed using an Attune instrument (ThermoFisher Scientific, Waltham, MA). Data were processed with the FlowJo software (version 10.5.3) using 50,000 events. Debris and doublets were excluded using FSC and SSC gating, and the percentage of EGFP-positive single cells was calculated for every sample.

Statistical analysis

All statistical calculations were performed with a two-tailed unpaired Student T test using Graph Pad Prism version 8.3.0. *P* values ≤ 0.05 were considered statistically significant.

Table 6.1. Antibody sources and conditions (hypothesis 3).

Protein	Primary antibody	Dilution	Source
ACTB/β-actin	Mouse monoclonal (C4) to ACTB/β-actin	1:1000	Sigma-Aldrich, MAB1501
BCL2	Mouse monoclonal (124) to BCL2	1:1000	Cell Signaling Technology, 15071S
BECN1	Rabbit monoclonal (D40C5) to BECN1	1:1000	Cell Signaling Technology, 3495S
GFP	Mouse monoclonal (4B10B2) and Rabbit monoclonal (E385) to GFP	1:1000 1:1000	Sigma-Aldrich, SAB5300167 Abcam, ab32146

Table 6.1. Continued

LC3	Rabbit polyclonal to LC3B	1:1000	Cell Signaling Technology, 2775S
HIV Nef	Mouse monoclonal (2H12(01-007)) to HIV-1 Nef	1:1000	ThermoFisher Scientific, MA1-71505
SIV Nef	Mouse monoclonal (17.2) to SIV Nef	1:1000	NIH AIDS Reagent Program, 2659
HIV-1 Gag p55/p24	Mouse monoclonal (183-H12-5C) to HIV p24	1:1000	NIH AIDS Reagent Program, 3537
SQSTM1/p62	Mouse monoclonal to SQSTM1/p62	1:1000	Abcam, ab56416
Mouse IgG	Goat polyclonal (HRP-conjugated)	1:2000	Pierce, 31430
Mouse IgG2a	Goat polyclonal (Alexa-568 conjugated)	1:500	ThermoFisher Scientific, A21134
Rabbit IgG	Goat polyclonal (HRP-conjugated)	1:2000	Abcam, ab97051
Rabbit IgG	Donkey polyclonal (HRP-conjugated)	1:2000	Abcam, ab16284

CHAPTER 7

CONCLUSIONS AND FUTURE DIRECTIONS

Autophagy is an important cellular defense mechanism against viruses with untapped therapeutic potential against HIV infection. Specifically, autophagy targets viral components needed for replication for lysosomal degradation. In addition to this primary role, the cleavage of viral structures allows their association with pattern recognition receptors and MHC-I/II complexes, triggering in turn innate and adaptive immune responses against these pathogens. Despite its antiviral potential, the interplay between HIV and the autophagy machinery has remained unclear for over a decade. Whereas some studies evidenced that the degradative nature of autophagy restricts HIV, others have claimed that this virus is able to exploit autophagy for its own replication benefits. What is more, these controversial findings seem to apply differently depending on the cell type studied. Hence, in order to consider the therapeutic potential of autophagy in the context of HIV infection, we must first improve our understanding of the reciprocal relationship between autophagy and HIV. In this study, we show that autophagy impairs HIV replication regardless of the cell type the virus is infecting through the clearance of the viral protein Gag, the main driver of virion assembly and release. Upon autophagy activation, Gag is targeted to autophagosomes for its subsequent degradation in autolysosomes. Consequently, if autophagy is intersected, Gag levels and virion production are restored. Our immunoprecipitation assays suggest that SQSTM1 is the autophagy receptor that targets Gag to phagophores. Since SQSTM1 generally binds to ubiquitinated cargo, our future studies will investigate the role of Gag ubiquitination, as well as other features (i.e. membrane association, protein domains, etc.) in this protein to understand the molecular mechanism by which Gag is sensed as a non-self protein that needs to be eliminated.

Importantly, our work also demonstrates that HIV circumvents autophagy restriction through a previously unappreciated mechanism involving the accessory protein Nef. We found that Nef strengthens the association between the initiator of

autophagy BECN1 and its natural inhibitor BCL2, halting autophagosome biogenesis and autophagy progression. Nef achieves this by promoting changes in the post-translational modifications that guide BECN1-BCL2 binding. In particular, HIV Nef enhances the PRKN-mediated mono-ubiquitination of BCL2, a post-translational modification that renders BCL2 more stable and, thus, enhances its inhibitory effect over BECN1. Because BECN1 is necessary for the formation and maturation of autophagosome structures, its sequestration by BCL2 causes defects in autophagosome formation and, consequently, in maturation, allowing in turn efficient virion assembly and release. The mechanism employed by Nef to enhance PRKN's effect on BCL2 is yet to be determined. Nef and BCL2 can be found in association with membranes at both, the ER and the mitochondria, whereas PRKN is a cytosolic protein reported to carry out its ubiquitin E3 ligase activity upon recruitment to particular locations[242,280,281]. Therefore, Nef might be responsible for the recruitment of PRKN to BCL2-enriched compartments where it can mediate BCL2 mono-ubiquitination. Due to the presence of BECN1 nearby ER locations, Nef-associated ubiquitination of ER-targeted BCL2 can detrimentally impact autophagy progression. In addition, our studies indicate that Nef also enhances BCL2 ubiquitination at the mitochondria. Importantly, modifications of BCL2 at this particular subcellular localization are usually linked to the regulation of apoptosis. However, while BCL2 phosphorylation strengthens BCL2's ability to inhibit apoptosis, little is known regarding the role of the ubiquitination of BCL2 in apoptotic events. In this matter, the phosphorylation of BCL2, leads to the dissociation from its inhibitor, the BCL2 associated agonist of cell death (BAD), enabling BCL2's anti-apoptotic activity [282]. Therefore, one could speculate that the mono-ubiquitination of BCL2 at the mitochondria, in an analogous manner to its role in BECN1-BCL2 interaction, could be enhancing BCL2-BAD association which would, in turn, facilitate cell death through apoptosis. These postulations could provide some mechanistic support to previous studies reporting that Nef is able to promote apoptosis in different cell types such as $CD4^+$ T cells, cardiomyocytes or brain endothelial cells[283-285]. Interestingly, this potential effect on apoptosis could account for some of the pathologies associated with the expression of Nef. In this context, the previously unrecognized ability of Nef

ability to inhibit autophagy might be also playing a pivotal role in the development of pathologies associated to HIV.

Nef expression has been recurrently associated with different pathologies in HIV^+ individuals even under ART treatments, including HIV-associated neurological disorders (HAND) or HIV-associated pulmonary hypertension (HIV-PH)[286-288]. These conditions are not only relevant due to their undesired symptomatology and prognosis, but also because it is usually associated with infected persons that live longer due to the effect the antiretroviral regimens. Whereas Nef expression has been linked to the development of these pathologies, the underlying mechanisms still remain unknown. Remarkably, several studies have demonstrated that autophagic disfunction is directly associated with pulmonary hypertension as well as numerous neurological disorders, including HAND[287,289,290]. Therefore, Nef's capacity to intersect autophagy, either at the initiation or maturation stages, might be the main driver in the development of these HIV-associated pathologies. In addition, PRKN malfunction seems to be associated with neurological disorders[281,291]. Hence, Nef-mediated recruitment of PRKN to down-regulate autophagy might also be involved in the progression of HAND due to its ability to intersect with PRKN.

Our mapping studies revealed that Nef uses two distinct regions, both within the N-terminal domain of the protein, to intersect with the early and late stages of autophagy. However, whereas the amino acids that constitute the PIKBD in Nef are known to mediate the maturation blockade, the residues responsible for the repression of the initiation stages are yet to be determined. In future studies, we will narrow down the amino acids in the Nef N-terminal domain responsible for this activity. Nonetheless, Nef's effect on the BCL2-mediated sequestration of BECN1 not only impair the early stages, but also the formation of autophagolysosomes and thus, might be accountable, at least partially, for the inhibitory impact on the late stages of autophagy. This ability of Nef to prevent autophagy could constitute yet another Nef-mediated mechanism to achieve immune evasion, in addition to its already known abilities to downregulate the immune receptors CD4, CD28 and major

histocompatibility complexes, as well as the restriction factors SERINC3 and SERINC5[118,119,121,124,274].

The fact that HIV Nef has developed two distinct mechanisms to neutralize autophagy restriction (initiation plus maturation) already denotes the critical role of this pathway in HIV replication. Our phylogenetic analyses support this conclusion and revealed that the unappreciated ability of Nef to prevent the early stages of autophagy is primarily observed in pandemic clades of HIV-1, such as the subtype B, and their direct ancestors SIV_{cpz}, while not present within the HIV-2/SIVsmm linage. The fact that HIV-2 is less pathogenic than HIV-1 and has failed to spread globally, further supports that the effective counteraction of autophagy might play a part in both, HIV pathogenesis and the successful spread of pandemic HIV-1 viruses in the human population. Additionally, Nef from different HIV-1 subtypes, including the subtype C, which despite having a high prevalence have not spread worldwide, did not show the capacity to down-regulate autophagy initiation. These data stresses the potential role of autophagy antagonism as a mechanism to facilitate viral propagation.

Interestingly, previous publications showed that Nef alleles derived from different HIV-1 subtypes exhibit variability in their abilities to counteract other restrictions factors. For instance, whereas Nef clones from subtype C efficiently internalize SERINC3, this activity seems more attenuated in subtype B strains, which is exactly the contrary of what we observe regarding autophagy antagonism[292]. Hence, the differential effects of HIV-1 pandemic clades on autophagy progression might also reflect an evolutionary strategy to compensate an underlying lack of activity to counteract other restriction factors. Moreover, due to the high plasticity that primate lentiviruses present to overcome the effect of different host restriction factors, we cannot rule out the possibility of convergent evolution in the context of autophagy antagonism. From this perspective, whereas SIV_{cpz} and HIV-1 subtype B use Nef to down-regulate the initiation of autophagy, other species and strains such as $SIV_{mac}239$ or the HIV-1 subtype C might be using other factors for the same antagonistic purpose. In compliance with this assumption, we found that the expression of all the

proteins encoded by the full-length proviral genome of transmitted/founder viruses from Subtype C successfully led to the down-regulation of the initiation of autophagy and thus, conferred these viruses resistance to autophagy-mediated restriction. This potential scenario, in which different viral clades have developed distinct strategies for a common inhibitory effect on autophagy would further highlight the importance of counteracting autophagy restriction as a conserved trait among primate lentiviruses.

Furthermore, our studies with primary HIV-1 transmitted/founder viruses indicate that autophagy antagonism might be associated with viral infectivity and pathogenesis. In line with these results, a recent publication showed that activation of autophagy within *ex vivo* mucosal tissues drastically reduces HIV infectivity. Therefore, transmitter/founder viruses might have evolved a potential mechanism to overcome this first barrier of defense by effectively downregulating the restrictive effect of autophagy. Our observations on transmitted/founder viruses not only suggest that autophagy antagonism is essential for infectivity and pathogenesis, but also that it represents a promising target for future therapeutic strategies or even PreP regimens aimed at intersecting mucosal transmission.

In summary, our work highlights the great therapeutic potential of autophagy against HIV and also identifies new cellular molecules used by HIV Nef (i.e. BECN1-BCL2, PRKN) that could represent targets for the design of therapies aimed at rendering the virus susceptible to autophagy elimination. These strategies could include the therapeutic as well as prophylactic treatments with drugs such as the FDA-approved rapamycin. Rapamycin could be used to restrict viral replication and infectivity through the autophagy-mediated degradation of HIV Gag as well as the enhancement of antigen presentation events that would shape subsequent immune responses. Rapamycin-induced autophagy relies on the direct inhibition of the pleiotropic kinase mTOR. Interestingly, phosphorylation cascades triggered by the activity of this kinase have been reported to lead to the Tat-dependent trans-activation of HIV transcription[293,294], and thus, enhancing HIV replication. Therefore, Rapamycin treatments might have the potential to prevent HIV replication not only by

promoting the autophagy-mediated elimination of Gag, but also by directly silencing the Tat-dependent proviral transcription through the inhibition of the mTOR. In addition, these treatments could improve the quality of life of infected individuals by preventing the development of different pathologies associated to HIV such as HAND or HIV-PH by restoring the protective effects of autophagy. Besides all these benefits, other studies have reported that rapamycin can be used to uncouple the cytotoxicity associated with some anti-HIV agents and reduce immune activation, a common characteristic observed in HIV^+ individuals, even those controlling HIV under cART[295-297]. While being extensively used in short-term treatments as an immunomodulator after solid organ transplantation, the full potential of long-term regimens with rapamycin is progressively being revealed, with very promising results in regard to its effect on general health parameters and longevity.

In a complementary manner, additional strategies could be implemented in order to activate autophagy while preventing the Nef-mediated counteracting activity. For instance, a previously identified mutant of BECN1, characterized by its inability to bind to BCL2, rises as a very interesting candidate due to its potential to mediate the effective activation of autophagy while bypassing its sequestration by BCL2 in a Nef-dependent manner[156]. Potentially, this mutant could be administered using different delivery strategies, such as the application of BECN1 mutant-containing liposomes selectively targeting $CD4^+$ cells in infected individuals. Remarkably, recent data have showed that therapies based on this particular mutant could also become promising prophylactic treatments applied in a long-term fashion. In that respect, Dr. Levin's team recently demonstrated that far from being associated with unwanted adverse effects, the exploitation of this BECN1 mutant to induce the endogenous activation of autophagy in genetically modified mice resulted in significantly longer and healthier lives[255]. Therefore, in addition to improve our capacity to design future autophagy-based therapies, this thesis project clearly evidences the great potential that the manipulation of autophagy represents in the fight against the HIV/AIDS pandemic.

REFERENCES

1 Castro-Gonzalez, S. *et al.* HIV-1 Nef counteracts autophagy restriction by enhancing the association between BECN1 and its inhibitor BCL2 in a PRKN-dependent manner. *Autophagy*, 1-25, doi:10.1080/15548627.2020.1725401 (2020).

2 Colomer-Lluch, M., Castro-Gonzalez, S. & Serra-Moreno, R. Ubiquitination and SUMOylation in HIV Infection: Friends and Foes. *Curr Issues Mol Biol* **35**, 159-194, doi:10.21775/cimb.035.159 (2020).

3 UNAIDS. 2020 Global AIDS Update— Seizing the moment —. (2020).

4 Bijkerk, H. [Kaposi's sarcoma, Pneumocystis carinii pneumonia and other opportunistic infections]. *Ned Tijdschr Geneeskd* **126**, 1886-1887 (1982).

5 Centers for Disease, C. Kaposi's sarcoma and Pneumocystis pneumonia among homosexual men--New York City and California. *MMWR Morb Mortal Wkly Rep* **30**, 305-308 (1981).

6 Altman, L. K. New Homosexual Disorder Worries Health Officials. *New York Times* (1982).

7 Ellrodt, A. *et al.* Isolation of human T-lymphotropic retrovirus (LAV) from Zairian married couple, one with AIDS, one with prodromes. *Lancet* **1**, 1383-1385, doi:10.1016/s0140-6736(84)91877-4 (1984).

8 Barre-Sinoussi, F. *et al.* Isolation of a T-lymphotropic retrovirus from a patient at risk for acquired immune deficiency syndrome (AIDS). *Science* **220**, 868-871, doi:10.1126/science.6189183 (1983).

9 Gallo, R. C. *et al.* Frequent detection and isolation of cytopathic retroviruses (HTLV-III) from patients with AIDS and at risk for AIDS. *Science* **224**, 500-503, doi:10.1126/science.6200936 (1984).

10 AIDS.gov. A timeline of HIV and AIDS.

11 Health Chief calls AIDS battle 'NO. 1 PRIORITY'. *New York Times* (1983).

12 Clavel, F. *et al.* Isolation of a new human retrovirus from West African patients with AIDS. *Science* **233**, 343-346, doi:10.1126/science.2425430 (1986).

13 Pebody, R. aidsmap. HIV-1 and HIV-2. (2019).

14 Avert.org. HIV strains and types. (2019).

15 WHO. HIV/AIDS. (2019).

16 Sharp, P. M. & Hahn, B. H. Origins of HIV and the AIDS pandemic. *Cold Spring Harb Perspect Med* **1**, a006841, doi:10.1101/cshperspect.a006841 (2011).

17 Hirsch, V. M., Olmsted, R. A., Murphey-Corb, M., Purcell, R. H. & Johnson, P. R. An African primate lentivirus (SIVsm) closely related to HIV-2. *Nature* **339**, 389-392, doi:10.1038/339389a0 (1989).

18 Huet, T., Cheynier, R., Meyerhans, A., Roelants, G. & Wain-Hobson, S. Genetic organization of a chimpanzee lentivirus related to HIV-1. *Nature* **345**, 356-359, doi:10.1038/345356a0 (1990).

19 Gao, F. *et al.* Human infection by genetically diverse SIVSM-related HIV-2 in west Africa. *Nature* **358**, 495-499, doi:10.1038/358495a0 (1992).

20 Takehisa, J. *et al.* Origin and biology of simian immunodeficiency virus in wild-living western gorillas. *J Virol* **83**, 1635-1648, doi:10.1128/JVI.02311-08 (2009).

21 Santiago, M. L. *et al.* Simian immunodeficiency virus infection in free-ranging sooty mangabeys (Cercocebus atys atys) from the Tai Forest, Cote d'Ivoire: implications for the origin of epidemic human immunodeficiency virus type 2. *J Virol* **79**, 12515-12527, doi:10.1128/JVI.79.19.12515-12527.2005 (2005).

22 Apetrei, C. *et al.* Molecular epidemiology of simian immunodeficiency virus SIVsm in U.S. primate centers unravels the origin of SIVmac and SIVstm. *J Virol* **79**, 8991-9005, doi:10.1128/JVI.79.14.8991-9005.2005 (2005).

23 Zhou, Y., Bao, R., Haigwood, N. L., Persidsky, Y. & Ho, W. Z. SIV infection of rhesus macaques of Chinese origin: a suitable model for HIV infection in humans. *Retrovirology* **10**, 89, doi:10.1186/1742-4690-10-89 (2013).

24 Shedlock, D. J., Silvestri, G. & Weiner, D. B. Monkeying around with HIV vaccines: using rhesus macaques to define 'gatekeepers' for clinical trials. *Nat Rev Immunol* **9**, 717-728, doi:10.1038/nri2636 (2009).

25 Taylor, B. S., Sobieszczyk, M. E., McCutchan, F. E. & Hammer, S. M. The challenge of HIV-1 subtype diversity. *N Engl J Med* **358**, 1590-1602, doi:10.1056/NEJMra0706737 (2008).

26 Sharp, P. M. & Hahn, B. H. The evolution of HIV-1 and the origin of AIDS. *Philos Trans R Soc Lond B Biol Sci* **365**, 2487-2494, doi:10.1098/rstb.2010.0031 (2010).

27 Vidal, N. *et al.* Unprecedented degree of human immunodeficiency virus type 1 (HIV-1) group M genetic diversity in the Democratic Republic of Congo suggests that the HIV-1 pandemic originated in Central Africa. *J Virol* **74**, 10498-10507, doi:10.1128/jvi.74.22.10498-10507.2000 (2000).

28 Osmanov, S. *et al.* Estimated global distribution and regional spread of HIV-1 genetic subtypes in the year 2000. *J Acquir Immune Defic Syndr* **29**, 184-190, doi:10.1097/00042560-200202010-00013 (2002).

29 Gartner, M. J., Roche, M., Churchill, M. J., Gorry, P. R. & Flynn, J. K. Understanding the mechanisms driving the spread of subtype C HIV-1. *EBioMedicine* **53**, 102682, doi:10.1016/j.ebiom.2020.102682 (2020).

30 Hemelaar, J., Gouws, E., Ghys, P. D. & Osmanov, S. Global and regional distribution of HIV-1 genetic subtypes and recombinants in 2004. *AIDS* **20**, W13-23, doi:10.1097/01.aids.0000247564.73009.bc (2006).

31 Carter, J. & Saunders, V. *Virology: Principles and applications*. (2007).

32 German Advisory Committee Blood, S. A. o. P. T. b. B. Human Immunodeficiency Virus (HIV). *Transfus Med Hemother* **43**, 203-222, doi:10.1159/000445852 (2016).

33 Malim, M. H. & Emerman, M. HIV-1 accessory proteins--ensuring viral survival in a hostile environment. *Cell Host Microbe* **3**, 388-398, doi:10.1016/j.chom.2008.04.008 (2008).

34 Vicenzi, E. & Poli, G. Novel factors interfering with human immunodeficiency virus-type 1 replication in vivo and in vitro. *Tissue Antigens* **81**, 61-71, doi:10.1111/tan.12047 (2013).

35 Berger, G. & Cimarelli, A. SIVSM/HIV-2 Vpx proteins: function and uses in the infection of primary myeloid cells. *Methods Mol Biol* **1087**, 159-165, doi:10.1007/978-1-62703-670-2_13 (2014).

36 Freed, E. O. HIV-1 assembly, release and maturation. *Nat Rev Microbiol* **13**, 484-496, doi:10.1038/nrmicro3490 (2015).

37 Zhu, P. *et al.* Distribution and three-dimensional structure of AIDS virus envelope spikes. *Nature* **441**, 847-852, doi:10.1038/nature04817 (2006).

38 Schiller, J. & Chackerian, B. Why HIV virions have low numbers of envelope spikes: implications for vaccine development. *PLoS Pathog* **10**, e1004254, doi:10.1371/journal.ppat.1004254 (2014).

39 Raska, M. *et al.* Glycosylation patterns of HIV-1 gp120 depend on the type of expressing cells and affect antibody recognition. *J Biol Chem* **285**, 20860-20869, doi:10.1074/jbc.M109.085472 (2010).

40 Woodham, A. W. *et al.* Human Immunodeficiency Virus Immune Cell Receptors, Coreceptors, and Cofactors: Implications for Prevention and Treatment. *AIDS Patient Care STDS* **30**, 291-306, doi:10.1089/apc.2016.0100 (2016).

41 Rankovic, S., Varadarajan, J., Ramalho, R., Aiken, C. & Rousso, I. Reverse Transcription Mechanically Initiates HIV-1 Capsid Disassembly. *J Virol* **91**, doi:10.1128/JVI.00289-17 (2017).

42 Arhel, N. Revisiting HIV-1 uncoating. *Retrovirology* **7**, 96, doi:10.1186/1742-4690-7-96 (2010).

43 Hu, W. S. & Hughes, S. H. HIV-1 reverse transcription. *Cold Spring Harb Perspect Med* **2**, doi:10.1101/cshperspect.a006882 (2012).

44 Ambrose, Z. & Aiken, C. HIV-1 uncoating: connection to nuclear entry and regulation by host proteins. *Virology* **454-455**, 371-379, doi:10.1016/j.virol.2014.02.004 (2014).

45 Castro-Gonzalez, S., Colomer-Lluch, M. & Serra-Moreno, R. Barriers for HIV Cure: The Latent Reservoir. *AIDS Res Hum Retroviruses* **34**, 739-759, doi:10.1089/AID.2018.0118 (2018).

46 Wu, Y. HIV-1 gene expression: lessons from provirus and non-integrated DNA. *Retrovirology* **1**, 13, doi:10.1186/1742-4690-1-13 (2004).

47 Karn, J. & Stoltzfus, C. M. Transcriptional and posttranscriptional regulation of HIV-1 gene expression. *Cold Spring Harb Perspect Med* **2**, a006916, doi:10.1101/cshperspect.a006916 (2012).

48 Basmaciogullari, S. & Pizzato, M. The activity of Nef on HIV-1 infectivity. *Front Microbiol* **5**, 232, doi:10.3389/fmicb.2014.00232 (2014).

49 Berkhout, B., Silverman, R. H. & Jeang, K. T. Tat trans-activates the human immunodeficiency virus through a nascent RNA target. *Cell* **59**, 273-282 (1989).

50 Fernandes, J., Jayaraman, B. & Frankel, A. The HIV-1 Rev response element: an RNA scaffold that directs the cooperative assembly of a homo-oligomeric ribonucleoprotein complex. *RNA Biol* **9**, 6-11, doi:10.4161/rna.9.1.18178 (2012).

51 Jia, B. *et al.* Species-specific activity of SIV Nef and HIV-1 Vpu in overcoming restriction by tetherin/BST2. *PLoS Pathog* **5**, e1000429, doi:10.1371/journal.ppat.1000429 (2009).

52 Gonzalez, M. E. Vpu Protein: The Viroporin Encoded by HIV-1. *Viruses* **7**, 4352-4368, doi:10.3390/v7082824 (2015).

53 Arrildt, K. T., Joseph, S. B. & Swanstrom, R. The HIV-1 env protein: a coat of many colors. *Curr HIV/AIDS Rep* **9**, 52-63, doi:10.1007/s11904-011-0107-3 (2012).

54 Wildum, S., Schindler, M., Munch, J. & Kirchhoff, F. Contribution of Vpu, Env, and Nef to CD4 down-modulation and resistance of human immunodeficiency virus type 1-infected T cells to superinfection. *J Virol* **80**, 8047-8059, doi:10.1128/JVI.00252-06 (2006).

55 Kogan, M. & Rappaport, J. HIV-1 accessory protein Vpr: relevance in the pathogenesis of HIV and potential for therapeutic intervention. *Retrovirology* **8**, 25, doi:10.1186/1742-4690-8-25 (2011).

56 Spragg, C. J. & Emerman, M. Antagonism of SAMHD1 is actively maintained in natural infections of simian immunodeficiency virus. *Proc Natl Acad Sci U S A* **110**, 21136-21141, doi:10.1073/pnas.1316839110 (2013).

57 Sundquist, W. I. & Krausslich, H. G. HIV-1 assembly, budding, and maturation. *Cold Spring Harb Perspect Med* **2**, a006924, doi:10.1101/cshperspect.a006924 (2012).

58 Usami, Y. *et al.* The ESCRT pathway and HIV-1 budding. *Biochem Soc Trans* **37**, 181-184, doi:10.1042/BST0370181 (2009).

59 Levine, A. M. AIDS-related malignancies: the emerging epidemic. *J Natl Cancer Inst* **85**, 1382-1397, doi:10.1093/jnci/85.17.1382 (1993).

60 Naif, H. M. Pathogenesis of HIV Infection. *Infect Dis Rep* **5**, e6, doi:10.4081/idr.2013.s1.e6 (2013).

61 Dinkins, C., Pilli, M. & Kehrl, J. H. Roles of autophagy in HIV infection. *Immunol Cell Biol* **93**, 11-17, doi:10.1038/icb.2014.88 (2015).

62 Garg, H., Mohl, J. & Joshi, A. HIV-1 induced bystander apoptosis. *Viruses* **4**, 3020-3043, doi:10.3390/v4113020 (2012).

63 Finkel, T. H. & Banda, N. K. Indirect mechanisms of HIV pathogenesis: how does HIV kill T cells? *Curr Opin Immunol* **6**, 605-615, doi:10.1016/0952-7915(94)90149-x (1994).

64 Simon, V., Ho, D. D. & Abdool Karim, Q. HIV/AIDS epidemiology, pathogenesis, prevention, and treatment. *Lancet* **368**, 489-504, doi:10.1016/S0140-6736(06)69157-5 (2006).

65 Levy, J. A. HIV pathogenesis: knowledge gained after two decades of research. *Adv Dent Res* **19**, 10-16 (2006).

66 Lackner, A. A., Lederman, M. M. & Rodriguez, B. HIV pathogenesis: the host. *Cold Spring Harb Perspect Med* **2**, a007005, doi:10.1101/cshperspect.a007005 (2012).

67 UNAIDS. UNAIDS data 2019. (2019).

68 Wandeler, G., Johnson, L. F. & Egger, M. Trends in life expectancy of HIV-positive adults on antiretroviral therapy across the globe: comparisons with general population. *Curr Opin HIV AIDS* **11**, 492-500, doi:10.1097/COH.0000000000000298 (2016).

69 Cohen, M. S. *et al.* Antiretroviral treatment of HIV-1 prevents transmission of HIV-1: where do we go from here? *Lancet* **382**, 1515-1524, doi:10.1016/S0140-6736(13)61998-4 (2013).

70 Latinovic, O. S., Reitz, M. & Heredia, A. CCR5 Inhibitors and HIV-1 Infection. *J AIDS HIV Treat* **1**, 1-5, doi:10.33696/AIDS.1.001 (2019).

71 Arts, E. J. & Hazuda, D. J. HIV-1 antiretroviral drug therapy. *Cold Spring Harb Perspect Med* **2**, a007161, doi:10.1101/cshperspect.a007161 (2012).

72 Tsou, L. K., Chen, C. H., Dutschman, G. E., Cheng, Y. C. & Hamilton, A. D. Blocking HIV-1 entry by a gp120 surface binding inhibitor. *Bioorg Med Chem Lett* **22**, 3358-3361, doi:10.1016/j.bmcl.2012.02.079 (2012).

73 Liu, H., Zhan, P. & Liu, X. Y. [Research progress of dual inhibitors targeting HIV-1 reverse transcriptase and integrase]. *Yao Xue Xue Bao* **48**, 466-476 (2013).

74 Lv, Z., Chu, Y. & Wang, Y. HIV protease inhibitors: a review of molecular selectivity and toxicity. *HIV AIDS (Auckl)* **7**, 95-104, doi:10.2147/HIV.S79956 (2015).

75 Siliciano, R. F. & Greene, W. C. HIV latency. *Cold Spring Harb Perspect Med* **1**, a007096, doi:10.1101/cshperspect.a007096 (2011).

76 Conway, J. M., Perelson, A. S. & Li, J. Z. Predictions of time to HIV viral rebound following ART suspension that incorporate personal biomarkers. *PLoS Comput Biol* **15**, e1007229, doi:10.1371/journal.pcbi.1007229 (2019).

77 Chun, T. W., Davey, R. T., Jr., Engel, D., Lane, H. C. & Fauci, A. S. Re-emergence of HIV after stopping therapy. *Nature* **401**, 874-875, doi:10.1038/44755 (1999).

78 Richman, D. D. Antiviral drug resistance. *Antiviral Res* **71**, 117-121, doi:10.1016/j.antiviral.2006.03.004 (2006).

79 Pinoges, L. *et al.* Risk factors and mortality associated with resistance to first-line antiretroviral therapy: multicentric cross-sectional and longitudinal analyses. *J Acquir Immune Defic Syndr* **68**, 527-535, doi:10.1097/QAI.0000000000000513 (2015).

80 Schackman, B. R. *et al.* The lifetime cost of current human immunodeficiency virus care in the United States. *Med Care* **44**, 990-997, doi:10.1097/01.mlr.0000228021.89490.2a (2006).

81 Nolan, D. & Mallal, S. Antiretroviral-therapy-associated lipoatrophy: current status and future directions. *Sex Health* **2**, 153-163, doi:10.1071/sh04058 (2005).

82 Freed, E. O. & Martin, M. A. in *Fields Virology* Vol. 2 (eds D.M. Knipe & P.M. Howley) Ch. 49, 59 (Lippincott Williams & Wilkins, 2013).

83 Akay, C. *et al.* Antiretroviral drugs induce oxidative stress and neuronal damage in the central nervous system. *J Neurovirol* **20**, 39-53, doi:10.1007/s13365-013-0227-1 (2014).

84 Clifford, D. B. & Ances, B. M. HIV-associated neurocognitive disorder. *Lancet Infect Dis* **13**, 976-986, doi:10.1016/S1473-3099(13)70269-X (2013).

85 Onen, N. F. *et al.* Aging and HIV infection: a comparison between older HIV-infected persons and the general population. *HIV Clin Trials* **11**, 100-109, doi:10.1310/hct1102-100 (2010).

86 Richardson, M. W., Guo, L., Xin, F., Yang, X. & Riley, J. L. Stabilized human TRIM5alpha protects human T cells from HIV-1 infection. *Mol Ther* **22**, 1084-1095, doi:10.1038/mt.2014.52 (2014).

87 Arhel, N. & Kirchhoff, F. Host proteins involved in HIV infection: new therapeutic targets. *Biochim Biophys Acta* **1802**, 313-321, doi:10.1016/j.bbadis.2009.12.003 (2010).

88 Mi, Z. *et al.* A small molecule compound IMB-LA inhibits HIV-1 infection by preventing viral Vpu from antagonizing the host restriction factor BST-2. *Sci Rep* **5**, 18499, doi:10.1038/srep18499 (2015).

89 Bogerd, H. P., Kornepati, A. V., Marshall, J. B., Kennedy, E. M. & Cullen, B. R. Specific induction of endogenous viral restriction factors using CRISPR/Cas-derived transcriptional activators. *Proc Natl Acad Sci U S A* **112**, E7249-7256, doi:10.1073/pnas.1516305112 (2015).

90 Cen, S. *et al.* Small molecular compounds inhibit HIV-1 replication through specifically stabilizing APOBEC3G. *J Biol Chem* **285**, 16546-16552, doi:10.1074/jbc.M109.085308 (2010).

91 Malim, M. H. & Bieniasz, P. D. HIV Restriction Factors and Mechanisms of Evasion. *Cold Spring Harb Perspect Med* **2**, a006940, doi:10.1101/cshperspect.a006940 (2012).

92 Stremlau, M. *et al.* Specific recognition and accelerated uncoating of retroviral capsids by the TRIM5alpha restriction factor. *Proc Natl Acad Sci U S A* **103**, 5514-5519, doi:10.1073/pnas.0509996103 (2006).

93 Laguette, N. *et al.* SAMHD1 is the dendritic- and myeloid-cell-specific HIV-1 restriction factor counteracted by Vpx. *Nature* **474**, 654-657, doi:10.1038/nature10117 (2011).

94 Mangeat, B. *et al.* Broad antiretroviral defence by human APOBEC3G through lethal editing of nascent reverse transcripts. *Nature* **424**, 99-103, doi:10.1038/nature01709 (2003).

95 Neil, S. J., Zang, T. & Bieniasz, P. D. Tetherin inhibits retrovirus release and is antagonized by HIV-1 Vpu. *Nature* **451**, 425-430, doi:10.1038/nature06553 (2008).

96 Goujon, C. *et al.* Human MX2 is an interferon-induced post-entry inhibitor of HIV-1 infection. *Nature* **502**, 559-562, doi:10.1038/nature12542 (2013).

97 Usami, Y., Wu, Y. & Gottlinger, H. G. SERINC3 and SERINC5 restrict HIV-1 infectivity and are counteracted by Nef. *Nature* **526**, 218-223, doi:10.1038/nature15400 (2015).

98 Stremlau, M. *et al.* The cytoplasmic body component TRIM5alpha restricts HIV-1 infection in Old World monkeys. *Nature* **427**, 848-853, doi:10.1038/nature02343 (2004).

99 Wu, F. *et al.* TRIM5alpha Resistance Escape Mutations in the Capsid Are Transferable between Simian Immunodeficiency Virus Strains. *J Virol* **90**, 11087-11095, doi:10.1128/JVI.01620-16 (2016).

100 Kratovac, Z. *et al.* Primate lentivirus capsid sensitivity to TRIM5 proteins. *J Virol* **82**, 6772-6777, doi:10.1128/JVI.00410-08 (2008).

101 Wei, W., Guo, H., Ma, M., Markham, R. & Yu, X. F. Accumulation of MxB/Mx2-resistant HIV-1 Capsid Variants During Expansion of the HIV-1 Epidemic in Human Populations. *EBioMedicine* **8**, 230-236, doi:10.1016/j.ebiom.2016.04.020 (2016).

102 Chaipan, C., Smith, J. L., Hu, W. S. & Pathak, V. K. APOBEC3G restricts HIV-1 to a greater extent than APOBEC3F and APOBEC3DE in human primary CD4+ T cells and macrophages. *J Virol* **87**, 444-453, doi:10.1128/JVI.00676-12 (2013).

103 Yu, X. *et al.* Induction of APOBEC3G ubiquitination and degradation by an HIV-1 Vif-Cul5-SCF complex. *Science* **302**, 1056-1060, doi:10.1126/science.1089591 (2003).

104 Lahouassa, H. *et al.* SAMHD1 restricts the replication of human immunodeficiency virus type 1 by depleting the intracellular pool of deoxynucleoside triphosphates. *Nat Immunol* **13**, 223-228, doi:10.1038/ni.2236 (2012).

105 Hrecka, K. *et al.* Vpx relieves inhibition of HIV-1 infection of macrophages mediated by the SAMHD1 protein. *Nature* **474**, 658-661, doi:10.1038/nature10195 (2011).

106 Wang, H. *et al.* Inhibition of Vpx-Mediated SAMHD1 and Vpr-Mediated Host Helicase Transcription Factor Degradation by Selective Disruption of Viral CRL4 (DCAF1) E3 Ubiquitin Ligase Assembly. *J Virol* **91**, d oi:10.1128/JVI.00225-17 (2017).

107 Heigele, A. *et al.* The Potency of Nef-Mediated SERINC5 Antagonism Correlates with the Prevalence of Primate Lentiviruses in the Wild. *Cell Host Microbe* **20**, 381-391, doi:10.1016/j.chom.2016.08.004 (2016).

108 Sood, C., Marin, M., Chande, A., Pizzato, M. & Melikyan, G. B. SERINC5 protein inhibits HIV-1 fusion pore formation by promoting functional inactivation of envelope glycoproteins. *J Biol Chem* **292**, 6014-6026, doi:10.1074/jbc.M117.777714 (2017).

109 Trautz, B. *et al.* The Antagonism of HIV-1 Nef to SERINC5 Particle Infectivity Restriction Involves the Counteraction of Virion-Associated Pools of the Restriction Factor. *J Virol* **90**, 10915-10927, doi:10.1128/JVI.01246-16 (2016).

110 Beitari, S., Ding, S., Pan, Q., Finzi, A. & Liang, C. Effect of HIV-1 Env on SERINC5 Antagonism. *J Virol* **91**, doi:10.1128/JVI.02214-16 (2017).

111 Van Damme, N. *et al.* The interferon-induced protein BST-2 restricts HIV-1 release and is downregulated from the cell surface by the viral Vpu protein. *Cell Host Microbe* **3**, 245-252, doi:10.1016/j.chom.2008.03.001 (2008).

112 Mangeat, B. *et al.* HIV-1 Vpu neutralizes the antiviral factor Tetherin/BST-2 by binding it and directing its beta-TrCP2-dependent degradation. *PLoS Pathog* **5**, e1000574, doi:10.1371/journal.ppat.1000574 (2009).

113 Serra-Moreno, R., Zimmermann, K., Stern, L. J. & Evans, D. T. Tetherin/BST-2 Antagonism by Nef Depends on a Direct Physical Interaction between Nef and Tetherin, and on Clathrin-mediated Endocytosis. *PLoS pathogens* **9**, e1003487, doi:10.1371/journal.ppat.1003487 (2013).

114 Sauter, D. & Kirchhoff, F. Tetherin antagonism by primate lentiviral nef proteins. *Current HIV research* **9**, 514-523 (2011).

115 Hauser, H. *et al.* HIV-1 Vpu and HIV-2 Env counteract BST-2/tetherin by sequestration in a perinuclear compartment. *Retrovirology* **7**, 51, doi:10.1186/1742-4690-7-51 (2010).

116 Arias, J. F. *et al.* Tetherin Antagonism by HIV-1 Group M Nef Proteins. *J Virol*, doi:10.1128/JVI.01465-16 (2016).

117 Watkins, R. L. *et al.* In vivo analysis of highly conserved Nef activities in HIV-1 replication and pathogenesis. *Retrovirology* **10**, 125, doi:10.1186/1742-4690-10-125 (2013).

118 Rosa, A. *et al.* HIV-1 Nef promotes infection by excluding SERINC5 from virion incorporation. *Nature* **526**, 212-217, doi:10.1038/nature15399 (2015).

119 Mangasarian, A., Piguet, V., Wang, J.-K., Chen, Y.-L. & Trono, D. Nef-induced CD4 and major histocompatibility complex class I (MHC-I) down-regulation are governed by distinct determinants: N-terminal alpha helix and proline repeat of Nef selectively regulate MHC-I trafficking. *Journal of Virology* **73**, 1964-1973 (1999).

120 Lundquist, C. A., Tobiume, M., Zhou, J., Unutmaz, D. & Aiken, C. Nef-mediated downregulation of CD4 enhances human immunodeficiency virus type 1 replication in primary T lymphocytes. *J Virol* **76**, 4625-4633, doi:10.1128/jvi.76.9.4625-4633.2002 (2002).

121 Swigut, T., Shody, N. & Skowronski, J. Mechanism for down-regulation of CD28 by Nef *EMBO J.* **20**, 1593-1604 (2001).

122 Roeth, J. F., Williams, M., Kasper, M. R., Filzen, T. M. & Collins, K. L. HIV-1 Nef disrupts MHC-I trafficking by recruiting AP-1 to the MHC-I cytoplasmic tail. *The Journal of cell biology* **167**, 903-913, doi:10.1083/jcb.200407031 (2004).

123 Chaudhry, A. *et al.* HIV-1 Nef promotes endocytosis of cell surface MHC class II molecules via a constitutive pathway. *J Immunol* **183**, 2415-2424, doi:10.4049/jimmunol.0804014 (2009).

124 Joas, S. *et al.* Nef-Mediated CD3-TCR Downmodulation Dampens Acute Inflammation and Promotes SIV Immune Evasion. *Cell Rep* **30**, 2261-2274 e2267, doi:10.1016/j.celrep.2020.01.069 (2020).

125 Geyer, M., Fackler, O. T. & Peterlin, B. M. Structure--function relationships in HIV-1 Nef. *EMBO Rep* **2**, 580-585, doi:10.1093/embo-reports/kve141 (2001).

126 Roeth, J. F. & Collins, K. L. Human immunodeficiency virus type 1 Nef: adapting to intracellular trafficking pathways. *Microbiol Mol Biol Rev* **70**, 548-563, doi:10.1128/MMBR.00042-05 (2006).

127 Piguet V, T. D. A structure-function analysis of the nef protein of primate lentiviruses. *Human retroviruses and AIDS*, p 448–459 (1999).

128 Buffalo, C. Z., Iwamoto, Y., Hurley, J. H. & Ren, X. How HIV Nef Proteins Hijack Membrane Traffic To Promote Infection. *J Virol* **93**, doi:10.1128/JVI.01322-19 (2019).

129 Pereira, E. A. & daSilva, L. L. HIV-1 Nef: Taking Control of Protein Trafficking. *Traffic* **17**, 976-996, doi:10.1111/tra.12412 (2016).

130 Kyei, G. B. *et al.* Autophagy pathway intersects with HIV-1 biosynthesis and regulates viral yields in macrophages. *J Cell Biol* **186**, 255-268, doi:10.1083/jcb.200903070 (2009).

131 Campbell, G. R., Rawat, P., Bruckman, R. S. & Spector, S. A. Human Immunodeficiency Virus Type 1 Nef Inhibits Autophagy through Transcription Factor EB Sequestration. *PLoS Pathog* **11**, e1005018, doi:10.1371/journal.ppat.1005018 (2015).

132 Chang, C. *et al.* Bidirectional Control of Autophagy by BECN1 BARA Domain Dynamics. *Mol Cell* **73**, 339-353 e336, doi:10.1016/j.molcel.2018.10.035 (2019).

133 Borel, S. *et al.* HIV-1 viral infectivity factor interacts with microtubule-associated protein light chain 3 and inhibits autophagy. *AIDS* **29**, 275-286, doi:10.1097/QAD.0000000000000554 (2015).

134 Blanchet, F. P. *et al.* Human immunodeficiency virus-1 inhibition of immunoamphisomes in dendritic cells impairs early innate and adaptive immune responses. *Immunity* **32**, 654-669, doi:10.1016/j.immuni.2010.04.011 (2010).

135 Hui, L., Chen, X., Haughey, N. J. & Geiger, J. D. Role of endolysosomes in HIV-1 Tat-induced neurotoxicity. *ASN Neuro* **4**, 243-252, doi:10.1042/AN20120017 (2012).

136 Munz, C. Regulation of innate immunity by the molecular machinery of macroautophagy. *Cell Microbiol* **16**, 1627-1636, doi:10.1111/cmi.12358 (2014).

137 Mizushima, N., Yoshimori, T. & Ohsumi, Y. The role of Atg proteins in autophagosome formation. *Annu Rev Cell Dev Biol* **27**, 107-132, doi:10.1146/annurev-cellbio-092910-154005 (2011).

138 Glick, D., Barth, S. & Macleod, K. F. Autophagy: cellular and molecular mechanisms. *J Pathol* **221**, 3-12, doi:10.1002/path.2697 (2010).

139 Nakatogawa, H., Suzuki, K., Kamada, Y. & Ohsumi, Y. Dynamics and d iversity in autophagy mechanisms: lessons from yeast. *Nat Rev Mol Cell Biol* **10**, 458-467, doi:10.1038/nrm2708 (2009).

140 Dikic, I. & Elazar, Z. Mechanism and medical implications of mammalian autophagy. *Nat Rev Mol Cell Biol* **19**, 349-364, doi:10.1038/s41580-018-0003-4 (2018).

141 Shi, C. S. & Kehrl, J. H. TRAF6 and A20 regulate lysine 63-linked ubiquitination of Beclin-1 to control TLR4-induced autophagy. *Sci Signal* **3**, ra42, doi:10.1126/scisignal.2000751 (2010).

142 Jewell, J. L., Russell, R. C. & Guan, K. L. Amino acid signalling upstream of mTOR. *Nat Rev Mol Cell Biol* **14**, 133-139, doi:10.1038/nrm3522 (2013).

143 Delgado, M. *et al.* Autophagy and pattern recognition receptors in innate immunity. *Immunol Rev* **227**, 189-202, doi:10.1111/j.1600-065X.2008.00725.x (2009).

144 Jung, C. H., Ro, S. H., Cao, J., Otto, N. M. & Kim, D. H. mTOR regulation of autophagy. *FEBS Lett* **584**, 1287-1295, doi:10.1016/j.febslet.2010.01.017 (2010).

145 Kim, J., Kundu, M., Viollet, B. & Guan, K. L. AMPK and mTOR regulate autophagy through direct phosphorylation of Ulk1. *Nat Cell Biol* **13**, 132-141, doi:10.1038/ncb2152 (2011).

146 Hurley, J. H. & Young, L. N. Mechanisms of Autophagy Initiation. *Annu Rev Biochem* **86**, 225-244, doi:10.1146/annurev-biochem-061516-044820 (2017).

147 Song, X. *et al.* AMPK-Mediated BECN1 Phosphorylation Promotes Ferroptosis by Directly Blocking System Xc(-) Activity. *Curr Biol* **28**, 2388-2399 e2385, doi:10.1016/j.cub.2018.05.094 (2018).

148 Menon, M. B. & Dhamija, S. Beclin 1 Phosphorylation - at the Center of Autophagy Regulation. *Front Cell Dev Biol* **6**, 137, doi:10.3389/fcell.2018.00137 (2018).

149 Nascimbeni, A. C., Codogno, P. & Morel, E. Local detection of PtdIns3P at autophagosome biogenesis membrane platforms. *Autophagy* **13**, 1602-1612, doi:10.1080/15548627.2017.1341465 (2017).

150 Matsunaga, K. *et al.* Autophagy requires endoplasmic reticulum targeting of the PI3-kinase complex via Atg14L. *J Cell Biol* **190**, 511-521, doi:10.1083/jcb.200911141 (2010).

151 Brier, L. W. *et al.* Regulation of LC3 lipidation by the autophagy-specific class III phosphatidylinositol-3 kinase complex. *Mol Biol Cell* **30**, 1098-1107, doi:10.1091/mbc.E18-11-0743 (2019).

152 Barth, S., Glick, D. & Macleod, K. F. Autophagy: assays and artifacts. *J Pathol* **221**, 117-124, doi:10.1002/path.2694 (2010).

153 Klionsky, D. J. *et al.* Guidelines for the use and interpretation of assays for monitoring autophagy (3rd edition). *Autophagy* **12**, 1-222, doi:10.1080/15548627.2015.1100356 (2016).

154 Mizushima, N., Yoshimori, T. & Levine, B. Methods in mammalian autophagy research. *Cell* **140**, 313-326, doi:10.1016/j.cell.2010.01.028 (2010).

155 Chang, N. C., Nguyen, M., Germain, M. & Shore, G. C. Antagonism of Beclin 1-dependent autophagy by BCL-2 at the endoplasmic reticulum requires NAF-1. *EMBO J* **29**, 606-618, doi:10.1038/emboj.2009.369 (2010).

156 Pattingre, S. *et al.* Bcl-2 antiapoptotic proteins inhibit Beclin 1-dependent autophagy. *Cell* **122**, 927-939, doi:10.1016/j.cell.2005.07.002 (2005).

157 Marquez, R. T. & Xu, L. Bcl-2:Beclin 1 complex: multiple, mechanisms regulating autophagy/apoptosis toggle switch. *Am J Cancer Res* **2**, 214-221 (2012).

158 Chen, D. *et al.* Parkin mono-ubiquitinates Bcl-2 and regulates autophagy. *J Biol Chem* **285**, 38214-38223, doi:10.1074/jbc.M110.101469 (2010).

159 Decuypere, J. P., Parys, J. B. & Bultynck, G. Regulation of the autophagic bcl-2/beclin 1 interaction. *Cells* **1**, 284-312, doi:10.3390/cells1030284 (2012).

160 Wei, Y., Pattingre, S., Sinha, S., Bassik, M. & Levine, B. JNK1-mediated phosphorylation of Bcl-2 regulates starvation-induced autophagy. *Mol Cell* **30**, 678-688, doi:10.1016/j.molcel.2008.06.001 (2008).

161 Tang, S. W., Ducroux, A., Jeang, K. T. & Neuveut, C. Impact of cellular autophagy on viruses: Insights from hepatitis B virus and human retroviruses. *J Biomed Sci* **19**, 92, doi:10.1186/1423-0127-19-92 (2012).

162 Kirkin, V., McEwan, D. G., Novak, I. & Dikic, I. A role for ubiquitin in selective autophagy. *Mol Cell* **34**, 259-269, doi:10.1016/j.molcel.2009.04.026 (2009).

163 Ding, W. X. & Yin, X. M. Mitophagy: mechanisms, pathophysiological roles, and analysis. *Biol Chem* **393**, 547-564, doi:10.1515/hsz-2012-0119 (2012).

164 Kraft, C., Peter, M. & Hofmann, K. Selective autophagy: ubiquitin-mediated recognition and beyond. *Nat Cell Biol* **12**, 836-841, doi:10.1038/ncb0910-836 (2010).

165 Kirkin, V. & Rogov, V. V. A Diversity of Selective Autophagy Receptors Determines the Specificity of the Autophagy Pathway. *Mol Cell* **76**, 268-285, doi:10.1016/j.molcel.2019.09.005 (2019).

166 Behrends, C. & Fulda, S. Receptor proteins in selective autophagy. *Int J Cell Biol* **2012**, 673290, doi:10.1155/2012/673290 (2012).

167 Kirkin, V., Lamark, T., Johansen, T. & Dikic, I. NBR1 cooperates with p62 in selective autophagy of ubiquitinated targets. *Autophagy* **5**, 732-733, doi:10.4161/auto.5.5.8566 (2009).

168 Reggiori, F. & Ungermann, C. Autophagosome Maturation and Fusion. *J Mol Biol* **429**, 486-496, doi:10.1016/j.jmb.2017.01.002 (2017).

169 Takats, S., Boda, A., Csizmadia, T. & Juhasz, G. Small GTPases controlling autophagy-related membrane traffic in yeast and metazoans. *Small GTPases* **9**, 465-471, doi:10.1080/21541248.2016.1258444 (2018).

170 Rusten, T. E. & Stenmark, H. How do ESCRT proteins control autophagy? *J Cell Sci* **122**, 2179-2183, doi:10.1242/jcs.050021 (2009).

171 Itakura, E., Kishi, C., Inoue, K. & Mizushima, N. Beclin 1 forms two distinct phosphatidylinositol 3-kinase complexes with mammalian Atg14 and UVRAG. *Mol Biol Cell* **19**, 5360-5372, doi:10.1091/mbc.E08-01-0080 (2008).

172 Matsunaga, K. *et al.* Two Beclin 1-binding proteins, Atg14L and Rubicon, reciprocally regulate autophagy at different stages. *Nat Cell Biol* **11**, 385-396, doi:10.1038/ncb1846 (2009).

173 Mizushima, N. & Yoshimori, T. How to interpret LC3 immunoblotting. *Autophagy* **3**, 542-545 (2007).

174 Liu, G., Bi, Y., Wang, R. & Wang, X. Self-eating and self-defense: autophagy controls innate immunity and adaptive immunity. *J Leukoc Biol* **93**, 511-519, doi:10.1189/jlb.0812389 (2013).

175 Levine, B. & Kroemer, G. Autophagy in the pathogenesis of disease. *Cell* **132**, 27-42, doi:10.1016/j.cell.2007.12.018 (2008).

176 Kizilarslanoglu, M. C. & Ulger, Z. Role of autophagy in the pathogenesis of Alzheimer disease. *Turk J Med Sci* **45**, 998-1003, doi:10.3906/sag-1407-75 (2015).

177 Cook, K. L., Shajahan, A. N. & Clarke, R. Autophagy and endocrine resistance in breast cancer. *Expert Rev Anticancer Ther* **11**, 1283-1294, doi:10.1586/era.11.111 (2011).

178 Lavandero, S., Chiong, M., Rothermel, B. A. & Hill, J. A. Autophagy in cardiovascular biology. *J Clin Invest* **125**, 55-64, doi:10.1172/JCI73943 (2015).

179 Randow, F. & Munz, C. Autophagy in the regulation of pathogen replication and adaptive immunity. *Trends Immunol* **33**, 475-487, doi:10.1016/j.it.2012.06.003 (2012).

180 Schmid, D. & Munz, C. Innate and adaptive immunity through autophagy. *Immunity* **27**, 11-21, doi:10.1016/j.immuni.2007.07.004 (2007).

181 Crotzer, V. L. & Blum, J. S. Autophagy and its role in MHC-mediated antigen presentation. *J Immunol* **182**, 3335-3341, doi:10.4049/jimmunol.0803458 (2009).

182 Rey-Jurado, E., Riedel, C. A., Gonzalez, P. A., Bueno, S. M. & Kalergis, A. M. Contribution of autophagy to antiviral immunity. *FEBS Lett* **589**, 3461-3470, doi:10.1016/j.febslet.2015.07.047 (2015).

183 Espert, L. *et al.* Autophagy is involved in T cell death after binding of HIV-1 envelope proteins to CXCR4. *J Clin Invest* **116**, 2161-2172, doi:10.1172/JCI26185 (2006).

184 Qian, M., Fang, X. & Wang, X. Autophagy and inflammation. *Clin Transl Med* **6**, 24, doi:10.1186/s40169-017-0154-5 (2017).

185 Andersen, A. N. *et al.* Coupling of HIV-1 Antigen to the Selective Autophagy Receptor SQSTM1/p62 Promotes T-Cell-Mediated Immunity. *Front Immunol* **7**, 167, doi:10.3389/fimmu.2016.00167 (2016).

186 Paludan, C. *et al.* Endogenous MHC class II processing of a viral nuclear antigen after autophagy. *Science* **307**, 593-596, doi:10.1126/science.1104904 (2005).

187 Schmid, D., Pypaert, M. & Munz, C. Antigen-loading compartments for major histocompatibility complex class II molecules continuously receive input from autophagosomes. *Immunity* **26**, 79-92, doi:10.1016/j.immuni.2006.10.018 (2007).

188 Kudchodkar, S. B. & Levine, B. Viruses and autophagy. *Rev Med Virol* **19**, 359-378, doi:10.1002/rmv.630 (2009).

189 Liyana Ahmad, S. M., Vanessa Sancho-Shimizu. Autophagy-Virus Interplay: From Cell Biology to Human Disease. *Front Cell Dev Biol* (2018).

190 Cheng, Y., Ren, X., Hait, W. N. & Yang, J. M. Therapeutic targeting of autophagy in disease: biology and pharmacology. *Pharmacol Rev* **65**, 1162-1197, doi:10.1124/pr.112.007120 (2013).

191 Kobayashi, S. *et al.* Autophagy inhibits viral genome replication and gene expression stages in West Nile virus infection. *Virus Res* **191**, 83-91, doi:10.1016/j.virusres.2014.07.016 (2014).

192 Shoji-Kawata, S. *et al.* Identification of a candidate therapeutic autophagy-inducing peptide. *Nature* **494**, 201-206, doi:10.1038/nature11866 (2013).

193 Talloczy, Z., Virgin, H. W. t. & Levine, B. PKR-dependent autophagic degradation of herpes simplex virus type 1. *Autophagy* **2**, 24-29, doi:10.4161/auto.2176 (2006).

194 Orvedahl, A. *et al.* HSV-1 ICP34.5 confers neurovirulence by targeting the Beclin 1 autophagy protein. *Cell Host Microbe* **1**, 23-35, doi:10.1016/j.chom.2006.12.001 (2007).

195 Liang, Q. *et al.* Identification of the Essential Role of Viral Bcl-2 for Kaposi's Sarcoma-Associated Herpesvirus Lytic Replication. *J Virol* **89**, 5308-5317, doi:10.1128/JVI.00102-15 (2015).

196 Liang, Q. *et al.* Zika Virus NS4A and NS4B Proteins Deregulate Akt-mTOR Signaling in Human Fetal Neural Stem Cells to Inhibit Neurogenesis and Induce Autophagy. *Cell Stem Cell* **19**, 663-671, doi:10.1016/j.stem.2016.07.019 (2016).

197 Chiramel, A. I. & Best, S. M. Role of autophagy in Zika virus infection and pathogenesis. *Virus Res* **254**, 34-40, doi:10.1016/j.virusres.2017.09.006 (2018).

198 Prentice, E., Jerome, W. G., Yoshimori, T., Mizushima, N. & Denison, M. R. Coronavirus replication complex formation utilizes components of cellular autophagy. *J Biol Chem* **279**, 10136-10141, doi:10.1074/jbc.M306124200 (2004).

199 Jackson, W. T. *et al.* Subversion of cellular autophagosomal machinery by RNA viruses. *PLoS Biol* **3**, e156, doi:10.1371/journal.pbio.0030156 (2005).

200 Maier, H. J. & Britton, P. Involvement of autophagy in coronavirus replication. *Viruses* **4**, 3440-3451, doi:10.3390/v4123440 (2012).

201 Cottam, E. M. *et al.* Coronavirus nsp6 proteins generate autophagosomes from the endoplasmic reticulum via an omegasome intermediate. *Autophagy* **7**, 1335-1347, doi:10.4161/auto.7.11.16642 (2011).

202 Gassen, N. C. *et al.* SKP2 attenuates autophagy through Beclin1-ubiquitination and its inhibition reduces MERS-Coronavirus infection. *Nat Commun* **10**, 5770, doi:10.1038/s41467-019-13659-4 (2019).

203 Cottam, E. M., Whelband, M. C. & Wileman, T. Coronavirus NSP6 restricts autophagosome expansion. *Autophagy* **10**, 1426-1441, doi:10.4161/auto.29309 (2014).

204 Carmona-Gutierrez, D. *et al.* Digesting the crisis: autophagy and coronaviruses. *Microb Cell* **7**, 119-128, doi:10.15698/mic2020.05.715 (2020).

205 Liao, K. *et al.* HIV Tat-mediated induction of autophagy regulates the disruption of ZO-1 in brain endothelial cells. *Tissue Barriers* **8**, 1748983, doi:10.1080/21688370.2020.1748983 (2020).

206 Bruno, A. P. *et al.* HIV-1 Tat protein induces glial cell autophagy through enhancement of BAG3 protein levels. *Cell Cycle* **13**, 3640-3644, doi:10.4161/15384101.2014.952959 (2014).

207 Mandell, M. A., Kimura, T., Jain, A., Johansen, T. & Deretic, V. TRIM proteins regulate autophagy: TRIM5 is a selective autophagy receptor mediating HIV-1 restriction. *Autophagy* **10**, 2387-2388, doi:10.4161/15548627.2014.984278 (2014).

208 Mandell, M. A. *et al.* TRIM proteins regulate autophagy and can target autophagic substrates by direct recognition. *Dev Cell* **30**, 394-409, doi:10.1016/j.devcel.2014.06.013 (2014).

209 Yu, A. *et al.* TRIM5alpha self-assembly and compartmentalization of the HIV-1 viral capsid. *Nat Commun* **11**, 1307, doi:10.1038/s41467-020-15106-1 (2020).

210 Valera, M. S. *et al.* The HDAC6/APOBEC3G complex regulates HIV-1 infectiveness by inducing Vif autophagic degradation. *Retrovirology* **12**, 53, doi:10.1186/s12977-015-0181-5 (2015).

211 Sagnier, S. *et al.* Autophagy restricts HIV-1 infection by selectively degrading Tat in CD4+ T lymphocytes. *J Virol* **89**, 615-625, doi:10.1128/JVI.02174-14 (2015).

212 Botbol, Y., Guerrero-Ros, I. & Macian, F. Key roles of autophagy in regulating T-cell function. *Eur J Immunol* **46**, 1326-1334, doi:10.1002/eji.201545955 (2016).

213 Hubbard, V. M. *et al.* Macroautophagy regulates energy metabolism during effector T cell activation. *J Immunol* **185**, 7349-7357, doi:10.4049/jimmunol.1000576 (2010).

214 Watson, R. O., Manzanillo, P. S. & Cox, J. S. Extracellular M. tuberculosis DNA targets bacteria for autophagy by activating the host DNA-sensing pathway. *Cell* **150**, 803-815, doi:10.1016/j.cell.2012.06.040 (2012).

215 Rasmussen, S. B. *et al.* Activation of autophagy by alpha-herpesviruses in myeloid cells is mediated by cytoplasmic viral DNA through a mechanism dependent on stimulator of IFN genes. *J Immunol* **187**, 5268-5276, doi:10.4049/jimmunol.1100949 (2011).

216 Rubinsztein, D. C., Codogno, P. & Levine, B. Autophagy modulation as a potential therapeutic target for diverse diseases. *Nat Rev Drug Discov* **11**, 709-730, doi:10.1038/nrd3802 (2012).

217 Lingappa, J. R., Reed, J. C., Tanaka, M., Chutiraka, K. & Robinson, B. A. How HIV-1 Gag assembles in cells: Putting together pieces of the puzzle. *Virus Res* **193**, 89-107, doi:10.1016/j.virusres.2014.07.001 (2014).

218 Scarlata, S. & Carter, C. Role of HIV-1 Gag domains in viral assembly. *Biochim Biophys Acta* **1614**, 62-72, doi:10.1016/s0005-2736(03)00163-9 (2003).

219 Dreux, M. & Chisari, F. V. Viruses and the autophagy machinery. *Cell Cycle* **9**, 1295-1307, doi:10.4161/cc.9.7.11109 (2010).

220 Daussy, C. F., Beaumelle, B. & Espert, L. Autophagy restricts HIV-1 infection. *Oncotarget* **6**, 20752-20753, doi:10.18632/oncotarget.5123 (2015).

221 Colomer-Lluch, M. & Serra-Moreno, R. BCA2/Rabring7 Interferes with HIV-1 Proviral Transcription by Enhancing the SUMOylation of IkappaBalpha. *J Virol* **91**, doi:10.1128/JVI.02098-16 (2017).

222 Nityanandam, R. & Serra-Moreno, R. BCA2/Rabring7 targets HIV-1 Gag for lysosomal degradation in a tetherin-independent manner. *PLoS pathogens* **10**, e1004151, doi:10.1371/journal.ppat.1004151 (2014).

223 Serra-Moreno, R., Jia, B., Breed, M., Alvarez, X. & Evans, D. T. Compensatory changes in the cytoplasmic tail of gp41 confer resistance to tetherin/BST-2 in a pathogenic nef-deleted SIV. *Cell Host Microbe* **9**, 46-57, doi:10.1016/j.chom.2010.12.005 (2011).

224 Fullgrabe, J., Ghislat, G., Cho, D. H. & Rubinsztein, D. C. Transcriptional regulation of mammalian autophagy at a glance. *J Cell Sci* **129**, 3059-3066, doi:10.1242/jcs.188920 (2016).

225 Napolitano, G. & Ballabio, A. TFEB at a glance. *J Cell Sci* **129**, 2475-2481, doi:10.1242/jcs.146365 (2016).

226 Settembre, C. & Ballabio, A. TFEB regulates autophagy: an integrated coordination of cellular degradation and recycling processes. *Autophagy* **7**, 1379-1381, doi:10.4161/auto.7.11.17166 (2011).

227 Wong, P. M., Feng, Y., Wang, J., Shi, R. & Jiang, X. Regulation of autophagy by coordinated action of mTORC1 and protein phosphatase 2A. *Nature communications* **6**, 8048, doi:10.1038/ncomms9048 (2015).

228 Axe, E. L. *et al.* Autophagosome formation from membrane compartments enriched in phosphatidylinositol 3-phosphate and dynamically connected to the endoplasmic reticulum. *J Cell Biol* **182**, 685-701, doi:10.1083/jcb.200803137 (2008).

229 Tang, D. *et al.* Endogenous HMGB1 regulates autophagy. *J Cell Biol* **190**, 881-892, doi:10.1083/jcb.200911078 (2010).

230 Nguyen, M. *et al.* Small molecule obatoclax (GX15-070) antagonizes MCL-1 and overcomes MCL-1-mediated resistance to apoptosis. *Proc Natl Acad Sci U S A* **104**, 19512-19517, doi:10.1073/pnas.0709443104 (2007).

231 Carroll, R. G., Hollville, E. & Martin, S. J. Parkin sensitizes toward apoptosis induced by mitochondrial depolarization through promoting d egradation of Mcl-1. *Cell reports* **9**, 1538-1553, doi:10.1016/j.celrep.2014.10.046 (2014).

232 Hollville, E., Carroll, R. G., Cullen, S. P. & Martin, S. J. Bcl-2 family proteins participate in mitochondrial quality control by regulating Parkin/PINK1-dependent mitophagy. *Mol Cell* **55**, 451-466, doi:10.1016/j.molcel.2014.06.001 (2014).

233 Lutz, A. K. *et al.* Loss of parkin or PINK1 function increases Drp1-dependent mitochondrial fragmentation. *J Biol Chem* **284**, 22938-22951, doi:10.1074/jbc.M109.035774 (2009).

234 Lama, J., Mangasarian, A. & Trono, D. Cell-surface expression of CD4 reduces HIV-1 infectivity by blocking Env incorporation in a Nef- and Vpu-inhibitable manner. *Curr Biol* **9**, 622-631, doi:10.1016/s0960-9822(99)80284-x (1999).

235 Rossi, F., Gallina, A. & Milanesi, G. Nef-CD4 physical interaction sensed with the yeast two-hybrid system. *Virology* **217**, 397-403, doi:10.1006/viro.1996.0130 (1996).

236 Harris, M. P. & Neil, J. C. Myristoylation-dependent binding of HIV-1 Nef to CD4. *J Mol Biol* **241**, 136-142, doi:10.1006/jmbi.1994.1483 (1994).

237 Grzesiek, S., Stahl, S. J., Wingfield, P. T. & Bax, A. The CD4 determinant for downregulation by HIV-1 Nef directly binds to Nef. Mapping of the Nef binding surface by NMR. *Biochemistry* **35**, 10256-10261, doi:10.1021/bi9611164 (1996).

238 Preusser, A., Briese, L., Baur, A. S. & Willbold, D. Direct in vitro binding of full-length human immunodeficiency virus type 1 Nef protein to CD4 cytoplasmic domain. *J Virol* **75**, 3960-3964, doi:10.1128/JVI.75.8.3960-3964.2001 (2001).

239 Bentham, M., Mazaleyrat, S. & Harris, M. The di-leucine motif in the cytoplasmic tail of CD4 is not required for binding to human immunodeficiency virus type 1 Nef, but is critical for CD4 down-modulation. *J Gen Virol* **84**, 2705-2713, doi:10.1099/vir.0.19274-0 (2003).

240 Jin, Y. J., Zhang, X., Boursiquot, J. G. & Burakoff, S. J. CD4 phosphorylation partially reverses Nef down-regulation of CD4. *J Immunol* **173**, 5495-5500, doi:10.4049/jimmunol.173.9.5495 (2004).

241 Cluet, D. *et al.* Detection of human immunodeficiency virus type 1 Nef and CD4 physical interaction in living human cells by using bioluminescence resonance energy transfer. *J Virol* **79**, 8629-8636, doi:10.1128/JVI.79.13.8629-8636.2005 (2005).

242 Thomenius, M. J. & Distelhorst, C. W. Bcl-2 on the endoplasmic reticulum: protecting the mitochondria from a distance. *J Cell Sci* **116**, 4493-4499, doi:10.1242/jcs.00829 (2003).

243 Akao, Y., Otsuki, Y., Kataoka, S., Ito, Y. & Tsujimoto, Y. Multiple subcellular localization of bcl-2: detection in nuclear outer membrane, endoplasmic reticulum membrane, and mitochondrial membranes. *Cancer Res* **54**, 2468-2471 (1994).

244 Krajewski, S. *et al.* Investigation of the subcellular distribution of the bcl-2 oncoprotein: residence in the nuclear envelope, endoplasmic reticulum, and outer mitochondrial membranes. *Cancer Res* **53**, 4701-4714 (1993).

245 Lee, S. T. *et al.* Bcl-2 targeted to the endoplasmic reticulum can inhibit apoptosis induced by Myc but not etoposide in Rat-1 fibroblasts. *Oncogene* **18**, 3520-3528, doi:10.1038/sj.onc.1202716 (1999).

246 Wang, N. S., Unkila, M. T., Reineks, E. Z. & Distelhorst, C. W. Transient expression of wild-type or mitochondrially targeted Bcl-2 induces apoptosis, whereas transient expression of endoplasmic reticulum-targeted Bcl-2 is protective against Bax-induced cell death. *J Biol Chem* **276**, 44117-44128, doi:10.1074/jbc.M101958200 (2001).

247 Narendra, D., Tanaka, A., Suen, D. F. & Youle, R. J. Parkin is recruited selectively to impaired mitochondria and promotes their autophagy. *J Cell Biol* **183**, 795-803, doi:10.1083/jcb.200809125 (2008).

248 Nguyen, T. N., Padman, B. S. & Lazarou, M. Deciphering the Molecular Signals of PINK1/Parkin Mitophagy. *Trends Cell Biol* **26**, 733-744, doi:10.1016/j.tcb.2016.05.008 (2016).

249 Renton, J. P., Xu, N., Clark, J. J. & Hansen, M. R. Interaction of neurotrophin signaling with Bcl-2 localized to the mitochondria and endoplasmic reticulum on spiral ganglion neuron survival and neurite growth. *J Neurosci Res* **88**, 2239-2251, doi:10.1002/jnr.22381 (2010).

250 Heise, T. *et al.* The La protein counteracts cisplatin-induced cell death by stimulating protein synthesis of anti-apoptotic factor Bcl2. *Oncotarget* **7**, 29664-29676, doi:10.18632/oncotarget.8819 (2016).

251 Zhao, X., Ogunwobi, O. O. & Liu, C. Survivin inhibition is critical for Bcl-2 inhibitor-induced apoptosis in hepatocellular carcinoma cells. *PLoS One* **6**, e21980, doi:10.1371/journal.pone.0021980 (2011).

252 Itakura, E. & Mizushima, N. Atg14 and UVRAG: mutually exclusive subunits of mammalian Beclin 1-PI3K complexes. *Autophagy* **5**, 534-536, doi:10.4161/auto.5.4.8062 (2009).

253 Kang, R., Zeh, H. J., Lotze, M. T. & Tang, D. The Beclin 1 network regulates autophagy and apoptosis. *Cell death and differentiation* **18**, 571-580, doi:10.1038/cdd.2010.191 (2011).

254 Kihara, A., Kabeya, Y., Ohsumi, Y. & Yoshimori, T. Beclin-phosphatidylinositol 3-kinase complex functions at the trans-Golgi network. *EMBO Rep* **2**, 330-335, doi:10.1093/embo-reports/kve061 (2001).

255 Fernandez, A. F. *et al.* Disruption of the beclin 1-BCL2 autophagy regulatory complex promotes longevity in mice. *Nature* **558**, 136-140, doi:10.1038/s41586-018-0162-7 (2018).

256 Adachi, A. *et al.* Production of acquired immunodeficiency virus syndrome-associated retrovirus in human and nonhuman cells transfected with an infectious molecular clone. *Journal of Virology* **59**, 284-291 (1986).

257 Strebel, K., Klimkait, T. & Martin, M. A. A novel gene of HIV-1, vpu, and its 16-kilodalton product. *Science* **241**, 1221-1223 (1988).

258 Zhang, H. *et al.* Novel single-cell-level phenotypic assay for residual drug susceptibility and reduced replication capacity of drug-resistant human immunodeficiency virus type 1. *J Virol* **78**, 1718-1729, doi:10.1128/jvi.78.4.1718-1729.2004 (2004).

259 Schwartz, O., Marechal, V., Danos, O. & Heard, J. M. Human immunodeficiency virus type 1 Nef increases the efficiency of reverse transcription in the infected cell. *J Virol* **69**, 4053-4059, doi:10.1128/JVI.69.7.4053-4059.1995 (1995).

260 Adachi, A. *et al.* Production of acquired immunodeficiency syndrome-associated retrovirus in human and nonhuman cells transfected with an infectious molecular clone. *J Virol* **59**, 284-291, doi:10.1128/JVI.59.2.284-291.1986 (1986).

261 Kirchhoff, F., Schindler, M., Specht, A., Arhel, N. & Munch, J. Role of Nef in primate lentiviral immunopathogenesis. *Cell Mol Life Sci* **65**, 2621-2636, doi:10.1007/s00018-008-8094-2 (2008).

262 Schmokel, J. *et al.* Conservation of Nef function across highly diverse lineages of SIVsmm. *Retrovirology* **6**, 36, doi:10.1186/1742-4690-6-36 (2009).

263 Serra-Moreno, R. & Evans, D. T. Adaptation of Human and Simian Immunodeficiency Viruses for Resistance to Tetherin/BST-2. *Curr HIV Res* **10**, 277-282 (2012).

264 Zhang, F. *et al.* Nef proteins from simian immunodeficiency viruses are tetherin antagonists. *Cell Host Microbe* **6**, 54-67, doi:10.1016/j.chom.2009.05.008 (2009).

265 Sauter, D. *et al.* Tetherin-driven adaptation of Vpu and Nef function and the evolution of pandemic and nonpandemic HIV-1 strains. *Cell Host Microbe* **6**, 409-421, doi:10.1016/j.chom.2009.10.004 (2009).

266 Le Tortorec, A. & Neil, S. J. Antagonism to and intracellular sequestration of human tetherin by the human immunodeficiency virus type 2 envelope glycoprotein. *J Virol* **83**, 11966-11978, doi:10.1128/JVI.01515-09 (2009).

267 Alexander, L. *et al.* Determinants of increased replicative capacity of serially passaged simian immunodeficiency virus with nef deleted in rhesus monkeys. *Journal of Virology* **77**, 6823-6835 (2003).

268 Joseph, S. B., Swanstrom, R., Kashuba, A. D. & Cohen, M. S. Bottlenecks in HIV-1 transmission: insights from the study of founder viruses. *Nat Rev Microbiol* **13**, 414-425, doi:10.1038/nrmicro3471 (2015).

269 Joseph, S. B. & Swanstrom, R. HIV/AIDS. A fitness bottleneck in HIV-1 transmission. *Science* **345**, 136-137, doi:10.1126/science.1257425 (2014).

270 Keele, B. F. *et al.* Identification and characterization of transmitted and early founder virus envelopes in primary HIV-1 infection. *Proc Natl Acad Sci U S A* **105**, 7552-7557, doi:10.1073/pnas.0802203105 (2008).

271 Kariuki, S. M., Selhorst, P., Arien, K. K. & Dorfman, J. R. The HIV-1 transmission bottleneck. *Retrovirology* **14**, 22, doi:10.1186/s12977-017-0343-8 (2017).

272 Magiorkinis, G. *et al.* The global spread of HIV-1 subtype B epidemic. *Infect Genet Evol* **46**, 169-179, doi:10.1016/j.meegid.2016.05.041 (2016).

273 DeGottardi, M. Q. *et al.* Selective downregulation of rhesus macaque and sooty mangabey major histocompatibility complex class I molecules by nef alleles of simian immunodeficiency virus and human immunodeficiency virus type 2. *Journal of Virology* **82**, 3139-3146 (2008).

274 Munch, J. *et al.* Nef-mediated enhancement of virion infectivity and stimulation of viral replication are fundamental properties of primate lentiviruses. *J Virol* **81**, 13852-13864, doi:10.1128/JVI.00904-07 (2007).

275 Salazar-Gonzalez, J. F. *et al.* Genetic identity, biological phenotype, and evolutionary pathways of transmitted/founder viruses in acute and early HIV-1 infection. *J Exp Med* **206**, 1273-1289, doi:10.1084/jem.20090378 (2009).

276 Deymier, M. J. *et al.* Particle infectivity of HIV-1 full-length genome infectious molecular clones in a subtype C heterosexual transmission pair following high fidelity amplification and unbiased cloning. *Virology* **468-470**, 454-461, doi:10.1016/j.virol.2014.08.018 (2014).

277 Deymier, M. J. *et al.* Heterosexual Transmission of Subtype C HIV-1 Selects Consensus-Like Variants without Increased Replicative Capacity or Interferon-alpha Resistance. *PLoS Pathog* **11**, e1005154, doi:10.1371/journal.ppat.1005154 (2015).

278 Kestler, H. W. *et al.* Importance of the nef gene for maintenance of high virus loads and for the development of AIDS. *Cell* **65**, 651-662 (1991).

279 Regier, D. A. & Desrosiers, R. C. The complete nucleotide sequence of a pathogenic molecular clone of simian immunodeficiency virus. *AIDS Research and Human Retroviruses* **6**, 1221-1231 (1990).

280 Van Nynatten, L. R. *et al.* Identification of Novel Subcellular Localization and Trafficking of HIV-1 Nef Variants from Reference Strains G (F1.93.HH8793) and H (BE.93.VI997). *Viruses* **10**, doi:10.3390/v10090493 (2018).

281 Ge, P., Dawson, V. L. & Dawson, T. M. PINK1 and Parkin mitochondrial quality control: a source of regional vulnerability in Parkinson's disease. *Mol Neurodegener* **15**, 20, doi:10.1186/s13024-020-00367-7 (2020).

282 Ito, T., Deng, X., Carr, B. & May, W. S. Bcl-2 phosphorylation required for anti-apoptosis function. *J Biol Chem* **272**, 11671-11673, doi:10.1074/jbc.272.18.11671 (1997).

283 Rasola, A., Gramaglia, D., Boccaccio, C. & Comoglio, P. M. Apoptosis enhancement by the HIV-1 Nef protein. *J Immunol* **166**, 81-88, doi:10.4049/jimmunol.166.1.81 (2001).

284 Acheampong, E. A. *et al.* Human Immunodeficiency virus type 1 Nef potently induces apoptosis in primary human brain microvascular endothelial cells via the activation of caspases. *J Virol* **79**, 4257-4269, doi:10.1128/JVI.79.7.4257-4269.2005 (2005).

285 Lenassi, M. *et al.* HIV Nef is secreted in exosomes and triggers apoptosis in bystander CD4+ T cells. *Traffic* **11**, 110-122, doi:10.1111/j.1600-0854.2009.01006.x (2010).

286 Lamers, S. L. *et al.* Brain-specific HIV Nef identified in multiple patients with neurological disease. *J Neurovirol* **24**, 1-15, doi:10.1007/s13365-017-0586-0 (2018).

287 Cheney, L. *et al.* HIV Nef and Antiretroviral Therapy Have an Inhibitory Effect on Autophagy in Human Astrocytes that May Contribute to HIV-Associated Neurocognitive Disorders. *Cells* **9**, doi:10.3390/cells9061426 (2020).

288 Almodovar, S. *et al.* Pathogenesis of HIV-associated pulmonary hypertension: potential role of HIV-1 Nef. *Proc Am Thorac Soc* **8**, 308-312, doi:10.1513/pats.201006-046WR (2011).

289 Zhang, C. F. *et al.* Autophagy in pulmonary hypertension: Emerging roles and therapeutic implications. *J Cell Physiol* **234**, 16755-16767, doi:10.1002/jcp.28531 (2019).

290 Dever, S. M., Rodriguez, M., Lapierre, J., Costin, B. N. & El-Hage, N. Differing roles of autophagy in HIV-associated neurocognitive impairment and encephalitis with implications for morphine co-exposure. *Front Microbiol* **6**, 653, doi:10.3389/fmicb.2015.00653 (2015).

291 Wasner, K., Grunewal, A. & Klein, C. Parkin-linked Parkinson's disease: From clinical insights to pathogenic mechanisms and novel therapeutic approaches. *Neurosci Res*, doi:10.1016/j.neures.2020.09.001 (2020).

292 Jin, S. W. *et al.* Variation in HIV-1 Nef function within and among viral subtypes reveals genetically separable antagonism of SERINC3 and SERINC5. *PLoS Pathog* **16**, e1008813, doi:10.1371/journal.ppat.1008813 (2020).

293 Besnard, E. *et al.* The mTOR Complex Controls HIV Latency. *Cell Host Microbe* **20**, 785-797, doi:10.1016/j.chom.2016.11.001 (2016).

294 Kumar, B., Arora, S., Ahmed, S. & Banerjea, A. C. Hyperactivation of mammalian target of rapamycin complex 1 by HIV-1 is necessary for

virion production and latent viral reactivation. *FASEB J* **31**, 180-191, doi:10.1096/fj.201600813R (2017).

295 Martin, A. R. *et al.* Rapamycin-mediated mTOR inhibition uncouples HIV-1 latency reversal from cytokine-associated toxicity. *J Clin Invest* **127**, 651-656, doi:10.1172/JCI89552 (2017).

296 Donia, M. Potential use of rapamycin in HIV infection. *British Pharmacological Society* (2020).

297 Rai, P. *et al.* Rapamycin-induced modulation of HIV gene transcription attenuates progression of HIVAN. *Exp Mol Pathol* **94**, 255-261, doi:10.1016/j.yexmp.2012.09.009 (2013).